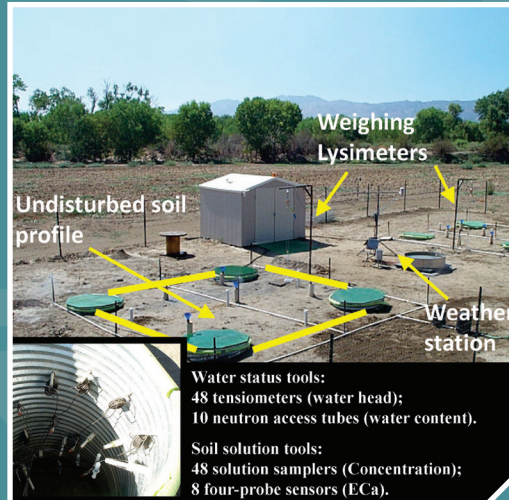


# Transport and Fate of Nutrients and Indicator Microorganisms at a Dairy Lagoon Water Application Site: AN ASSESSMENT OF NUTRIENT MANAGEMENT PLANS





# **Transport and Fate of Nutrients and Indicator Microorganisms at a Dairy Lagoon Water Application Site:**

AN ASSESSMENT OF NUTRIENT  
MANAGEMENT PLANS

**Scott Bradford**

*USDA, ARS, US Salinity Laboratory*

# Notice

This work was supported through Interagency Agreement DW-12-92189901-0 between EPA's Ground Water & Ecosystems Restoration Division, National Risk Management Research Laboratory (Stephen Hutchins, Project Officer) and USDA-ARS's U.S. Salinity Laboratory (Scott Bradford, Principal Investigator). Although this work was funded substantially by the U.S. Environmental Protection Agency, it has not been subjected to Agency review and therefore does not necessarily reflect the views of the Agency, and no official endorsement should be inferred.

Corresponding author. Scott Bradford, USDA, ARS, US Salinity Laboratory, 450 W. Big Springs Road, Riverside, CA 92507; Tel.:951-369-4857; Fax: 951-342-4964; E-mail: [Scott.Bradford@ars.usda.gov](mailto:Scott.Bradford@ars.usda.gov)

# Foreword

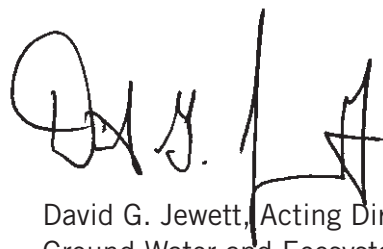
The U.S. Environmental Protection Agency (EPA) is charged by Congress with protecting the Nation's land, air, and water resources. Under a mandate of national environmental laws, the Agency strives to formulate and implement actions leading to a compatible balance between human activities and the ability of natural systems to support and nurture life. To meet this mandate, EPA's research program is providing data and technical support for solving environmental problems today and building a science knowledge base necessary to manage our ecological resources wisely, understand how pollutants affect our health, and prevent or reduce environmental risks in the future.

The National Risk Management Research Laboratory (NRMRL) is the Agency's center for investigation of technological and management approaches for preventing and reducing risks from pollution that threatens human health and the environment. The focus of the Laboratory's research program is on methods and their cost-effectiveness for prevention and control of pollution to air, land, water, and subsurface resources; protection of water quality in public water systems; remediation of contaminated sites, sediments and ground water; prevention and control of indoor air pollution; and restoration of ecosystems. NRMRL collaborates with both public and private sector partners to foster technologies that reduce the cost of compliance and to anticipate emerging problems. NRMRL's research provides solutions to environmental problems by: developing and promoting technologies that protect and improve the environment; advancing scientific and engineering information to support regulatory and policy decisions; and providing the technical support and information transfer to ensure implementation of environmental regulations and strategies at the national, state, and community levels.

EPA currently requires that application of concentrated animal feeding operation wastes to agricultural fields follows a Nutrient Management Plan (NMP). The tacit assumption is that a well-designed and executed NMP ensures that all lagoon water contaminants (nutrients and pathogens) are retained or taken up in the root zone so that ground water is inherently protected. This research was designed to test the assumption that appropriate NMPs are protective of ground water and to address potential weaknesses in the land-application design and operation processes. A well-designed and managed NMP was implemented on two 6-by-6-meter plots at a dairy farm in San Jacinto, California, for several years using different forage and application patterns. The selected site was intensively characterized and instrumented for the experimental studies. Lagoon water application rates were determined by following NMP guidelines from the National Resource Conservation Service (NRCS).

Spatial and temporal variations in water, nutrient, and indicator microbe levels at the site were determined using a system of nested tensiometers and soil solution samplers, neutron probe readings, weighing lysimeters, periodic soil coring, plant tissue analysis, and measurements of apparent soil electrical conductivity. Along with the field experiments, laboratory experiments were also conducted, using microbes, lagoon water, well water, and soils from the NMP field site. Microcosm and batch studies were conducted to quantify microbial retention and survival. Transport experiments were conducted to quantify the influence of water content, microorganism size, grain-size distribution, and lagoon water composition on the movement and retention of microbes. Transport parameters were estimated by fitting numerical simulations to experimental data.

This project is completed and has resulted in multiple journal articles that provide detailed information on the various aspects of the project. This EPA report summarizes these results.



David G. Jewett, Acting Director  
Ground Water and Ecosystems Restoration Division  
National Risk Management Research Laboratory



# Contents

Notice . . . . .	ii
Foreword . . . . .	iii
Contents . . . . .	v
Figures . . . . .	vii
Tables . . . . .	ix
Abbreviations . . . . .	x
Executive Summary . . . . .	xi
1.0 Literature Review . . . . .	1
Background . . . . .	1
Review . . . . .	2
Environmental Contaminants . . . . .	2
Nutrients and Organics . . . . .	3
Salts . . . . .	3
Pathogens . . . . .	3
Land Application . . . . .	5
Water Flow . . . . .	7
Nutrient Transport . . . . .	8
Pathogen Transport . . . . .	10
Treatments . . . . .	12
2.0 Site Characterization for Detailed NMP Studies . . . . .	16
Background . . . . .	16
Materials and Methods . . . . .	16
Results and Discussion . . . . .	18
Soft Data . . . . .	18
Hard Data . . . . .	19
Validation and Simulations . . . . .	21
Bromide Travel Times . . . . .	21
Averaging of Bromide Transport . . . . .	21
3.0 NMP Results - Nutrients . . . . .	25
Background . . . . .	25
Materials and Methods . . . . .	25
Field . . . . .	25
Water and Nitrogen Mass Balances in the Root Zone . . . . .	27
Results and Discussion . . . . .	30
Management Considerations for Salinity . . . . .	30
Management Considerations for Organic Nitrogen . . . . .	33
Plant Available N, P, and K . . . . .	35
Nitrogen Fixation – Alfalfa 2008 . . . . .	36
4.0 NMP Results – Indicator Microorganisms . . . . .	40
Background . . . . .	40
Materials and Methods . . . . .	40
NMP Field Site . . . . .	40
Analysis and Sampling for Indicator Microorganisms . . . . .	40

Laboratory Experiments . . . . .	42
Results and Discussion . . . . .	43
NMP Field Site. . . . .	43
Laboratory Experiments . . . . .	46
5.0 Laboratory Studies Investigating Mechanisms of Colloid Retention . . . . .	52
Background . . . . .	52
Materials and Methods. . . . .	52
Colloids . . . . .	52
Sand . . . . .	53
Electrolyte Solution Chemistry . . . . .	53
DLVO Calculations . . . . .	53
Batch Experiments . . . . .	54
Column Experiments . . . . .	54
Colloid Transport Model for Saturated and Unsaturated Systems. . . . .	54
Results and Discussion . . . . .	55
6.0 Mathematical Models to Simulate Pathogen and Nutrient Fate . . . . .	58
Background . . . . .	58
Physical Chemical Nonequilibrium (PCNE) Model . . . . .	59
Dual-Permeability Model . . . . .	60
Stochastic Stream Tube Model. . . . .	63
7.0 Summary and Conclusions. . . . .	66
Quality Assurance . . . . .	70
8.0 References . . . . .	71

# Figures

Figure 1.1.	A schematic of the processes and nitrogen species that are involved in the nitrogen cycle. . . . .	9
Figure 1.2.	A flowchart that illustrates the steps that may be used to assess and improve the performance of lagoon water application sites. . . . .	12
Figure 2.1.	A schematic of the field site. Squares represent two 6x6 m plots. . . . .	17
Figure 2.2.	A 4 ha map of the vertical component of the apparent soil electrical conductivity in the field as measured using a mobile remote electromagnetic induction sensor system on a 5x5 m grid. . . . .	19
Figure 2.3.	North-south and east-west transects of estimated values of $K_s$ on plot 1. . . . .	20
Figure 2.4.	Field measurements of the relative bromide concentration over time for the bromide tracer experiment. . . . .	23
Figure 2.5.	Field measurements (circle) and 2D-MIM simulation (lines and triangle) of relative bromide concentration over time at -95, -126 and -155 cm. . . . .	24
Figure 3.1.	Schematic of the field site. . . . .	26
Figure 3.2.	The absolute value of the soil water pressure head ( $ h $ ) in the soil profile as a function of day after emergence (DAE) for the cyclic and blending water application strategies during the sorghum 2007 growing season. . . . .	31
Figure 3.3.	Electrical conductivity of the soil solution ( $EC_w$ ) over depth and total dissolved solids (TDS) load during 2007 for the blending and cyclic water application strategies. . . . .	32
Figure 3.4.	Nitrogen from ammonium ( $N-NH_4$ ) and nitrogen from combined nitrite and nitrate ( $N-(NO_2+NO_3)$ ) concentration in the soil profile at the end (final) and beginning (initial) of two consecutive growing seasons (triticale 2007/sorghum 2007 and sorghum 2007/alfalfa 2008). . . . .	33
Figure 3.5.	Three conceptual approaches for nitrogen NMPs based on low (top figure-333 g of $N\cdot m^{-2}$ ), intermediate (middle figure-1666 g of $N\cdot m^{-2}$ ), and high (lower figure-3333 g of $N\cdot m^{-2}$ ) soil organic N reservoirs. . . . .	34
Figure 3.6.	The composition, distribution, and amount of organic and inorganic N species ( $mg\ L^{-1}$ ) in dairy wastewater during the triticale 2007 growing season. . . . .	35
Figure 3.7:	Soil inorganic and organic N reservoirs ( $N_{soil}^I$ and $N_{soil}^O$ ) and cumulative values of N uptake by plant ( $N_{plant}^I$ ), exchange to/from organic and inorganic N forms ( $E_{OI}$ ), N loss to drainage ( $N_{drainage}^I$ ), supplied organic N ( $N_{application}^O$ ), and supplied inorganic N minus loss to the atmosphere ( $N_{application}^I - N_{atmosphere}^I$ ) in the root zone are presented over time. . . . .	37
Figure 3.8.	Plant available phosphorus ( $P-PO_4$ ) and potassium (K) in the soil profile at the beginning (initial) of the triticale and end (final) of the sorghum growing seasons in 2007 for the blending and cyclic water application strategies. . . . .	38
Figure 3.9.	Dry phytomass, cumulative water application and actual evapotranspiration throughout the five growing cycles of alfalfa in 2008. . . . .	38
Figure 4.1.	Plots of the concentration of <i>Enterococcus</i> (Figure 4.1a), fecal coliform (Figure 4.1b), somatic coliphage (Figure 4.1c), and total <i>E. coli</i> (Figure 4.1d) in soil ( $S, N\ g^{-1}$ ) as a function of depth at several different days after emergence (DAE) during the winter triticale growing season at the NMP field site. . . . .	45

Figure 4.2.	Plots of the gravimetric water content ( $\theta_g$ ) (Figure 4.2a), and the normalized concentration of <i>Enterococcus</i> (Figure 4.2b), fecal coliform (Figure 4.2c), somatic coliphage (Figure 4.2d), and total <i>E. coli</i> (Figure 4.2e) in soil ( $S/C_T$ ) as a function of depth at selected sampling times (initial, and times = 0, 14, 62, 134, and 206 h after wastewater application) during the summer alfalfa growing season at the NMP field site. . . . .	47
Figure 4.3.	A semi-log plot of the relative total concentration ( $C_T/C_{T0}$ ) as a function of time in batch survival experiments under sterile (Figure 4.3a) and native (Figure 4.3b) conditions at 80% water saturation for the various indicator microorganisms . . . . .	48
Figure 4.4.	Breakthrough curves (Figure 4.4a) and retention profiles (Figure 4.4b) for <i>Enterococcus</i> , total <i>E. coli</i> , and $\phi X174$ in a column experiment packed with sterilized field soil. . . . .	49
Figure 4.5.	Plots of the normalized concentration of the indicator microorganisms in soil ( $S/C_T$ ) as a function of depth at a sampling time of 24 h after ponded infiltration of wastewater ceased on the undisturbed soil core from the NMP site. . . . .	50
Figure 4.6.	A semi-log plot of the relative total concentration ( $C_T/C_{T0}$ ) of the various indicator microorganisms as a function of time in the ponded infiltration undisturbed soil column experiment. . . . .	51
Figure 5.1	Observed and simulated breakthrough curves of colloids for various saturation levels in 360 $\mu\text{m}$ sand at an ionic strength of 6 mM (Figure 5.1a) and 30 mM (Figure 5.1b) . . . . .	57
Figure 6.1.	Plots of simulated breakthrough curves (Figure 6.1a) and retention profiles (Figure 6.1b) when $q_t$ was equal to 0.0918 $\text{cm min}^{-1}$ and the value of $wq_2$ was 0, 0.001, 0.002, 0.004, and 0.008 $\text{cm min}^{-1}$ . . . . .	63
Figure 6.2.	Plots of the simulated breakthrough curves (Figure 6.2a) and retention profiles (Figure 6.2b) when $wq_2$ was 0.001 $\text{cm min}^{-1}$ and $q_t$ was equal to 0.024, 0.046, 0.091, 0.181, and 0.361 $\text{cm min}^{-1}$ . . . . .	64
Figure 6.3.	(a) Plot of the relative flux concentration, $\langle vC \rangle / (\langle v \rangle C_r)$ , at a depth of 10 cm as a function of time when $v$ and $k_d$ are both stochastic parameters and values of $\rho_{vd} = -1, -0.5, 0, 0.5,$ and 1. (b, c) Corresponding normalized solid phase colloid concentration, $\langle S \rangle / N_{ic}$ , and associated variance after 250 min with depth, respectively. Model parameters that were employed in these simulations were $D = 0.0313 \text{ cm}^2 \text{ min}^{-1}$ , $\langle v \rangle = 0.313 \text{ cm min}^{-1}$ , $\langle k_d \rangle = 0.03 \text{ min}^{-1}$ , $k_r = 0.001 \text{ min}^{-1}$ , $\sigma_v = 1$ , and $\sigma_d = 1$ . . . . .	65

# Tables

Table 1.1.	A summary of measured total suspended solids (TSS), electrical conductivity (EC), oxidation-reduction potentials (ORP), ammonium (NH <sub>4</sub> -N), nitrite and nitrate (NO <sub>2</sub> +NO <sub>3</sub> -N), total Kjeldahl nitrogen (TKN), total phosphorus (TP), total organic carbon (TOC), and potassium (K) concentrations from several swine, poultry, dairy, and beef lagoon water samples. . . . .	2
Table 1.2.	Indicator microbial populations in whole lagoon samples from different CAFOs. . . . .	4
Table 1.3.	Nutrient uptake parameters for selected crops (Kellogg et al., 2000). . . . .	6
Table 1.4.	Hypothetical blending ratio (well water to lagoon water) for various lagoon waters when winter wheat and summer corn are grown using semi-arid and temperate climates. . . . .	6
Table 1.5.	The estimated environmental loading of total salts and indicator microorganisms when the various lagoon waters were applied to a 1 m <sup>2</sup> area of agricultural field to meet the nitrogen needs of corn during a 90 d summer growing season. . . . .	7
Table 2.1.	The hydraulic properties ( $\theta_s$ is the saturated water content; $\theta_r$ is the residual water content; $\alpha$ is the reciprocal of the air entry pressure; and $n$ is the pore size distribution parameter of the van Genuchten model) of the three major layers in the upper soil profile of the field plot. Soft data was estimated from particle size distribution and bulk density data using the ROSETTA program. . . . .	20
Table 2.2.	Mean and standard deviation of bromide travel time (units in hours, $h$ ) at each sampling depth and culvert pipe location, and associated average and variance values for each depth. . . . .	22
Table 3.1.	Ammonia volatilization from the sprinkler irrigation system and soil surface. . . . .	29
Table 3.2.	Potential and actual evapotranspiration (ET), crop coefficient, rainfall and water application during the growing season of triticale during winter 2007 (A) and sorghum during summer 2007 (B), DAE is day after emergence. . . . .	31
Table 3.3.	Salts and macro-nutrients of a raw and treated dairy wastewater (DWW). DWW was sequentially treated by solid separator, sedimentation tank and sand filter. . . . .	35
Table 4.1.	Representative concentrations of indicator microorganisms in raw and treated dairy wastewater, and the percent removal by treatment. . . . .	43
Table 4.2.	Actual evapotranspiration (ET), rainfall, well water application, wastewater application, and drainage amounts during the winter (triticale) and summer (sorghum) growing seasons as a function of day after emergence (DAE). . . . .	44
Table 4.3.	Fitted parameters ( $\lambda_0$ and $\alpha$ ) from the time dependent decay model (Equation 4.2) for the various indicator microorganisms under native conditions at 80% water saturation. . . . .	48
Table 6.1.	Expressions for the second- and third-order moments for breakthrough after a Dirac delta input according to physical nonequilibrium (PNE), chemical nonequilibrium (CNE), and PCNE models. . . . .	61

# Abbreviations

AWI	air water interface
CAFO	concentrated animal feeding operation
CML	carboxyl modified latex
CNE	chemical nonequilibrium
DAE	day after emergence
DWW	dairy wastewater
DLVO	Derjaguin, Landau, Verwey and Overbeek
EC	electrical conductivity
ET	evapotranspiration
FC	fecal coliform
IS	ionic strength
MPN	most probable number
NMP	nutrient management plan
ORP	oxidation–reduction potentials
PET	potential evapotranspiration
PCNE	physical and chemical nonequilibrium
PDF	probability density function
PNE	physical nonequilibrium
SWI	solid water interface
TKN	total Kjeldahl nitrogen
TOC	total organic carbon
TP	total phosphorus
TSS	total suspended solids

# Executive Summary

The Environmental Protection Agency (EPA) currently requires that application of Concentrated Animal Feeding Operation (CAFO) wastes to agricultural fields follow an approved Nutrient Management Plan (NMP). The tacit assumption is that a well designed and executed NMP ensures that all lagoon water contaminants (nutrients and pathogens) are retained or taken up in the root zone, so that groundwater is inherently protected. Recent research by the EPA, however, has demonstrated that land application of CAFO lagoon water can cause nitrate contamination of groundwater at significant depths in short time frames. The research outlined in this report was designed to test the assumption that a well designed and executed NMP is protective of groundwater from nutrients, salts, and indicator microorganisms, and to address potential weaknesses in the land application design and operation processes of NMPs.

The report is divided into seven chapters. Chapter 1 provides a detailed review of the literature examining the reuse of CAFO wastewater on agricultural fields, with special emphasis on nutrients and pathogens. A dairy farm in San Jacinto, California, was selected for our NMP research experiments. A well designed and managed NMP was implemented on two 6x6 m plots at this site for several years to study the fate of nutrients and indicator microorganisms. This study required a high level of confidence in the water flow and solute transport behavior and therefore detailed information on the associated soil properties was needed. Chapter 2 provides a description of our field site and extensive experiments that were conducted to characterize the flow and transport properties at this site. Chapter 3 provides a detailed description of the NMP implemented at this site and results pertaining to the fate of nutrients and salts. Chapter 4 describes field and laboratory research that was conducted to study the fate of indicator microorganisms under NMP conditions. Many gaps still exist with regard to our understanding of microorganism transport and retention in the field. Laboratory experiments and mathematical model development were therefore initiated to overcome some of these limitations. Chapter 5 outlines results from laboratory studies that examined the coupled effects of pore structure, solution chemistry, and water velocity on colloid retention in saturated and unsaturated porous media, whereas Chapter 6 describes the development and application of the mathematical models for colloid transport and retention. Chapter 7 provides a summary of the research, and the main conclusions and recommendations.

Collectively, this research led to the development of recommendations to improve NMP performance to protect groundwater under CAFO waste application sites from both nutrients and indicator microorganisms. The main NMP lessons learned from the study include:

- Only minor differences in NMP performance were found between cyclic and blending application strategies for dairy lagoon water.
- NMPs need to account for the soil organic N reservoir in the N mass balance. This may induce difficulties in conservative NMP implementation that is protective of the environment due to: i) difficulties in estimation of mineralization rates and their spatial variability; ii) delayed availability of the organic N for plant uptake; and iii) continuous mineralization and potential nutrient leaching during fallow periods.
- NMPs should be designed to meet plant N uptake and to minimize the migration of nutrients below the root zone. This was achieved in this research by accurately applying inorganic N in dairy wastewater (DWW) that was treated to remove most of the suspended solids, and minimizing the soil

organic reservoir by applying only a fraction of the plant N uptake with DWW. Additional research is needed to optimize the use of soil organic reservoirs under other NMPs.

- The use of leguminous crops, such as alfalfa, in NMPs is more complicated than cereal crops. Potential advantages of leguminous crops are their deeper root system and greater plant N uptake. However, atmospheric N fixation is a nutrient source for leguminous crops that is difficult to quantify, and this creates potential challenges for implementing environmentally protective NMPs. Additional research is therefore needed to optimize NMP performance with leguminous crops.
- DWW contain much higher quantities of salts than typical irrigation water. NMPs that precisely apply water and DWW to meet evapotranspiration (ET) will therefore accumulate salts in the root zone that may restrict plant growth, and water and nutrient uptake. If this reduction in ET is not considered at NMP sites, additional leaching and contaminant migration will occur. This point is strongly dependent on the salt tolerance of the crop, suggesting that NMPs should use only salt tolerant crops.
- The leaching timing of excess salts below the root zone is a crucial aspect in NMP design because of continuous mineralization of organic N during fallow periods. In order to minimize  $\text{NO}_3^-$  leaching, pre-irrigations should be scheduled at the end of the growing season, when the soil profile is depleted from  $\text{NO}_3^-$  by plant uptake.
- A comprehensive measurement of N mass balance in the root zone requires information on losses to the atmosphere during irrigation. Atmospheric losses may be minimized by applying DWW during times that are associated with low potential ET (i.e., early morning), or through drip systems that minimize the exposure of DWW to the atmosphere.
- Differences in the concentration ratios of N, P, and K between DWW and plant uptake may lead to accumulation of P and K in the root zone.
- Improve measurements of water and nutrient requirements by the crop to obtain accurate information on the required timing and quantities for application and to minimize drainage (contaminant flux to groundwater).
- Increase the water and N use efficiency by irrigating to meet plant uptake requirements using a high uniformity application system. Minimize runoff and ponding conditions by matching the water application rate to the soil infiltration rate.
- The transport potential of microorganisms can be significantly reduced by minimizing water leaching below the root zone and surface water runoff. This can be achieved by: precise estimation of the ET rate; uniform application of wastewater; and selecting water application timing and quantities based on considerations of soil permeability and ET.
- Special caution is warranted for NMPs on coarse textured and structured soils, and during water flow transients where enhanced microorganism transport potential has been reported in the literature.
- Timing of water application should allow for adequate die-off of microorganisms before leaching the root zone by irrigation or natural precipitation.
- Develop a “hydrological sensitivity index” based on the soil and groundwater properties (depth, quality, hydraulic properties, and mineralogy of the vadose zone and aquifer). This index should categorize high and low potential zones of contamination from agricultural activity. Application of liquid and solid dairy wastes in low sensitivity zones would be more flexible than in other zones.

# 1.0 Literature Review

## Background

New technological innovations and the economic advantage of size have driven a structural shift from small to large concentrated animal feeding operations (CAFOs) in the USA. It has been estimated that confined livestock and poultry animals in the USA generate about 453 million tonnes of manure annually (Kellogg et al., 2000; USEPA, 2003). Water use at CAFOs includes drinking water for animals and water used in cooling facilities, sanitation and wash down of facilities, and animal waste-disposal systems. The United States Geological Survey estimated that livestock water use accounted for nearly 1% of the total freshwater withdrawals (excluding thermoelectric power) in the USA (Hutson et al., 2004). Daily use of water for farm animals was reported to be 159 L d<sup>-1</sup> for a milking cow, 18 L d<sup>-1</sup> for a hog, and 18 L d<sup>-1</sup> for 100 chickens. Large volumes of animal manure-containing wastewater, wash water, and storm water runoff can be generated at CAFOs (USEPA, 2001a). This manure-contaminated water is typically collected and stored in wastewater lagoons on farms (USEPA, 2001a).

Transportation, storage, and treatment of manure and manure-contaminated water are costly (Gleick, 2000). The large volume of waste generated, and the lack of disposal area at CAFOs, further limit the ability for effective manure management. Manure and wastewater are, therefore, usually land applied within about 16 km of CAFO facilities. When applied to agricultural lands at agronomic rates, manure and wastewater can be a valuable fertilizer and soil amendment that can improve the physical condition of the soil for plant growth (Jokela, 1992; Kapkiyai et al., 1999), reduce power required for tillage (Sommerfeldt and Chang, 1985, 1987), and increase the organic content of soil (Sommerfeldt et al., 1988). The reuse of CAFO wastewater in

irrigated agriculture also provides a potential means to reduce the demand for high quality water that is a scarce natural resource in many arid and semi-arid regions (Pimentel et al., 2004). Conversely, CAFO manure and wastewater have also been reported to pose a potential risk to environmental resources and to human health (Thorne, 2007; Burkholder et al., 2007). Contaminants of potential concern in animal wastes include excess amounts of nutrients (Jongbloed and Lenis, 1998; Mallin, 2000), salts (Chang and Entz, 1996; Hao and Chang, 2003), organics rich in biochemical oxygen-demanding material (Webb and Archer, 1994), heavy metals (Barker and Zublena, 1996), microbial pathogens (Gerba and Smith, 2005; Schets et al., 2005), antibiotics (Shore et al., 1988 and 1995; Nichols et al., 1997; Peterson et al., 2000), and natural and synthetic hormones (Hanselman et al., 2003; Raman et al., 2004).

This review contains three sections, namely: (i) Environmental Contaminants; (ii) Land Application; and (iii) Treatments. The Environmental Contaminants section reviews the nutrients and pathogens that are found in CAFO lagoon water and why they may pose a risk to the environment and/or human health. The Land Application section reviews the current regulatory framework for land application of CAFO wastewater that is based upon Nutrient Management Plans (NMPs), the implicit assumptions and possible weaknesses in NMP design and application, illustrative nutrient and pathogen loading rates at NMP sites, and potential transport pathways for nutrients and pathogens. Finally, the section on Treatments discusses potential best management practices and lagoon water treatments that may be needed before land application of CAFO wastewater to minimize risks and dissemination of nutrients and pathogens in the environment.

## Review

### Environmental Contaminants

Three classes of potential lagoon water contaminants are considered in this section, namely: (i) nutrients and organics, (ii) salts, and (iii) pathogens. Tables 1.1 and 1.2 provide illustrative examples of concentrations of the various nutrients, salts and indicator microorganisms that were measured in CAFO lagoon water from several farms. Considerable variability is expected in the concentration of these contaminants at different farms due to differences in animal and waste management practices. Hence, the concentration values provided in these tables should be viewed as only reflecting site specific conditions at the indicated farm, and general trends should not be ascribed to these data. Wastewater from these lagoons, however, is actually used for land application at these farms, and therefore these data can be used to provide an estimate of potential environmental concentrations for the various contaminants.

Table 1.1 provides a summary of measured total suspended solids (TSS), electrical conductivity (EC), oxidation-reduction potentials (ORP), ammonium ( $\text{NH}_4\text{-N}$ ), nitrite and nitrate ( $\text{NO}_2+\text{NO}_3\text{-N}$ ), total Kjeldahl nitrogen (TKN), total phosphorus (TP), total organic carbon (TOC), and potassium (K) concentrations from several swine, poultry, dairy, and beef lagoon water samples (Hutchins et al., 2007). Concentrations of indicator microorganisms in these lagoon water samples are provided in Table 1.2. For these data, separate analyses were conducted on the samples collected as described previously (Hutchins et al., 2007). Microbial indicators were analyzed on whole lagoon samples using a commercial most probable number (MPN) method (IDEXX Laboratories, ME). More general information on nutrient characteristics and other properties of various types of lagoon water samples is also available in the literature (MWPS, 1993; NCSU, 1994; USDA, 1996; ASAE, 1999; USEPA, 2001a; Bradford et al., 2008).

**Table 1.1.** A summary of measured total suspended solids (TSS), electrical conductivity (EC), oxidation-reduction potentials (ORP), ammonium ( $\text{NH}_4\text{-N}$ ), nitrite and nitrate ( $\text{NO}_2+\text{NO}_3\text{-N}$ ), total Kjeldahl nitrogen (TKN), total phosphorus (TP), total organic carbon (TOC), and potassium (K) concentrations from several swine, poultry, dairy, and beef lagoon water samples (mean with standard deviation, three locations for each lagoon).

CAFO	TSS	EC	ORP	$\text{NH}_4\text{-N}$	$\text{NO}_2+\text{NO}_3\text{-N}$	TKN	TP	TOC	K
Type	mg $\text{L}^{-1}$	dS $\text{m}^{-1}$	mV	mg $\text{L}^{-1}$	mg $\text{L}^{-1}$	mg $\text{L}^{-1}$	mg $\text{L}^{-1}$	mg $\text{L}^{-1}$	mg $\text{L}^{-1}$
Beef Feedlot <sup>2</sup>	212 ± 28	2.6 ± 0.0	73 ± 26	33 ± 3	0.2 ± 0.01	63 ± 1	14 ± 0	155 ± 6	277 ± 2
Dairy <sup>2</sup>	718 ± 150	3.1 ± 0.0	-277 ± 24	84 ± 12	0.5 ± 0.1	185 ± 11	30 ± 1	576 ± 94	178 ± 29
Poultry <sup>1</sup>	847 ± 15	11.3 ± 0.2	-331 ± 21	656 ± 34	1.2 ± 0.01	802 ± 7	50 ± 1	1050 ± 40	1430 ± 200
Poultry <sup>2</sup>	865 ± 79	8.0 ± 0.0	-337 ± 2	289 ± 11	0.5 ± 0.01	407 ± 2	23 ± 0	374 ± 15	1490 ± 30
Poultry <sup>3</sup>	253 ± 75	4.4 ± 0.0	207 ± 28	58 ± 5	10.4 ± 2.3	96 ± 0	30 ± 0	114 ± 15	811 ± 14
Swine Sow <sup>1</sup>	1230 ± 30	12.6 ± 0.0	-348 ± 16	944 ± 23	2.8 ± 0.04	1290 ± 15	264 ± 5	944 ± 304	137 ± 2
Swine Finisher <sup>1</sup>	5310 ± 2430	19.4 ± 0.0	-368 ± 2	1630 ± 20	8.0 ± 0.1	2430 ± 40	324 ± 14	4780 ± 280	242 ± 3
Swine Nursery <sup>1</sup>	4220 ± 1940	21.5 ± 0.1	-368 ± 5	1370 ± 90	5.7 ± 0.8	2040 ± 60	368 ± 35	1440 ± 130	4150 ± 210

<sup>1</sup> – Primary lagoon; <sup>2</sup> – Secondary lagoon; <sup>3</sup> – Tertiary lagoon; CAFO – Concentrated Animal Feeding Operation

### **Nutrients and Organics**

Table 1.1 provides illustrative concentrations of nutrients ( $\text{NH}_4\text{-N}$ , TKN, TP, and K) and organics (TOC) that were measured in several swine, poultry, dairy, and beef lagoon water samples. Ayers and Westcot (1989) reported severe restrictions on the use of irrigation water that had total nitrogen values greater than  $30 \text{ mg L}^{-1}$  due to potential problems discussed below. These same authors also reported that typical ranges for  $\text{NH}_4\text{-N}$ ,  $\text{PO}_4\text{-P}$ , and  $\text{K}^+$  in irrigation water were 0-5, 0-2, and 0-2  $\text{mg L}^{-1}$ , respectively. The EPA has set the Maximum Contaminant Level (MCL) in groundwater for nitrate ( $\text{NO}_3^-$ ) and nitrite ( $\text{NO}_2^-$ ) at  $10 \text{ mg L}^{-1}$   $\text{NO}_3\text{-N}$  and  $1 \text{ mg L}^{-1}$   $\text{NO}_2\text{-N}$ , respectively. The EPA-recommended guideline for TOC in drinking water is  $4 \text{ mg L}^{-1}$ . Hence, Table 1.1 indicates that nutrient and organic concentrations are very high in these lagoon water samples, relative to irrigation and drinking water standards.

Published literature also indicates that animal wastes frequently contain high concentrations of nutrients (Chang and Entz, 1996; Hao and Chang, 2003) and organics rich in biochemical oxygen-demanding material (Webb and Archer, 1994) that can adversely impact soil and water quality (Jokela, 1992; Chang and Entz, 1996; Craun and Calderon, 1996; USEPA, 1997; USEPA, 2000). Potential environmental problems from excess amounts of nutrients and organics in water include algal blooms, reduced biodiversity, objectionable tastes and odors, and growth of toxic organisms in surface waters that are used for recreation and sources of drinking water (Mallin, 2000; Burkholder et al., 2007). These degraded conditions, especially the associated hypoxia/anoxia and high ammonia, have caused major kills of freshwater species (Burkholder et al., 2007). High nitrate levels in water have been associated with increased risk of methemoglobinemia for infants (blue-baby syndrome), as well as diarrhea and respiratory disease (Ward et al., 2005).

### **Salts**

Table 1.1 provides illustrative concentrations of EC that were measured in several swine, poultry, dairy, and beef lagoon water samples. Ayers and Westcot (1989) reported severe restrictions on the use of irrigation water that had EC values greater than  $3 \text{ dS m}^{-1}$ . The salinity levels that are associated with these lagoon waters are very high relative to the irrigation quality guidelines.

Prolonged exposure of agricultural lands to animal wastes that have high salinity levels may alter many soil physical and chemical properties, and crop yields (Burns et al., 1985; King et al., 1985; Chang et al., 1991). For example, Chang et al. (1991) studied the effects of 11 years of cattle manure addition on soil chemical properties. Accumulation of specific ions (soluble sodium, calcium, magnesium, chloride, sulfate, bicarbonate, and zinc), nutrients (total N, nitrate, total P, available P), and organic matter increased with increasing application rates of manure and lagoon water. Near the soil surface the EC and the sodium adsorption ratio (SAR) increased and the pH decreased with increasing addition rates of manure. Changes in these soil chemical properties can in turn influence soil hydraulic properties. For example, high SAR values are frequently associated with decreases in the saturated hydraulic conductivity (Ayers and Westcot, 1989) as a result of dispersion of the clay (colloidal) fraction of soils. High levels of EC as well as specific ions (sodium, chloride, boron, nitrate, and bicarbonate) can also severely influence crop yields (Maas and Hoffman, 1977; Maas, 1984) as a result of increases in osmotic stress and specific ion toxicities.

### **Pathogens**

Animal wastes frequently contain pathogenic viruses, bacteria, and protozoa that pose a risk to human and/or animal health (USDA, 1992; USEPA, 1998; Gerba and Smith, 2005). Although more than 130 microbial pathogens have been identified from all animal

species that may be transmitted to humans by various routes (USDA, 1992; USEPA, 1998), the most significant manure-borne zoonotic pathogens are the protozoan parasites *Cryptosporidium parvum* and *Giardia duodenalis*, and the bacterial pathogens *Salmonella* spp., *Campylobacter* spp., *Escherichia coli* O157:H7, and *Listeria monocytogenes*. Viruses of potential concern include: poliovirus, coxsackie virus, echovirus, hepatitis A, rotavirus, and Norwalk virus (Gerba and Smith, 2005).

The EPA has set drinking water goals for pathogens to be no detection, because of the low infectious dose for many pathogens (Loge et al., 2002) and variability of individual responses to infection (Gerba, 1996). Regulations to protect public health from pathogens, however, are largely based on measured concentrations of indicator microorganisms such as total or fecal (thermotolerant) coliform (FC). For example, the World Health Organization (WHO) recommended standard for use of degraded water for irrigating crops eaten raw is <1000 FC per 100 mL (WHO, 2006), whereas in the USA the standard for unrestricted urban use varies with the state from non-detectable to 200 FC per 100 mL (USEPA, 2004). Table 1.2 provides

illustrative concentrations of various indicator microorganisms of fecal contamination (Total Coliforms, Fecal Coliforms, and Fecal Enterococci) that were measured in several swine, poultry, dairy, and beef lagoon water samples. The concentration of indicator microorganisms in the various lagoon water samples is very high, and significantly exceeds the recommended US standards for unrestricted irrigation (USEPA, 2004).

Surface and groundwater contamination by pathogenic microorganisms is common in many areas of the USA (USEPA, 1997). Drinking water exposures may occur in vulnerable private wells, whereas recreation exposures and illnesses can happen due to accidental ingestion of contaminated water and dermal contact during swimming. Surveys of waterborne disease outbreaks frequently demonstrate a farm animal source (Centers for Disease Control and Prevention, 1998). Pathogenic microorganisms in groundwater have been estimated to cause between 750,000 and 5 million illnesses per year in the USA (Macler and Merkle, 2000). Greater risks of serious illness occur for the very young, elderly, pregnant women, the immunocompromised, and those predisposed with other illnesses (Gerba, 1996).

**Table 1.2.** Indicator microbial populations in whole lagoon samples from different CAFOs (mean with standard deviation, three locations for each lagoon).

CAFO Type	Total Coliforms cfu per 100 mL	Fecal Coliforms cfu per 100 mL	Fecal Enterococci cfu per 100 mL
Beef Feedlot <sup>2</sup>	3.89E03 ± 0.99E03	1.57E03 ± 0.28E03	2.94E03 ± 1.07E03
Dairy <sup>2</sup>	1.91E07 ± 0.16E07	1.08E06 ± 0.11E06	1.53E05 ± 0.23E05
Poultry <sup>1</sup>	4.73E04 ± 2.09E04	2.91E04 ± 1.07E04	1.41E05 ± 0.67E05
Poultry <sup>2</sup>	2.42E03 ± 0.00E03	2.42E03 ± 0.00E03	8.51E04 ± 2.75E04
Poultry <sup>3</sup>	5.83E04 ± 0.28E04	2.03E01 ± 0.06E01	2.68E03 ± 1.24E03
Swine Sow <sup>1</sup>	4.89E05 ± 0.70E05	3.34E05 ± 0.43E05	3.69E05 ± 0.39E05
Swine Finisher <sup>1</sup>	1.02E06 ± 0.12E06	9.52E05 ± 3.44E05	8.50E05 ± 4.63E05
Swine Nursery <sup>1</sup>	1.87E05 ± 0.95E05	7.93E04 ± 8.30E04	2.43E05 ± 0.00E05

<sup>1</sup> – Primary lagoon; <sup>2</sup> – Secondary lagoon; <sup>3</sup> – Tertiary lagoon; CAFO – Concentrated Animal Feeding Operation

Manure-contaminated water resources have also been implicated in food-borne disease outbreaks on a variety of fresh produce (Gerba and Smith, 2005). The health impacts of such outbreaks can be very significant. For example, the 2006 outbreak of *E.coli* O157:H7 on spinach from the Salinas Valley, California, resulted in 205 illnesses and 3 deaths (USFDA, 2007). Furthermore, loss of confidence in the safety of agricultural produce can have significant economic impacts. For example, the 2005 spinach crop from this same region was estimated to be worth around \$188 million.

### Land Application

The Environmental Protection Agency (EPA) currently requires that CAFO waste application to agricultural lands follow approved Nutrient Management Plans (NMPs). The National Resources Conservation Service (NRCS) defines a NMP as, “Managing the amount, source, placement, form and timing of the application of nutrients and soil amendments” (USDA, 2000). The purpose of a NMP is to meet the nutrient needs of the crop to be grown, while minimizing the loss of nutrients to surface and groundwater (USEPA, 2003). Nutrient management plans are developed to adhere to state-specific NRCS guidelines. In general, a NMP is developed by considering all nutrient input sources (such as manure, fertilizer, lagoon water, and well water), the nutrient content at the soil surface, nutrient volatilization losses to the atmosphere (e.g., nitrogen losses as ammonia), nutrient mineralization rates, and plant uptake rates for nutrients. The nutrient concentrations are typically measured directly for the input sources, at the soil surface, and in plant tissues, whereas nutrient volatilization and mineralization rates are commonly estimated from literature values. The amount of lagoon water or other nutrient source that can be used in a given irrigation cycle is determined based on nutrient mass-balance considerations for a limiting nutrient (e.g., nitrogen or

phosphorus). A review of several state NMP guidelines shows that they are typically written so as to be protective of surface water resources, and only provide limited direction on land application site characterization and design to protect groundwater from contamination (such as in regions with shallow water tables).

A brief example of NMP implementation is given below. In this example we assume that nitrogen is the limiting nutrient for plant growth, and use the CAFO lagoon water composition information for nutrients presented in Table 1.1. Nitrate and nitrite only contributed a small fraction to the total N in the lagoon water samples (see Table 1.1) and were therefore neglected in this analysis. Table 1.3 lists nutrient uptake parameters for selected crops (Kellogg et al., 2000) that were used in this example. For simplicity we also make the following assumptions: N volatilization loss of 20%, N mineralization (ammonification) of 50% during the growing season, initially zero N in the soil profile and in the well water, and the only water source to the plants was irrigation water. Table 1.4 presents the blending ratios that were calculated to meet the nutrient (nitrogen) requirements for winter wheat and summer corn for silage assuming final yields of 27 and 56 tonne-hectare<sup>-1</sup>, respectively, and 90 d of full cover crop. We performed this calculation for two climatic conditions, inducing different evapotranspiration (ET) fluxes that correspond to semi-arid and temperate areas. Table 1.4 indicates that the higher ET flux produces a higher blending ratio. Lagoon water with a low N concentration (Dairy and Beef) provides insufficient N at low ET fluxes and therefore an additional N source is required (fertilizer) in order to meet crop needs.

**Table 1.3.** Nutrient uptake parameters for selected crops (Kellogg et al., 2000).

Crop	Nitrogen	Phosphorus
	kg per ton of product	kg per ton of product
Corn for silage	3.6	0.5
Sorghum for silage	7.4	1.2
Barley	18.6	3.8
Wheat	20.6	3.6
Alfalfa	25.2	2.4
Grass silage	6.8	0.8

Data in Tables 1.1-1.4 can be used to provide an illustrative estimate of the environmental loading for the various contaminants identified in the lagoon water under NMP application conditions. As an example, Table 1.5 provides the estimated environmental loading of total salts (from EC values given in Table 1.1) and indicator microorganisms (sum of Total coliform and Enterococcus in a given row of Table 1.2) when the various lagoon waters (blended with well water) were applied to a 1 m<sup>2</sup> area of agricultural field to meet the nitrogen needs of corn during a 90 d summer growing season with an evapotranspiration rate of 10 mm d<sup>-1</sup>. In contrast to Tables 1.1-1.2, Table 1.5 is dependent on both the contaminant concentration in the lagoon water and on the blending ratio given in Table 1.4.

**Table 1.4.** Hypothetical blending ratio (well water to lagoon water) for various lagoon waters when winter wheat and summer corn are grown using semi-arid and temperate climates.

CAFO Type	Plant available N* mg L <sup>-1</sup>	Winter wheat blending ratio		Summer corn blending ratio	
		Semi arid climate ET=5 mm d <sup>-1</sup>	Temperate climate ET=2.5 mm d <sup>-1</sup>	Semi arid climate ET=10 mm d <sup>-1</sup>	Temperate climate ET=5 mm d <sup>-1</sup>
Beef Feedlot <sup>2</sup>	41	insufficient N	insufficient N	0.93	0.46
Dairy <sup>2</sup>	118	0.05	insufficient N	4.56	2.28
Poultry <sup>1</sup>	598	3.88	1.43	27.46	12.90
Poultry <sup>2</sup>	290	1.37	0.18	12.79	5.74
Poultry <sup>3</sup>	65	insufficient N	insufficient N	2.07	0.50
Swine Sow <sup>1</sup>	928	6.58	2.78	43.22	20.59
Swine Finisher <sup>1</sup>	1704	12.93	5.94	80.21	38.66
Swine Nursery <sup>1</sup>	1431	10.70	4.82	67.19	32.30

\* Total N minus amount due to volatilization and ammonification; <sup>1</sup> – Primary lagoon; <sup>2</sup> – Secondary lagoon; <sup>3</sup> – Tertiary lagoon; CAFO – Concentrated Animal Feeding Operation; ET – Evapotranspiration

**Table 1.5.** The estimated environmental loading of total salts and indicator microorganisms when the various lagoon waters were applied to a 1 m<sup>2</sup> area of agricultural field to meet the nitrogen needs of corn during a 90 d summer growing season. An evapotranspiration rate of 10 mm d<sup>-1</sup> was assumed.

<b>CAFO</b>	<b>Total Salts</b>	<b>Total Indicator Microbes</b>
<b>Type</b>	<b>g m<sup>-2</sup></b>	<b>number m<sup>-2</sup></b>
Beef Feedlot <sup>2</sup>	1755.0	6.1E+07
Dairy <sup>2</sup>	458.9	3.8E+10
Poultry <sup>1</sup>	277.8	6.2E+07
Poultry <sup>2</sup>	422.2	6.2E+07
Poultry <sup>3</sup>	1434.8	2.7E+08
Swine Sow <sup>1</sup>	196.8	1.8E+08
Swine Finisher <sup>1</sup>	163.3	2.1E+08
Swine Nursery <sup>1</sup>	216.0	5.8E+07

<sup>1</sup> – Primary lagoon; <sup>2</sup> – Secondary lagoon; <sup>3</sup> – Tertiary lagoon; CAFO – Concentration Animal Feeding Operation

Nutrient management plans assume that a limiting nutrient is the primary environmental concern. In order to minimize surface water runoff and leaching to groundwater, NMPs also imply that water is applied to the crop to meet the potential evapotranspiration demands. The environmental loading information presented in Table 1.5 indicates that significant amounts of salts and indicator microorganisms will be added to agricultural lands where a NMP is being implemented. An implicit assumption of a NMP is that all CAFO contaminants will be taken up, inactivated, retained, or degraded in the root zone, so that surface and groundwater are inherently protected. The validity of these assumptions for all lagoon water contaminants has not yet been thoroughly studied. Below we discuss possible weaknesses in NMP design and application, as well as potential transport pathways and processes for nutrients and pathogens.

### **Water Flow**

The basic premise of a NMP is that water and nutrients are applied to the root zone at agronomic rates so that both surface and groundwater resources will be protected from all contaminants in lagoon water. Potential water inputs at a NMP application site include irrigation water (well and/or CAFO lagoon water), precipitation, surface water, snow melt, soil water, and shallow groundwater tables. The water application amount per irrigation should be based on measurements or estimates of potential evapotranspiration (PET) and water-balance considerations at the application site. If water input at a NMP application site equals PET then surface and groundwater contamination should theoretically be eliminated because all of the applied water to the site is used by the crop.

When water in excess of PET is applied to a NMP site then both surface and groundwater contamination problems are possible. This situation can arise from a number of different scenarios that may be beyond human control. Potential problems may arise due to inaccuracies in the estimation of PET, or from not accounting for all the sources of plant available water (perched water tables, precipitation, snow melt, and surface water runoff). For example, significant amounts of unexpected precipitation (a thunderstorm) after application of nutrients may lead to surface water runoff and/or leaching of contaminants. Other problems can occur due to nonuniform water application practices during flood or furrow irrigation or as a result of spatial variability of soil hydraulic properties (e.g., different amounts of water are applied to specific locations in the field) and evapotranspiration. Changes in surface topography that produce surface water runoff and lateral flow to other locations in the field pose other NMP difficulties.

Nutrient management plans implicitly assume that water flow and lagoon water contaminant transport are controlled by the soil matrix.

Preferential flow is a potentially important mechanism for water and contaminant transport to bypass portions of the soil matrix and root zone. Several recent reviews and other papers provide detailed discussions of the various processes and conditions leading to preferential flow (Ritsema et al., 1993; de Rooij, 2000; Evans et al., 2001; National Research Council, 2001; Bodvarsson et al., 2003; Šimůnek et al., 2003; Wang et al., 2004). In summary, preferential water flow can occur as a result of funneling of water at textural interfaces (capillary barriers), unstable flow behavior that is induced by spatial and/or temporal variations in capillary characteristics (wettability or hysteresis), dynamic capillary properties (nonequilibrium capillary pressure - water content characteristics), macropores, and fractured systems. All of these factors can potentially accelerate the movement of lagoon water contaminants through the root zone to underlying groundwater. Some mechanisms of preferential flow are also anticipated to depend on the initial soil water content and water application rate. For example, soil water repellency is reported to occur below some critical water content (Ritsema and Dekker, 2000), hysteresis is induced when infiltration stops and redistribution occurs (Wang et al., 2003), and filling of macropores occurs primarily near saturated conditions (Mohanty et al., 1997). Improved NMP designs are needed to provide guidelines to minimize transport processes that bypass the root zone. For example, it may be possible to minimize preferential flow in macropores by applying irrigation water at rates lower than the saturated conductivity of the soil.

### ***Nutrient Transport***

It should be mentioned that NMPs are only as good as the information on evapotranspiration and nutrient mass balance. Errors in water and nutrient application rates, or nonuniform water application will likely lead to excesses and/or shortages in lagoon water application in certain locations. Such errors are potentially responsible for some of the reported

environmental problems associated with lagoon water application sites (Evans et al., 1984; King et al., 1985; Sims et al., 1998; Correll, 1998). Another potential problem arises when the relative content of nitrogen and phosphorus in lagoon water differs from that in the crop. In this case, NMPs that are designed to meet the nitrogen requirement for crops may result in the over-application of phosphorus. Conversely, NMPs based on crop phosphorus needs may significantly reduce the lagoon water application rates, and thus require nitrogen fertilizers to meet plant needs.

The biogeochemistry of nutrients at NMP sites can be quite complex. For example, Figure 1.1 shows a schematic of the processes and nitrogen species that are involved in the nitrogen cycle. The most important inorganic forms of nitrogen are ammonium ions ( $\text{NH}_4^+$ ), ammonia gas ( $\text{NH}_3$ ), nitrite ( $\text{NO}_2^-$ ), nitrate ( $\text{NO}_3^-$ ), nitrogen gas ( $\text{N}_2$ ), nitrous oxide ( $\text{N}_2\text{O}$ ), and nitric oxide (NO). Organic nitrogen compounds in lagoon water occur as urea, amino acids, amines, purines, and pyrimidines, as well as a fraction of the dry weight of plants, microorganisms, detritus, and soils. Organic and inorganic forms of nitrogen are continually involved in biogeochemical transformations. The major processes involved in the nitrogen cycle are ammonification (mineralization of organic nitrogen to ammonium), nitrification (oxidation of ammonia to nitrate), denitrification (reduction of nitrate to nitrogen gas), nitrogen fixation (reduction of nitrogen gas to ammonia), nitrogen assimilation (conversion of inorganic nitrogen to organic forms), and nitrogen volatilization (conversion of ammonium ion to ammonia gas).

The biogeochemistry of phosphorus at NMP sites is also very complex. Most phosphorus (63 to 92%) in manure and lagoon water occurs in inorganic forms (Sharpley and Moyer, 2000). Bohn et al. (1985) presents a speciation diagram of phosphorus species of dissolved orthophosphoric acid ( $\text{H}_3\text{PO}_4$ )

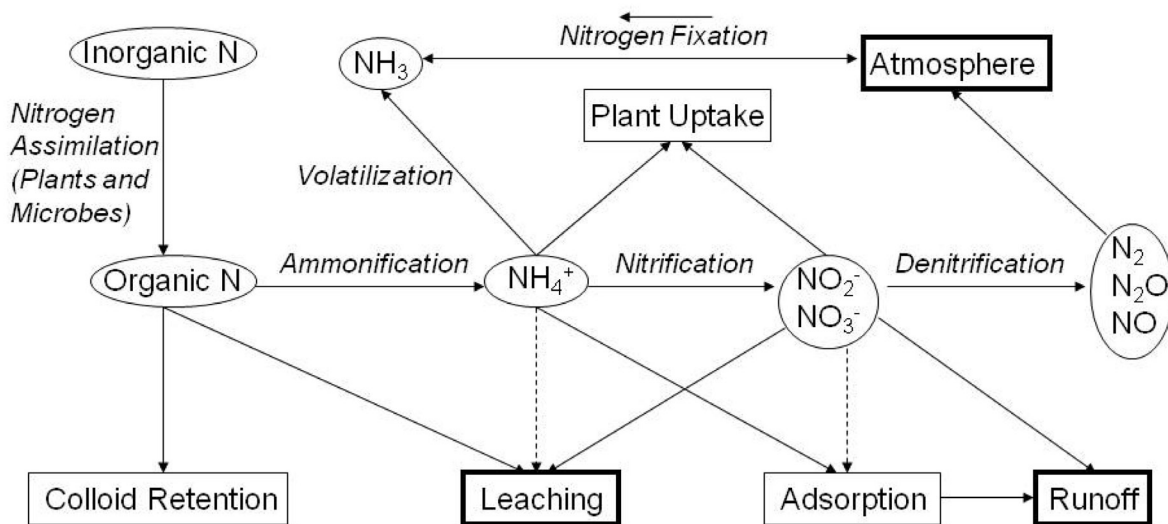


**Figure 1.1.** A schematic of the processes and nitrogen species that are involved in the nitrogen cycle. Important inorganic forms of nitrogen are ammonium ions ( $\text{NH}_4^+$ ), ammonia gas ( $\text{NH}_3$ ), nitrite ( $\text{NO}_2^-$ ), nitrate ( $\text{NO}_3^-$ ), nitrogen gas ( $\text{N}_2$ ), nitrous oxide ( $\text{N}_2\text{O}$ ), and nitric oxide ( $\text{NO}$ ). The dashed lines denote secondary transport processes.

as a function of pH. The three acid dissociation constants for  $\text{H}_3\text{PO}_4$  at  $25^\circ\text{C}$  are  $7.5 \times 10^{-3}$  ( $\text{pK}_{a1}=2.1$ ),  $6.2 \times 10^{-8}$  ( $\text{pK}_{a2}=7.2$ ), and  $5.0 \times 10^{-13}$  ( $\text{pK}_{a3}=12.3$ ). The dominant phosphate species in the pH range of 2.1-7.2 is  $\text{H}_2\text{PO}_4^-$ , whereas  $\text{HPO}_4^{2-}$  is the main species in the pH range of 7.2-12.3. Both of these species are available for plant uptake. Phosphorus, however, forms complex minerals with many elements (Arai and Sparks, 2007). For example, phosphorus species frequently precipitate out of solution with calcium, iron, and aluminum ions (Yeoman et al., 1988; Moore and Reddy, 1994). Furthermore, phosphorus species can strongly adsorb to positively charged surfaces in soils (Torkzaban et al., 2006b; Arai and Sparks, 2007), such as on metal oxide surfaces and clay edges. The solubility of phosphorus in soil solution is, therefore, a complex function of biogeochemical variables and processes such as pH, oxidation-reduction potential, the concentrations of cations (such as  $\text{Ca}^{2+}$ ,  $\text{Mg}^{2+}$ ,  $\text{Al}^{3+}$ , and  $\text{Fe}^{3+}$ ) and phosphorus species, soil mineralogy and organic matter content, and the mineralization rate of organic (manure) compounds (Moore and Reddy, 1994; Sharpley, 1995;

Arai and Sparks, 2007). Measurements of total phosphorus in soils may, therefore, not accurately assess the potential for plant uptake of phosphorus and the potential for subsurface transport losses (Brock et al., 2007).

The subsurface fate of nutrient species at NMP sites depends on a variety of transport and mass transfer processes. For example, dissolved inorganic nitrogen ions such as ammonium, nitrite, and nitrate can be transported with flowing water (advection), as well as by diffusive and dispersive solute fluxes. Interface mass transfer processes may play important roles between dissolved nitrogen species and soil/sediment surfaces (e.g., sorption/desorption of ammonium) or the air phase (e.g., volatilization of ammonia), and uptake of nitrogen species by plants and microorganisms is anticipated. The presence of colloidal forms (manure suspension) containing organic nitrogen and phosphorus that are mobile in the water phase provide another nutrient transport pathway.

Environmental losses of nutrient species that are primarily associated with the solid

phase (such as ammonium and phosphorus) will occur mainly in conjunction with high sediment loads during surface water runoff (Sims et al., 1998; Correll, 1998). For a well designed NMP that is conducted on most mineral soils, little leaching and subsurface transport of phosphorus is expected. Sims et al. (1998), however, review the literature that indicates that phosphorus species may also be leached through soils under certain environmental conditions (e.g., deep sandy soils, high organic matter soils, or soils with high soil phosphorus concentrations from long-term over fertilization and/or excessive use of organic wastes). Pautler and Sims (2000) suggested that the degree of phosphorus saturation, DPS (defined as the ratio of the amount of phosphorus sorbed by the soil to the phosphorus sorption capacity), is a better indicator for the potential losses to subsurface transport than the total phosphorus. Increased addition of manure has been reported to nonlinearly increase the phosphorus sorption capacity of the soil (Brock et al., 2007). When the DPS was greater than around 30%, phosphorus transport from soils increased dramatically (Brock et al., 2007).

### ***Pathogen Transport***

The root and vadose zones at NMP application sites play a critical role in protecting water supplies from pathogen contamination. Effective treatment relies on the retention and inactivation of pathogens in unsaturated or variably saturated porous media. Inactivation of pathogenic microorganisms is commonly assumed to occur within 60 d, although many viruses and protozoa are known to be viable for a longer duration (Schijven et al., 2006). Considerable research has been devoted to the fate and transport of microorganisms and other colloids in porous media (reviews are given by Herzig et al., 1970, McDowell-Boyer et al., 1986; McCarthy and Zachara, 1989, Ryan and Elimelech, 1996; Khilar and Fogler, 1998; Schijven and Hassanizadeh, 2000; Harvey and Harms, 2002; Jin and Flury, 2002; Ginn et al., 2002; de Jonge et al.,

2004; DeNovio et al., 2004; Rockhold et al., 2004; Sen and Khilar, 2006; Tufenkji et al., 2006). Most of the published research pertains to saturated media, less is known about microbe transport and retention in unsaturated systems (Wan and Wilson, 1994b; Choi and Corapcioglu, 1997; Wan and Tokunaga, 1997; Schafer et al., 1998ab; Saiers et al., 2003; Saiers and Lenhart, 2003; de Jonge et al., 2004; DeNovio et al., 2004). Below we briefly review the literature about processes and factors that will potentially influence the transport and fate of pathogens and surrogates (indicator microorganisms, latex microspheres, and other colloids) at NMP sites.

Microorganism retention mechanisms in the vadose zone are more complicated than in the saturated zone mainly due to the presence of air in the system. In unsaturated porous media water flow is restricted by capillary forces to the smaller regions of the pore space and flow rates are relatively small. Microorganism transport may be influenced by increased attachment to the solid-water interface (Chu et al., 2001; Lance and Gerba, 1984; Torkzaban et al. 2006a), attachment to the air-water interface (Wan and Wilson, 1994ab; Schafer et al., 1998b; Torkzaban et al., 2006b), straining of microorganisms near multiple interfaces in the smallest regions of the pore space (McDowell-Boyer et al., 1986; Cushing and Lawler, 1998; Bradford et al., 2006a), film straining in water films enveloping the solid phase (Wan and Tokunaga, 1997; Saiers and Lenhart, 2003), and retention at the solid-air-water triple point (Crist et al., 2004 and 2005; Chen and Flury, 2005; Zevi et al., 2005; Steenhuis et al., 2006). Transients in water content and composition during infiltration and drainage processes can also significantly influence these unsaturated retention mechanisms (Saiers et al., 2003; Saiers and Lenhart, 2003; Torkzaban et al., 2006b).

Size exclusion affects the mobility of microorganisms in the vadose zone by constraining

them to more conductive flow domains and larger pore networks that are physically accessible (Ryan and Elimelech, 1996; Ginn, 2002). As a result, microbes can be transported faster than a conservative solute tracer (Cumbie and McKay, 1999; and Harter et al., 2000; Bradford et al., 2003). Differences in the dispersive flux for microbes and a conservative solute tracer may also occur as a result of size exclusion (Sinton et al., 2000; Bradford et al., 2002).

Various combinations of well, surface, and lagoon water, encompassing a range in solution chemistry, are used for irrigation at NMP sites. Many chemical factors (i.e., pH, ionic strength, surface charge, etc.) are known to influence the transport behavior of pathogens. For example, using colloids as pathogen models, colloids are stabilized when the electrical double layers are expanded and when the net particle charge does not equal zero (Ouyang et al., 1996). Increasing electrolyte concentration and ionic strength decreases the double layer thickness and thereby promotes aggregation and microorganism-porous medium interactions. Aggregation will in turn impact the colloid size distribution and therefore straining. Aqueous phase pH influences the net microorganism and solid surface charge by changing pH-dependent surface charge sites. McCarthy and Zachara (1989) reported that colloids can be produced through disaggregation when the ion balance is shifted from one dominated by  $\text{Ca}^{2+}$  to one dominated by  $\text{Na}^+$ . These chemical factors (pH, ionic strength, surface charge, and chemical composition) are also known to influence soil structure (disaggregation) and pore size distribution (shrinking and swelling) when the soil contains clays and other colloidal materials (Ayers and Westcot, 1989).

Most transport experiments with pathogens have been conducted in the absence of dissolved manure suspensions. Pathogens in lagoon water, however, constitute only a small portion of the colloidal suspension.

Large quantities of manure components are also present. Several researchers have examined the influence of organic matter or manure suspensions on microbe transport. Some researchers reported that dissolved organic matter (DOM) or manure suspensions enhanced microbe transport (Johnson and Logan, 1996; Pieper et al., 1997; Powelson and Mills, 2001; Guber et al., 2005ab; Bradford et al., 2006cd). Blocking of favorable attachment sites by organic matter has typically been used to explain this enhanced transport (Johnson and Logan, 1996; Pieper et al., 1997; Guber et al., 2005ab), although filling of straining sites provides an alternative explanation (Bradford et al., 2006c). Dissolved organic matter has also been reported to sorb onto bacterial cell walls and alter their electrophoretic mobility (Gerritson and Bradley, 1987). Increasing the negative charge of the bacterial surface diminishes its attachment onto negatively charged solid surfaces (Sharma et al., 1985). Other researchers have reported that organic matter inhibits microbe transport due to hydrophobic interactions between microbe and grain surfaces that are coated with organic matter (Bales et al., 1993). Adsorption of pathogens onto mobile manure colloids could also facilitate their transport potential (Jin et al., 2000; de Jonge et al., 2004).

Many microbiological factors will also play important roles in pathogen migration at NMP sites. Microbe growth, death, and inactivation are of special importance. The ability of many pathogens to survive in manure (Wang et al., 1996), lagoon water (Ibekwe et al., 2003), and soil (Gagliardi and Karns, 2000 and 2002) has been well documented. The survival and subsequent transport of viruses have also been reported to be enhanced in the presence of manure suspensions (Bradford et al., 2006d), likely due to sorption of organic components onto metal oxide surfaces that would otherwise inactivate the viruses (Sagripanti et al., 1993; Pieper et al., 1997; Schijven et al., 1999; Chu et al., 2001; and

Ryan et al., 2002). Some microbes can also alter their surface characteristics and surrounding environment so as to promote attachment or release (detachment) (Ginn et al., 2002). Other mobile microbes possess the ability to move in the direction of increasing concentration gradient of chemoattractants or a decreasing concentration gradient of chemorepellents (Nelson and Ginn, 2001). Many of these microbiological processes are expected to be strongly coupled with temperature and nutrient conditions at NMP sites.

### Treatments

Figure 1.2 presents a flowchart that illustrates the potential steps that may be used to assess and improve the performance of lagoon water application sites. To determine whether the reuse of CAFO wastewater on agricultural lands poses an acceptable environmental risk, it is necessary to monitor the transport and fate of relevant contaminants at these sites. At

present, land application of CAFO lagoon water is based upon a nutrient balance. As mentioned earlier, other potential contaminants of concern at NMP sites include salts, heavy metals, pathogens, antibiotics, and hormones. If the risk (measured concentration of a particular contaminant below or in the root zone) is deemed to be unacceptable, then management practices for animals will have to be modified and/or wastewater treatment will have to be implemented before this water can be used in NMPs. Based on current technologies and associated costs, it is not practical for this level of monitoring to be done for typical farm operations. Additional field research is, therefore, needed to determine appropriate contaminant loadings for effective NMPs, and to assess whether additional treatment steps are needed. Below we discuss potential tools, treatments, and management practices that may be needed.

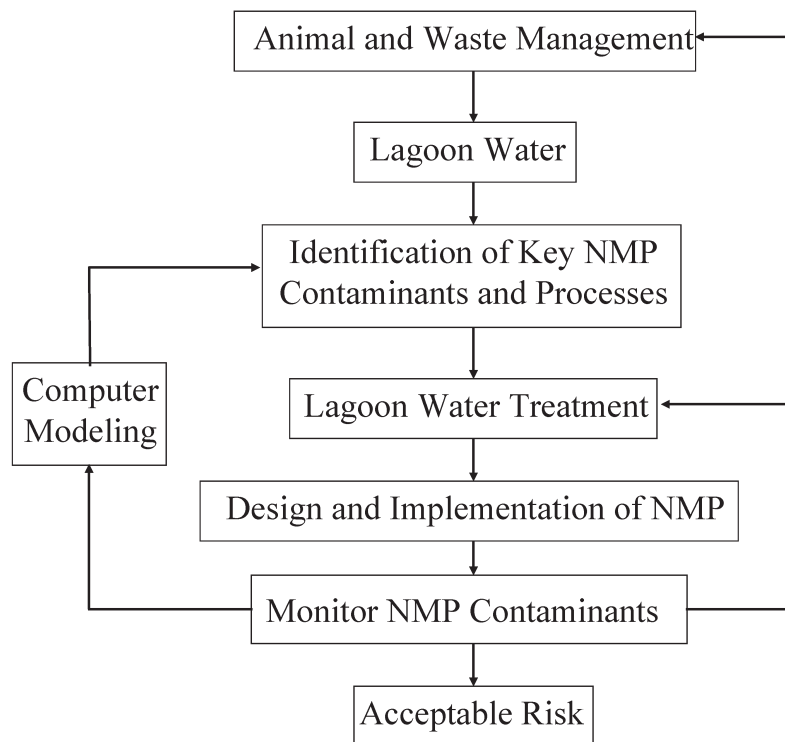


**Figure 1.2.** A flowchart that illustrates the steps that may be used to assess and improve the performance of lagoon water application sites.

Computer models are valuable tools that can be used by researchers to study the transport and fate of lagoon water contaminants under various environmentally relevant scenarios that are found at NMP sites. Conventional models for contaminant transport are based upon solution of mass conservation equations for flowing water (Richards equation) and solute transport (advection-dispersion equation), subject to a variety of equilibrium or kinetic reactions (e.g., Šimůnek et al., 2009). Improved NMPs could potentially be designed with the aid of computer models to maximize desirable effects such as nutrient uptake by plants, soil retention of pathogens, and to minimize the leaching and/or runoff of contaminants.

To efficiently utilize CAFO lagoon water and diminish the potential of manure contaminants to be transported to groundwater and surface water bodies it is essential to plan and implement proper management. Manipulation of animal diet and veterinary practices are likely to be some of the most simple and cost effective ways to minimize the potential release of some contaminants into the environment. For example, it has been reported that changing cattle diet from grain to forage will reduce the numbers of pathogenic *E. coli* O157:H7 in cattle manure (Russell et al., 2000; Callaway et al., 2003). Selection of CAFO locations away from vulnerable water resources such as shallow water tables and surface water, and on soils with relatively little structure and moderate infiltration rates are other common sense practices to minimize the potential for water contamination. Sufficient agricultural land should also be located adjacent to CAFOs so that the manure and lagoon water that is generated may be applied to these lands at agronomic rates. Actions to further avoid water resource contamination may include: proper timing of lagoon water application (not during rainy seasons); leveling the CAFO facilities to a small incline towards a draining conduit and channeling runoff water to a designated storage reservoir (lagoon);

and avoiding manure accumulation on CAFO grounds, especially during rainy seasons.

Physical separation is commonly used as an effective pretreatment method to reduce the organic load to CAFO wastewater and therefore decrease nutrient and pathogen concentrations in lagoons. Separation methods to remove organic solids from the wastewater include using stationary inclined screens, vibrating screens, rotary screens, a horizontal decanter centrifuge, hydrocyclone, as well as roller, belt, and screw presses (Zhang and Westerman, 1997). The separated manure sludge may in turn have to be treated (composted) before it can be used as a soil amendment and as a source for nutrients.

Lagoons for CAFO wastewater storage act in a similar fashion as sedimentation basins in municipal wastewater treatment. Given sufficient retention time in lagoons, significant reductions in total suspended solids are expected (35-65%). Most lagoons operate anaerobically. Aerated lagoons have received less attention because of their higher costs and their increased potential of transferring reactive nitrogen to the atmosphere through volatilization of ammonia. However, the potential for decreased odor and increased nitrogen reduction might increase their use if economical treatment methods emerge to mitigate ammonia loss. Typically, CAFO wastewater storage in lagoons can reduce the amount of nitrogen by 30 to 75% through volatilization (depending on whether the lagoon is anaerobic or aerobic) (Svoboda, 1995; USEPA, 2001a). Phosphorus tends to be associated with the particulate fraction of lagoon water, and nitrogen and potassium are usually in dissolved form. Hence, as particles settle out of solution the lagoon sludge contains less nitrogen and potassium but more phosphorus than the lagoon liquid. Up to 80% of the phosphorus in lagoons can accumulate in bottom sludge (MWPS, 1993; Lander et al., 1998). The bottom of CAFO lagoons should be properly sealed to prevent

deep percolation of wastewater towards groundwater resources. Most states have regulations regarding permissible levels of percolation rates from lagoon storage systems. For example, regulations in Kansas stipulate that percolation rates should be less than 0.3-0.63 cm d<sup>-1</sup>.

Lagoon water from CAFOs may have to be adjusted to become a stable, balanced, and nutrient-rich product for reuse as irrigation water and fertilizer during implementation of NMPs. This may require active management and treatments that are not currently practiced on farms. Many municipal wastewater treatment techniques may be applied to CAFO wastewater (Zhang and Lei, 1998; Chastain et al., 2001; Vanotti et al., 2005ab; Loughrin et al., 2006). For example, chemical treatments may be used to promote flocculation of particles by neutralizing the electrostatic forces that keep them apart, causing the particles to form aggregate flakes (flocs) that rapidly settle out of solution. Commonly used flocculants include various salts of multivalent cations such as aluminum, iron, calcium or magnesium, and/or long-chain polymers (Dobias, 1993). Other factors such as pH, temperature, aeration, and salinity can be controlled to induce flocculation (Lindeburg, 2001). Given optimum amounts of chemical additives and sufficient settling time, flocs will form and settle out of solution to clarify wastewater. Chemical flocculation treatments involve equipment, chemicals, and maintenance that are not typically found on CAFOs. Vanotti and Hunt (1999) and Vanotti et al. (2002) estimated it would cost an additional \$1.27 to \$2.79 per finished hog to remove 90-95% of the suspended solids in swine lagoon water using chemical treatments. Additional research is needed to assess whether such approaches will be economically viable to implement.

Alternatively, it may also be possible to adapt a variety of low cost soil treatments for wastewater to remove excess amounts

of organics, nutrients, pathogens, and other contaminants in CAFO lagoon water. Potential soil treatments for wastewater include: infiltration ponds and galleries, sand filtration, and subsurface flow wetlands (Schijven and Hassanizadeh, 2000; Tufenkji et al., 2002; Ray et al., 2002; Hunt et al., 2002; Weiss et al., 2005). Treatment by passage through sands can provide a physical treatment for particles in wastewater due to size limitations imposed by the pore sizes (Bradford et al., 2006a), but also provides solid-water and air-water interfaces where chemical and microbiological reactions and transformations may occur (Tufenkji et al., 2002). Furthermore, proper selection and design of the solid surface chemistry of the porous media can be used to target the retention and/or degradation of specific contaminants of interest. For example, metal oxide coatings on solid surfaces can be created to adsorb and/or inactivate a variety of microbial pathogens, as well as inorganic and organic compounds (Joshi and Chaudhuri, 1996; Ahammed and Chaudhuri, 1999). Soil treatment forms the theoretical basis for many permeable reactive barrier technologies that have been developed and applied to treat contaminated groundwater plumes (Gu et al., 1999; Benner et al., 1999; Scherer et al., 2000; Waybrant et al., 2002). The collected CAFO wastewater effluent from soil treatment could in turn be used in NMPs to irrigate agricultural lands with mitigated risk to the environment.

Maintaining soil and groundwater quality is the key to the long-term successful use of NMPs. If leaching is inadequate, then dissolved salts will concentrate and accumulate in soil profiles when irrigation water that is applied to crops subsequently returns to the atmosphere via evapotranspiration. The total dissolved solids of CAFO wastewater typically range between 1500 to 3500 mg L<sup>-1</sup>, equivalent to electrical conductivity levels of 2.4-5.5 dS m<sup>-1</sup>. Salt, sodium, and osmotic effects of salinity can restrict crop establishment and growth due to changes in soil

physical structure, tillage, infiltration and permeability, sodium toxicity, and salt accumulation (Ayers and Westcot, 1989; Chang et al., 1991). Selective use of gypsum, aggregate stability imparted by crops, direct seeding of crops, and careful irrigation timing of lagoon water application under a site-specific management regime are potential methods that may be used to ameliorate the negative effects of CAFO lagoon waters on soil and groundwater quality (Ayers and Westcot, 1989). Salt deposits can also be flushed away by adding excess amounts of fresh water, but at a significant cost (Bouwer, 2002). Furthermore, desalination of wastewater and removing the excess salt to the ocean can cost up to \$2 per 1000 L. Selection of salt-tolerant crops and timing of nutrient application are, therefore, important considerations for NMPs. The salt tolerance characteristics of various crops are provided in Ayers and Westcot (1989).

## 2.0

# Site Characterization for Detailed NMP Studies

### Background

Field research was designed to study the transport and fate of nutrients and indicator microorganisms at a NMP site. To achieve a high level of confidence in the water flow and solute transport behavior at this site, detailed information on the associated soil properties was required and is discussed in this chapter. The first phase of our approach was site selection. Since the transport and fate of nutrients and microorganisms in the vadose zone are very complex processes (Bradford et al., 2008; Bradford and Torkzaban, 2008) measurements of the apparent soil electrical conductivity were used to select a highly uniform location in a 4 ha field to reduce the level of complexity and uncertainty. The second phase of our approach involved an initial site characterization to identify the soil stratigraphy, approximate particle size distribution, and bulk density information on soil cores and pits. Results revealed that a uniform layer of sandy loam was situated from the surface down to a depth of about -70 cm, followed by a white sand layer (-70 to -80 cm). The deeper profile (less than -80 cm) was characterized by a sandy loam layer, which incorporated various sand and clay lenses at different depths. In the third stage, pedotransfer functions and interpolation algorithms were used to generate an initial conceptual model about the soil profile, including initial estimates of hydraulic properties (soft data). This conceptual model guided the selection location for undisturbed cores that capture the dominant water flow behavior under study.

The hydraulic properties of and conservative solute transport in undisturbed core samples were subsequently measured in the laboratory (hard data) and used to further refine the

conceptual model of the site properties. The next phase of site characterization was field validation of the conceptual model of the soil hydraulic and solute transport properties. Water flow and solute transport experiments were used for this purpose, and to ensure good agreement between measured and simulated data. A feedback between field experiments and computer simulations was used to identify locations in the field where additional measurements or computer simulations were needed to improve the conceptual model and level of understanding at the site.

### Materials and Methods

A mobile remote electromagnetic induction sensor system (Geonics EM-38DD) was used to measure the apparent soil electrical conductivity ( $EC_a$ ) across a 4 ha field (Corwin and Lesch, 2005a). This system includes two EM-38 units synchronized to operate simultaneously, enabling measurements of both vertical and horizontal dipole conductivity. Data was collected following the protocols of Corwin and Lesch (2005b) to generate an approximately 5x5 m grid  $EC_a$  map of our field site. The map coordinates were determined using a global positioning system (GPS).

Selection of our experimental field plot for nitrate and microorganism transport studies was based upon the generated  $EC_a$  map. The agricultural field in San Jacinto, CA (33°50'22" North, 117°00'46" West) was chosen for this purpose because it was associated with minimal spatial variability in  $EC_a$  readings, which implies relatively low heterogeneity in soil texture. The experimental plot is located next to a dry river bed and has a shallow perched water table at a depth of -220 cm.

The experimental site consisted of two 6x6 m plots (Figure 2.1). At the corners of each plot a backhoe was used to expose the soil profile and to install 120-cm diameter by 220-cm long culvert pipes vertically into the soil (Figure 2.1 - circles marked with letters). Soil profiles in each culvert pipe hole were photographed and notes on soil stratification were taken before installing each culvert pipe. Each culvert pipe was instrumented with 6 tensiometers and 6 solution samplers to measure the soil water pressure and to extract soil solution with depth. Tensiometers and solution samplers (90 cm in length) were installed radially from the culvert pipe into the undisturbed soil profile (parallel to the soil surface). A staggered configuration of the sensors in the culvert pipe was selected to minimize the potential for preferential flow and interference from other sensors, and to maximize the area of the profile that was sampled (Figure 2.1). The arc in Figure 2.1 represents the area of water potential and soil solution sampling. Pressure transducers (MPX2100DP, Motorola LTD., Denver, Colorado) and a data logger (CR7, Campbell Scientific, Inc., Logan, Utah) recorded the tensiometer readings every

15 min. Five neutron access tubes (220 cm long) were installed vertically on each plot (Figure 2.1 - circle marked with Roman numerals). The water content with depth at desired times was determined using a neutron probe (503-DRHYDROPROBE®, CPN, Martinez, CA) and an established calibration curve in this soil profile.

To minimize the sampling time of the solution samplers, it was necessary to increase the water flux through the soil solution sampler. This was accomplished by replacing the traditional ceramic cup with filter paper (MF-0.45  $\mu\text{m}$ , Millipore, Billerica, MA) that had a high saturated conductivity ( $60 \text{ cm}\cdot\text{h}^{-1}$ ) and a small thickness (180  $\mu\text{m}$ ).

The instantaneous profile method (Watson, 1966) was used to evaluate the hydraulic conductivity of the upper 60 cm of the profile at the field site. This method uses simultaneous measurements of the volumetric water content ( $\theta$ ) and soil water pressure head ( $h$ ) in a soil profile during the course of drainage to determine the hydraulic conductivity.

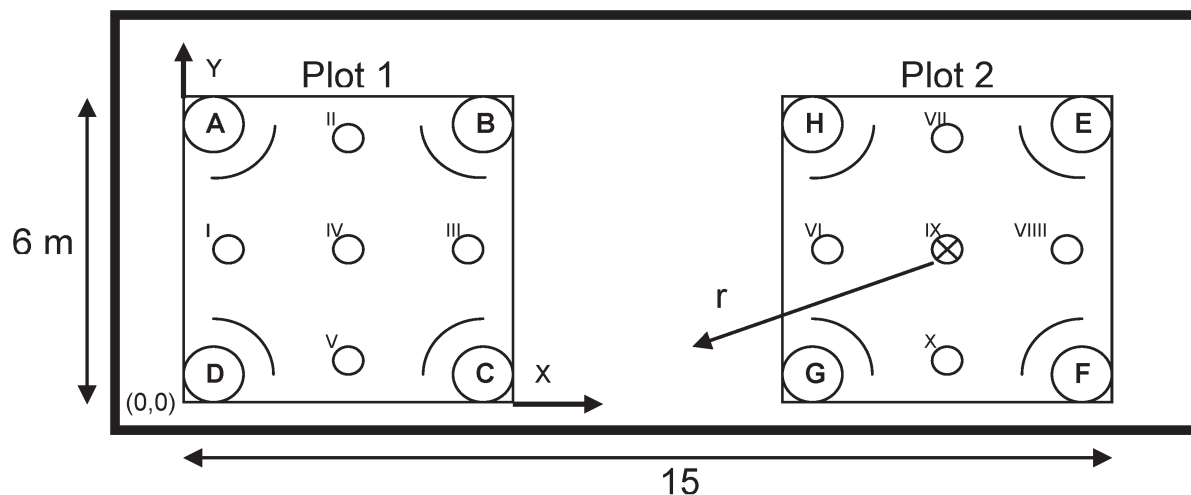


**Figure 2.1.** A schematic of the field site. Squares represent two 6x6 m plots. Circles with letters are vertical culvert pipes (120 cm diameter by 220 cm long) installed with six tensiometers. Circles with roman numerals are vertical neutron probe access tubes. Arcs represent the area of water potential sampling. The crossed circle in the center of Plot 2 denotes the origin of a radial axis ( $r$ ).

An additional set of  $\theta$  and  $h$  data was measured near saturation ( $h= 0$  to  $-30$  cm) during redistribution of water immediately after ponded infiltration ceased (Hillel, 1998). In this case the value of  $\theta$  was acquired using a time domain reflectometry (TDR) system (Trase system, Soilmoisture Equip. Corp., Santa Barbara, CA) as well as gravimetrically, and  $h$  was monitored with a tensiometer (Tensimeter, Soil Measurement Systems, Tucson, AZ).

A step pulse conservative tracer (Potassium Bromide, KBr) experiment was conducted under steady-state water flow on bare soil at the plot, after plowing the upper 20 cm of the soil. We employed a 0.2 x 0.2 m staggered grid drip irrigation system (Typhoon 630, Netafim, Fresno, CA) to uniformly apply small water and solute fluxes to the soil surface that induced unsaturated flow conditions in the upper 120 cm of the soil profile. The surface boundary condition was a steady infiltration rate of  $0.275 \pm 0.025$  cm·h<sup>-1</sup>. The soil surface was covered with a black nylon tarp to avoid water evaporation during the tracer experiment.

When a steady-state water flow condition was established in the soil profile after 100 h, the water application system was switched between well water to a step pulse of KBr solution for 47 h and then switched back to well water for an additional 280 h. The KBr solution had 2.4 g·L<sup>-1</sup> Br, and was mixed well before and during application. Soil solution samples were collected over an interval of 24 h and analyzed for Br concentration with a Colorimetric system (O.I. Analytical, Flow Solution IV, College Station, Texas). The Br data from the field is presented at the median time of the sampling interval.

Additional information was collected to evaluate the transverse dispersivity in the root zone (0 to -60 cm) and the effect of non-uniform upper boundary condition on the soil water and bromide application uniformity. These experiments are described in detail in Segal et al. (2009).

Undisturbed cores from the experimental site were collected for measurements of bulk density ( $\rho_b$ ), hydraulic properties, and conservative solute transport. Details on these experiments and results are provided in Segal et al. (2008 and 2009).

The HYDRUS-2D code (Šimůnek et al., 1999) was used to simulate the water flow in the upper profile during steady-state infiltration and drainage experiments. Other simulations were conducted to determine the lateral water flux that may occur directly above or through the sand layer relative to the vertical surface water flux. The two-dimensional water flow and bromide transport at the field site during the tracer experiment under a non-uniform top boundary condition (drip) and when considering a heterogeneous distribution of hydraulic properties in the lower profile (depths <-80 cm) was also simulated using this model. Details on the simulation conditions and parameters are in Segal et al. (2008, 2009).

## Results and Discussion

### *Soft Data*

In this section we discuss the use of soft data to select a location for flow and transport studies and to develop a conceptual model of the soil hydraulic properties at this field site.

Electromagnetic induction technology was employed to quantify the field spatial variability of  $EC_a$ . Figure 2.2 shows a map of the vertical component of  $EC_a$ . The experimental study site was selected from this soft  $EC_a$  data to be located in a “relatively uniform” section of the field with low  $EC_a$  values (coarser textured material) as indicated in Figure 2.2.

Our initial conceptual model of the soil profile stratigraphy at the experimental site was developed from photographic information (Segal et al., 2008). The particle size distribution (PSD) and bulk density data (Segal et al., 2008) were used in conjunction with the ROSETTA program to estimate values of saturated hydraulic conductivity ( $K_s$ ) at sampled

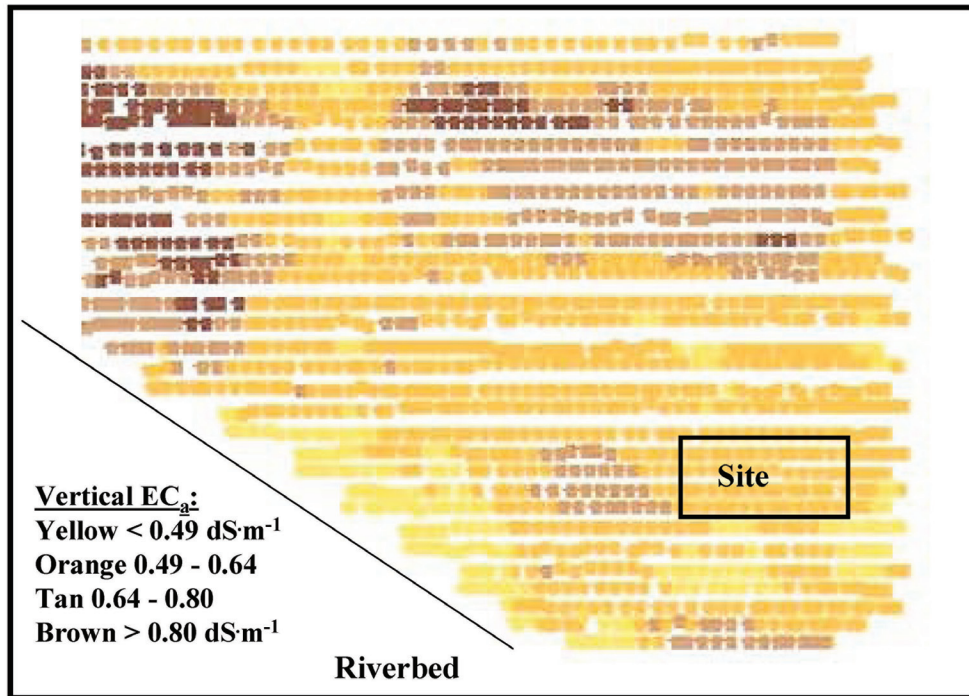


**Figure 2.2.** A 4 ha map of the vertical component of the apparent soil electrical conductivity in the field as measured using a mobile remote electromagnetic induction sensor system on a 5x5 m grid.

locations. The nearest neighbor algorithm was then used to interpolate values of  $K_s$  at other locations that were not sampled. Figure 2.3 presents the estimated values of  $K_s$  on north-south and east-west transects of the plot. The dark uniform layer between the soil surface and -70 cm was the cultivated layer. The light-colored thin layer underneath the cultivated layer was the sandy layer (-70 to -80 cm). The lower soil profile (-80 cm to -210 cm) was scattered with multiple lenses of different texture. The data can be further analyzed in terms of one-dimensional vertical conductivity (Segal et al., 2008).

#### **Hard Data**

The soft data discussed above provided valuable information that was used to guide our strategy for collecting additional hard data in the field and the laboratory. This hard data was used to further refine our conceptual model and to improve our quantification of key soil hydraulic properties at the field site. Furthermore, comparison of field and laboratory data was used to identify potential

limitations of the various types of hard data, and to assess the predicted hydraulic properties that were estimated from the soft data.

Undisturbed cores were collected for hydraulic property analysis at several locations in the root zone (0 to -70 cm), at the capillary barrier (sand layer), and in the lower profile (below -80 cm). These sampling locations were chosen to improve our understanding of water flow in areas of the site where distinct differences in estimated soil hydraulic properties were identified (soft data shown in Figure 2.3). The fitted hydraulic model parameters to the measured soil core data are provided in Table 2.1.

Field data collected during steady-state infiltration and redistribution were analyzed using the instantaneous profile method to determine hydraulic properties at depths of -30 and -60 cm. Analysis of the entire profile with this method was not possible due to the layering at the site, which violated an assumption of this approach (no lateral flow).

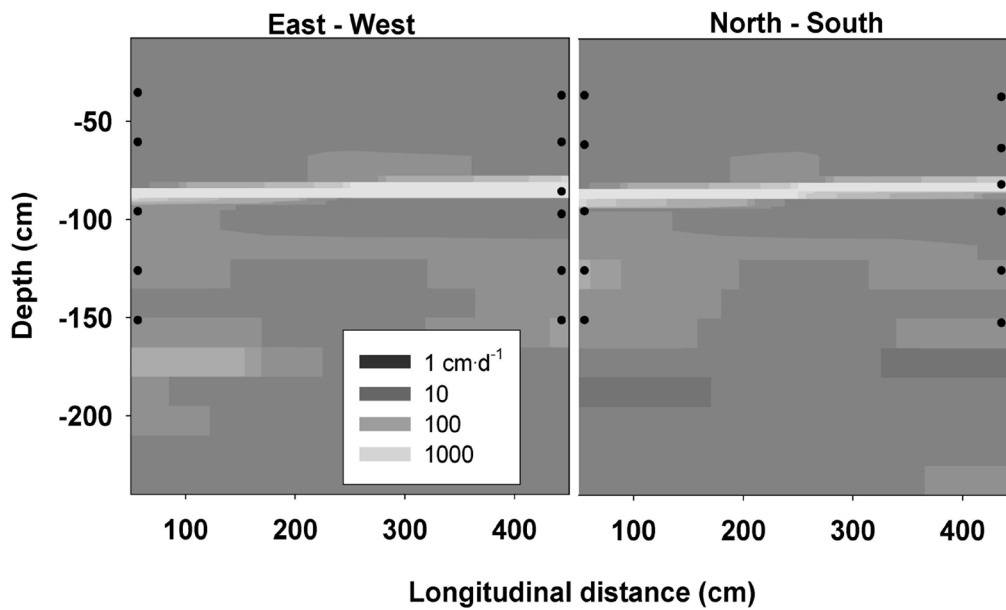


**Figure 2.3.** North-south and east-west transects of estimated values of  $K_s$  on plot 1. These transects were generated from a three dimensional map of  $K_s$  that was estimated using particle size distribution and bulk density data from locations I-V using ROSETTA, and the nearest neighbor interpolation algorithm. Circles represent the undisturbed core sampling locations.

Fitted field-scale hydraulic properties parameters also are presented in Table 2.1. Field and laboratory values of  $h(S_e)$  matched reasonably well. In contrast, field and laboratory values of  $h$  showed considerable dissimilarity

and revealed limitations of using only lab information to described field-scale hydraulic properties. A potential explanation for this difference could be entrapped air in the field.

**Table 2.1.** The hydraulic properties ( $\theta_s$  is the saturated water content;  $\theta_r$  is the residual water content;  $\alpha$  is the reciprocal of the air entry pressure; and  $n$  is the pore size distribution parameter of the van Genuchten model) of the three major layers in the upper soil profile of the field plot. Soft data was estimated from particle size distribution and bulk density data using the ROSETTA program. Hard data was measured on undisturbed core samples using the multistep outflow, pressure plate, and constant head permeameter techniques or from TDR readings in the field site.

Hydraulic property	Layer 1 Sandy loam 0 to -70cm		Layer 2 Sand -70 to -80cm		Layer 3 Silt loam -80 to -90cm	
	Soft data	Hard data	Soft data	Hard data	Soft data	Hard data
$K_s$ (cm.h <sup>-1</sup> )	1.95	5	9.25	71.2	1.4	1.6
$\theta_s$	0.37	0.43	0.35	0.33	0.41	0.45
$\theta_r$	0.033	0.03	0.04	0.01	0.056	0.04
$\alpha$ (cm <sup>-1</sup> )	0.018	0.0085	0.042	0.016	0.0047	0.007
$n$	1.45	1.6	2.41	1.96	1.70	1.57

### **Validation and Simulations**

In this section we compare soft and hard estimates of hydraulic properties from several locations in the field. Numerical simulations were subsequently conducted to independently “validate” our field scale hydraulic properties where possible, and to further improve our understanding of water flow at specific locations in the field. Moreover, the reliability of using soft and hard data as input for simulations of water flow was demonstrated.

Table 2.1 presents a comparison between the hydraulic properties generated from soft and hard data. This information was obtained for three layers in the upper soil profile of the field site (0 to -70 cm; -70 to -80 cm; and -80 to -90 cm). In general, soft and hard estimates of the hydraulic properties for the silt loam layer were very consistent. In contrast, soft estimates of the hydraulic properties were poorer for the coarser textured sandy loam layer and especially the sand layer. In general, the soft data provides a reasonable prediction of soil textural characteristics, but that the specific magnitudes of the hydraulic properties are only approximately predicted. Hence, soft data may likely be used to infer trends in spatial variability in soil textural properties, but not to deterministically simulate water flow at the site. Observed and simulated steady-state water infiltration and redistribution in the relatively uniform upper soil profile (0 to -70 cm) support this statement (Segal et al., 2008). In this case, simulations which employed measured hydraulic properties as model input provided a better agreement of observed water flow and drainage. Nevertheless, simulations which employed the soft-data-derived hydraulic properties did capture the general water flow behavior and trends. Numerical modeling in conjunction with measured hydraulic properties also proved to be an effective tool to gain additional insight on field scale water flow. For example, we used numerical simulations to quantify the influence of water application

rate on the lateral water flux at a location of pronounced soil textural discontinuity in the field at a depth of -70 to -80 cm (Segal et al., 2008).

### **Bromide Travel Times**

The mean and standard deviation of the bromide travel time for each BTC is presented in Table 2.2, as well as average and variance of these values at each depth. Minor changes in the variance of the mean travel time were measured in the upper profile (-32 and -61 cm), due to high uniformity in soil texture and water content (Segal et al. 2008). In contrast, the variance significantly increased immediately below the sand layer (-95 cm). This high variability in travel time can be attributed to three reasons, namely: (i) the sand layer was associated with a lower water content and consequently a higher pore water velocity; (ii) low permeability lenses just below the sand layer caused lateral flow of Br; and (iii) variability in the soil permeability directly below the sand layer generated variability in water and bromide mass inputs.

The average standard deviation in travel time (Table 2.2) tended to increase with depth as expected due to dispersion. However, similar values occurred at -95 and -126 cm, likely due to greater variability in travel times at -95 cm. The ratio between the variance and the average values was much larger in the mean travel time than in the standard deviations of the travel times. This observation suggests that local scale effects on the BTCs were much less significant than plot scale factors.

### **Averaging of Bromide Transport**

The influence of soil heterogeneity, water content, and location of the solution samplers on the tracer data may be overcome by averaging the 4 collected samples at the same depth and time on a plot, and then analyzing the depth averaged bromide transport behavior. Bromide transport in the root zone and in the lower profile will be separately discussed in detail below due to the previously noted

**Table 2.2.** Mean and standard deviation of bromide travel time (units in hours,  $h$ ) at each sampling depth and culvert pipe location, and associated average and variance values for each depth.

Depth	-32 cm	-61 cm	-95 cm	-126 cm	-155 cm
Location	Estimated mean bromide travel time (h)				
A	82	120	280	190	250
B	64	110	160	265	250
C	75	130	200	210	300
D	NA	110	145	250	270
Average mean travel time (h)	73.6	117.5	196.2	228.7	267.5
Variance of mean travel time ( $h^2$ )	82.3	91.6	3656.2	1206.2	558.3

Depth	-32 cm	-61 cm	-95 cm	-126 cm	-155 cm
Location	Estimated standard deviation of bromide travel time (h)				
A	52	50	69	60	80
B	37	46	61	62	63
C	38	56	66	68	79
D	NA	46	62	66	76
Average standard deviation of travel time (h)	42	50	65	64	75
Variance of standard deviation of travel time ( $h^2$ )	70	22	13	13	62

differences in soil and water flow characteristics in these regions.

Observed field measurements of the depth averaged bromide transport data is presented in Figure 2.4. The average relative bromide concentration at a given time is denoted using filled circles for the -32 cm depth and with empty circles for the -61 cm depth. Integration of the area under the breakthrough curve provided very good mass balance at -32 and -61 cm (99.5-102%) which is presented in the figure. The vertical bars represent standard deviations and the horizontal bars represent the sampling time range. Standard deviations account for the inherent soil spatial variability, and the variable location of each solution sampler. The modeled breakthrough curves, based on the mobile-immobile (MIM) transport parameters evaluated in the laboratory, are also depicted in Figure 2.4. Additional information is provided in Segal et al. (2009). The modeled curves provide a reasonable prediction of the average measured

value of bromide at -32 and -61 cm and total Br recovery. In general, the attempt to independently predict the bromide transport in the root zone by using only laboratory derived model parameters was fairly successful at this scale. In addition, both one- and two-dimensional simulations (average value of a cross section at a specific depth and time) provided nearly an identical description of the data, indicating that the water flow and solute transport in the upper 60 cm of the soil profile could be described as a uniform one-dimensional process when using our drip irrigation setup and measured values of dispersivity.

The water flow and solute transport pattern in the lower profile (-70 to -200 cm) is much more complex than in the root zone (0 to -70 cm). In particular, the coarse sand layer at about -70 cm generates high water velocities and a lateral component to water flow (Segal et al. 2008). The presence of interconnected layers and fine textured lenses of variable thickness below -80 cm produce a

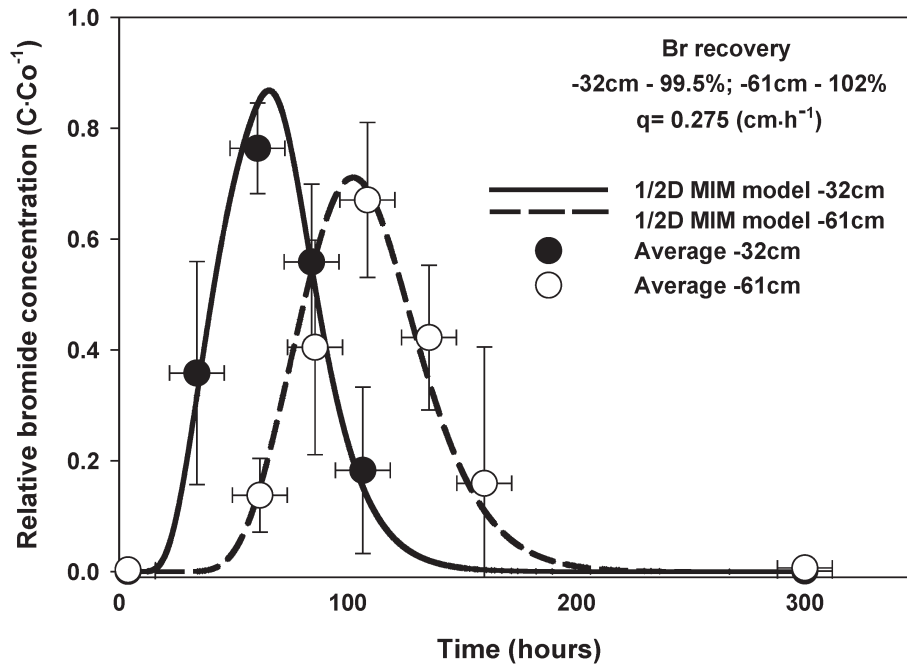


**Figure 2.4.** Field measurements of the relative bromide concentration over time for the bromide tracer experiment. Data is presented at two depths in the field plot, -32 and -61 cm (circles). Each data point is an average of the four locations at the same time and depth. The vertical bars are standard deviations and the horizontal bars represent the sampling time range. The corresponding 1D and 2D (depth averaged) MIM simulation results are also presented in this figure based on transport parameters derived from the undisturbed core.

location specific pattern of solute transport through the lower soil profile of the field plot. Two-dimensional solute transport simulations were conducted to study the relative importance of nonuniform boundary conditions and soil heterogeneity on solute transport in the lower profile. Results indicate that soil heterogeneity is the major contributor to solute transport behavior in the lower soil profile. Specifically, variations in bromide travel time and total mass suggested that the sand layer in conjunction with fine textured lenses slow down the bromide propagation and generates bypassing of water and solute through lower resistance pathways. Yet, the lower water velocities below this region (due to the raised water table) decrease the variability of the mean travel time (Table 2.2) and generate a more uniform Br front. This finding coupled with the fact that the exact soil type that is associated with a particular soil solution sampler is unknown, hampers the application of a

completely deterministic approach for describing solute transport in the lower profile.

Considering the above information, the bromide transport data in the lower profile is presented below in terms of the one-dimensional average concentration (4 sample locations) at a specific depth as a function of time. Figure 2.5 presents measured and simulated bromide breakthrough curves in the lower profile at -95, -126, -155 cm and the Br mass recovery under the BTCs. The horizontal bars are standard deviations of the concentration measurements. It should be mentioned that the one-dimensional modeling data that are presented in this figure were generated from a two-dimensional simulation that was averaged over a specific depth at a given time. A transect of spatially heterogeneous hydraulic properties was generated from measurements taken from the field plot that was used as input for this simulation (Figure 2.3). Good

agreement between measured and modeled data was found (Correlation coefficient above 84%). In general, travel time and mass balance of the average bromide concentration over depth is conserved (>88.4% bromide mass recovery). However, the observed and simulated standard deviations have the same order of magnitude as the average value, suggesting high variability of bromide at a specific depth and time.

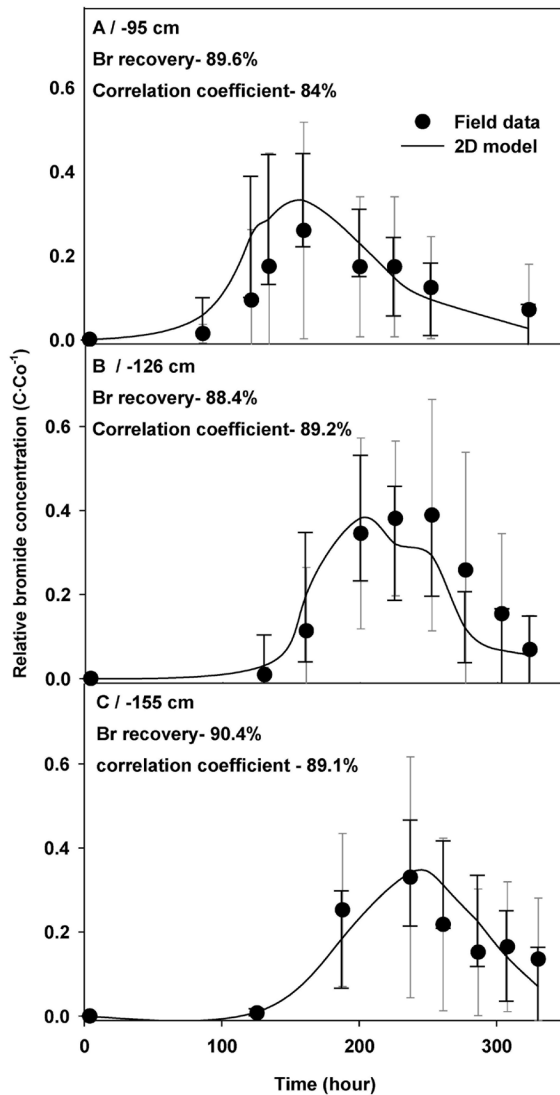


**Figure 2.5.** Field measurements (circle) and 2D-MIM simulation (lines and triangle) of relative bromide concentration over time at -95, -126 and -155 cm. Measured data is an average value from four sampling locations at the same time and depth. Simulated data is presented as an average value at these same depths. The horizontal bars are standard deviations.

# 3.0

## NMP Results - Nutrients

### Background

NMPs are designed to meet the water and nutrient needs of crops, while minimizing the loss of nutrients to surface water and groundwater (USEPA, 2003). However, researchers with the USEPA have observed significant migration of pollutants (e.g., nitrate) towards surface water and groundwater bodies at NMP sites (Hutchins and Bradford, 2005 - personal communication). These observations suggest that implementing a NMP based on current agronomic practices may not always protect the environment. The literature review (Chapter 1) indicates that potential problems with NMP implementation include: (i) inaccurate quantification of water and nutrient mass balances due to inadequate information on soil properties, climatic data, wastewater constituents or crop water and nutrient uptake rates; (ii) inherent spatial and temporal variability in soil properties, manure and nutrient distribution, irrigation uniformity, and crop growth; and (iii) NMP management constraints, such as quantifying the amount of water and wastewater application and managing the timing of the application. The objective of this study was to measure the fate of nitrogen, phosphorus, potassium and salts from land application of dairy wastewater under a well-designed and implemented NMP in a semi-arid environment. We also present key management practices that minimize the potential leaching of nutrients and salts toward groundwater.

### Materials and Methods

Traditional NMP studies have been conducted from an agronomic perspective to determine the impact of specific NMP factors on a given field. The statistical design for such experiments include blocks and random repetitions because the spatial variability of the field and application systems is typically unknown. In

contrast, our experiment was a process-based (mechanistic) study of flow and transport processes under NMP conditions. Accurate implementation of a process-based NMP requires the determination of water, salt and nutrient mass balances in the root zone, and the ability to quantify flow and transport processes. To collect this type of information requires the use of measurement tools such as weighing lysimeters, weather station, tensiometers and solution samplers with depth, and irrigation systems with a high level of uniformity and precision. The traditional agronomic design cannot achieve such high precision in measuring and implementing a NMP on each repetition due to economic constraints, and this further increases the variability of traditional NMP studies. Below we highlight the design of our process-based NMP that was needed to overcome the limitations of the traditional agronomic approach.

### Field

Our field site was located in San Jacinto, CA (33°50'22" North, 117°00'46" West) and was chosen to be in a relatively homogenous part of the field in order to minimize variability in soil hydraulic properties. This objective was achieved by acquiring preliminary information on the field soil spatial variability using a remote electromagnetic induction system (Segal et al., 2008). This procedure eliminated the need of repetitions scattered across the field in traditional agronomic NMP studies, and allowed us to focus on within plot variability. The experiment site was also chosen to have no recent history of CAFO wastewater application. The field was cultivated only during winter (triticale, TRICAL<sup>®</sup> Resource Seeds, Inc.) and manure was applied twice (the last manure application was three years prior to this experiment) during the last ten years prior to this experiment.

The experimental site consists of two 6 m × 6 m plots (Figure 3.1, more detailed description of the site is given in Segal et al., 2008 and 2009). Within plot variability was overcome by taking multiple measurements over depth at several locations within the plots. Briefly, one culvert pipe was installed at each corner of both plots (8 pipes total). Each pipe was instrumented with 6 tensiometers and 6 soil solution samplers installed over depth at approximately 30 cm intervals, which were installed 90 cm horizontally from the culvert pipe into the undisturbed soil profile. The staggered configuration of the sensors (represented by the arc in Figure 3.1), was selected to maximize the area of the profile that was sampled. Each plot was also equipped with five neutron probe (503-DRHYDROPROBE®, CPN, Martinez, CA) access tubes for measuring the water content with depth.

An intensive study on water flow and soil hydraulic properties was conducted on the two plots at our experimental site (Segal et al., 2008) and no significant difference was found between the plots. The soil texture of the root zone (0-65 cm) was a sandy loam (Grangeville fine sandy loam, a coarse-loamy, mixed, superactive, thermic fluvaquent haploxeroll) with average contents of 55% sand, 40% silt and 5% clay. The average bulk density was 1.35 g·cm<sup>-3</sup> and the saturated and residual water contents were 0.43 and 0.03, respectively. The average saturated hydraulic conductivity was 2.35 cm·h<sup>-1</sup>, the longitudinal dispersivity was 0.56 cm, the immobile water content was 0.0978, and the mass transfer coefficient between mobile and immobile regions was 0.0035 h<sup>-1</sup> (Segal et al., 2008 and 2009).

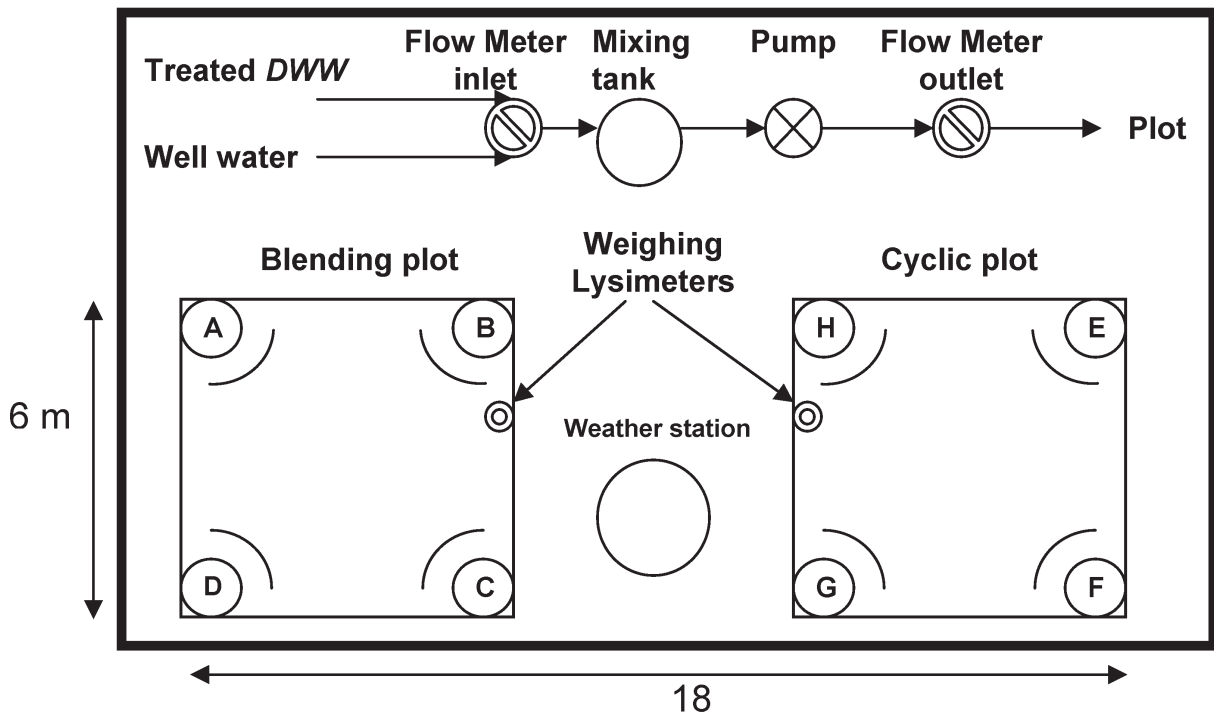


**Figure 3.1.** Schematic of the field site. Squares represent two six-by-six meter plots. Circles with letters (A-H) are 220 cm in length vertical culvert pipes installed with tensiometers and solution samplers. Arcs represent the area of water potential sampling. The controlled mixing and application system is illustrated at the top of the figure.

Raw DWW was treated prior to land application with a stationary inclined screen separator (Zhang and Westerman, 1997), a sedimentation tank (Sukias et al., 2001), and a sand filter (Rodgers et al., 2005) packed with crushed silica (0.45-0.5 mm in diameter, AGF, Netafim, Fresno, CA). In contrast to traditional agronomic designs, our process-based NMP minimized variability through uniform application of water and nutrient with a high level of precision. Specifically, well water and/or DWW were uniformly applied to each plot using a pump and nine emitters (R184CT, Raindrip, Fresno, CA) in 3 m spacing. The water application rates varied between 0.6 to 0.95 cm·h<sup>-1</sup> (25 to 40% of the soil saturated hydraulic conductivity) with a Christiansen uniformity coefficient of 94% under low wind conditions. The water and wastewater application system consisted of a mixing tank, a controller, solenoid valves, pumps and two electrical water meters with a resolution of 3.78 L ± 1.5% (JSJ075, Carlon meter, Grand Haven, MI) to achieve desired blending ratios for treated DWW and well water (Figure 3.1). Dairy wastewater was applied using cyclic and blending strategies. The blending strategy employed a selected mixture of treated DWW and well water to meet the needs of the crop for N and water. Conversely, the cyclic strategy applied separate irrigations of treated DWW and well water to meet the crop needs for N and water.

A NMP was implemented on winter and summer crops during 2007, and a perennial crop in 2008. Triticale (TRICAL<sup>®</sup> Resource Seeds, Inc.) served as the 2007 winter crop and was planted on February 10<sup>th</sup>, seedlings emerged and established a full stand on February 25<sup>th</sup>, and the crop was harvested on May 8<sup>th</sup>. The 2007 summer crop was NK 300 hybrid forage sorghum (Syngenta Global) and was planted on May 30<sup>th</sup>, seedlings emerged and established a full stand on June 5<sup>th</sup>, and the crop was harvested on August 13<sup>th</sup>. The 2008 perennial crop was alfalfa (Grandslam cv. Western Farm Service,

CA). Alfalfa is an important crop for the dairy industry due to its high yield, feeding value and efficiency in N removal. Alfalfa has three major differences relative to the crops used in 2007, namely: i) it is a perennial crop with multi-cuts; ii) it has a deeper root system; and iii) it may assimilate N from the atmosphere through nodules (symbiotic nitrogen fixation). Alfalfa was planted on the blending field plot at agronomical rate of 2.75 Kg·ha<sup>-1</sup> on April 1<sup>st</sup>, emerged on April 10<sup>th</sup>, and established full cover 30 days later. Five consecutive growing cycles (five cuttings with harvest interval between 37 to 45 days) were achieved during 2008. The NMP was implemented by dividing the growing season into multi-cut segments that represent the growing cycle. Each growing cycle was considered a separate period with a new initial condition. The first growing cycle started on May 10<sup>th</sup> and lasted until June 17<sup>th</sup>. However, extensive weed growth interfered with the normal development of the alfalfa during this period. Therefore, the plot was treated with herbicide (Pursuit, BASF, NC) at the rate of 150 ml·ha<sup>-1</sup> on June 25<sup>th</sup>. A fallow season (time between harvest and planting that is associated with minimal ET and nutrient uptake) occurred between successive growing seasons for the crops described above.

Blumenthal and Russelle (1996) reported that atmospheric N fixation through nodules will be less active during periods of high  $N_{soil}^I$ . The alfalfa NMP therefore attempted to maintain high N concentrations in the root zone during the growing season in order to minimize the amount of N fixation and to maximize the amount of DWW addition. No DWW was applied between the last two alfalfa harvests in order to deplete the soil profile of plant available N.

#### **Water and Nitrogen Mass Balances in the Root Zone**

Plot scale water balance information in the root zone over a given time interval was used to determine the amount of applied irrigation

water,  $I$  ( $\text{ML}^{-3}\Delta\text{T}^{-1}$ ) to meet crop ET ( $\text{ML}^{-3}\Delta\text{T}^{-1}$ ) at the end of this interval as:

$$I = ET + D + \Delta W - P_w \quad [3.1]$$

where  $D$  ( $\text{ML}^{-3}\Delta\text{T}^{-1}$ ) is water loss due to drainage,  $P_w$  ( $\text{ML}^{-3}\Delta\text{T}^{-1}$ ) is the water input due to precipitation, and  $\Delta W$  ( $\text{ML}^{-3}\Delta\text{T}^{-1}$ ) is the change in soil water storage (final – initial).

Water balance parameters in Equation [3.1] were measured as described below. Potential ET ( $ET_p$ ), with a resolution of 0.1 mm, was estimated using data from a weather station (Penman, 1948) located between the plots. Temperature, relative humidity, solar radiation, wind speed and rain were recorded every 15 min. Actual ET ( $ET_{\text{actual}}$ ) was estimated from weighing lysimeters, 20 cm in diameter and 100 cm length, installed at the perimeter of each plot (Figure 3.1). The top of the lysimeter was at the soil surface connected to a load cell that measured the total weight continuously (resolution of 50 g). A suction cup (filter paper; MF-0.45  $\mu\text{m}$ , Millipore, Billerica, MA) was connected to the bottom of the lysimeter, where vacuum was applied to collect the drainage. The crop coefficient ( $K_c$ ) was calculated as the ratio of  $ET_{\text{actual}}$  to  $ET_p$  during a given time period. The value of  $P_w$  (resolution of 0.25 mm) was measured using a rain gauge (CS700, Campbell Scientific, Logan, Utah). The values of  $D$  and  $\Delta W$  were determined from neutron probe and tensiometer readings in the root zone and measured soil hydraulic properties. The value of  $I$  was verified from flow meter readings.

In this study the following inorganic and organic N mass balance equations for the root zone were employed:

$$N_{\text{application}}^I + E_{OI} = N_{\text{plant}}^I + N_{\text{drainage}}^I + N_{\text{atmosphere}}^I + \Delta N_{\text{soil}}^I \quad [3.2]$$

$$N_{\text{application}}^O = \Delta N_{\text{soil}}^O + E_{OI} \quad [3.3]$$

where  $N_{\text{application}}^I$  is the inorganic N applied to the soil surface ( $\text{ML}^{-3}\Delta\text{T}^{-1}$ ),  $E_{OI}$  ( $\text{ML}^{-3}\Delta\text{T}^{-1}$ ) is the amount of N converted from/to organic

to/from inorganic forms,  $N_{\text{plant}}^I$  ( $\text{ML}^{-3}\Delta\text{T}^{-1}$ ) is the inorganic N uptake by the plant,  $N_{\text{drainage}}^I$  ( $\text{ML}^{-3}\Delta\text{T}^{-1}$ ) is the inorganic N drained below the root zone,  $N_{\text{atmosphere}}^I$  ( $\text{ML}^{-3}\Delta\text{T}^{-1}$ ) is the inorganic N lost to the atmosphere,  $\Delta N_{\text{soil}}^I$  is the difference in inorganic N storage in the root zone (final-initial),  $N_{\text{application}}^O$  ( $\text{ML}^{-3}\Delta\text{T}^{-1}$ ) is the organic N applied to the soil surface and  $\Delta N_{\text{soil}}^O$  ( $\text{ML}^{-3}\Delta\text{T}^{-1}$ ) is the difference in organic N storage in the root zone (final-initial). The total N mass balance is equal to the sum of Equations [3.2] and [3.3]. Equation [3.3] assumes that losses of organic N are only due to mineralization (volatilization and drainage of organic N are assumed to be negligible).

The N mass balance was calculated over the upper 30 cm for the triticale, 60 cm for the sorghum and 90 cm for the alfalfa, where roots are most active in water and nutrient uptake under irrigated conditions (Kätterer et al., 1993; Merrill and Rawlins, 1979; Abdul-Jabbar et al., 1982). Nitrogen balance parameters were quantified as described below. Total N and C in the solid phase of the DWW, soil, and plant tissues were measured using the combustion method (Flash EA 1112, Thermo-Finnigan, Waltham, MA). Measurement of nitrogen from ammonium ( $\text{N-NH}_4$ ) (Keeney and Nelson, 1982) and nitrogen from combined nitrite and nitrate ( $\text{N-(NO}_2+\text{NO}_3)$ ) concentrations in soil solution and DWW were performed using a colorimetric system (O.I. Analytical, Flow Solution IV, College Station, Texas) after filtering the sample through a 0.22  $\mu\text{m}$  filter. Values of  $N_{\text{application}}^I$  and  $N_{\text{application}}^O$  were directly measured in the DWW before each application. The value of  $\Delta N_{\text{soil}}^I$  was determined from sequential measurements of soil inorganic N concentrations in the root zone before DWW application events. The value of  $N_{\text{drainage}}^I$  was determined from measured inorganic N concentrations in soil solution below the root zone and from information about the water fluxes.

$N_{\text{atmosphere}}^I$  accounts for volatilization of ammonia ( $\text{NH}_3$ ) during application and from the

soil surface. We assumed denitrification was negligible under the low nitrate and unsaturated conditions of the root zone (Luo et al., 1999). The loss of  $\text{NH}_3$  during irrigation was measured using the concentration ratio of  $\text{N-NH}_4$  in the irrigation water at the emitter outlet and at the soil surface. Volatilization of  $\text{NH}_3$  from the soil surface was measured following DWW wastewater application for a period of one week during the 2007 winter crop season using a standard chamber and acid-trap technique to capture  $\text{NH}_3$  emissions (Black et al. 1985). The loss of  $\text{N-NH}_4$  during irrigation and the  $ET_p$  are presented for two application events in Table 3.1. The  $\text{N-NH}_4$  losses during irrigation varied between 9 and 32%, and higher rates were associated with higher  $\text{N-NH}_4$  concentrations in the irrigation water and higher  $ET_p$ . The atmospheric loss of  $\text{N-NH}_4$  during irrigation was measured and taken into account in the N balance before each application. The loss of  $\text{N-NH}_4$  from the soil after irrigation was measured to be three orders of magnitude smaller than the  $\text{N-NH}_4$  loss to the atmosphere during irrigation (Table 3.1). These findings are consistent with other data presented in the literature (Cameron et al., 1995; Sharpe and Harper, 1997; Cameron et al., 2002; Hawke and Summers, 2006).

$N'_{plant}$  was determined from measurements of dry phytomass and its N content. Before each water application, a 1 m long row of plants of the triticale and sorghum (0.2 to 0.4 m<sup>2</sup>) or 0.3 by 0.3 m of the alfalfa was collected for N analysis from the middle of the plot, where minimal effects from the measuring devices are expected. Since the root system was not removed during the harvesting, it was not considered as an N sink.

For triticale and sorghum during 2007 the value of  $E_{O1}$  accounts for the net exchange due to mineralization. In contrast, for alfalfa (a legume) during 2008 the value of  $E_{O1}$  also accounts for N fixation from the atmosphere. The value of  $E_{O1}$  was determined from Equation [3.2], while all other parameters were measured, and this information was used in conjunction with Equation [3.3] to determine the changes in  $N_{soil}^O$  using measured average values of the initial  $N_{soil}^O$  at the field site. The exchange rate was subsequently calculated as  $E_{O1}$  divided by the initial  $N_{soil}^O$  for a given time period. Final total N (dominated by  $N_{soil}^O$ ) and its spatial variability in the plots were measured on March, 2008. Ten soil cores, 30 cm long by 1.25 cm in diameter, were sampled from each plot in random locations. Three samples were taken from each

**Table 3.1.** Ammonia volatilization from the sprinkler irrigation system and soil surface.

<b>N-NH<sub>3</sub> volatilization from sprinkler irrigation system</b>				
Late winter DAE	Application Strategy	N-NH <sub>4</sub> in Irrigation water mg·L <sup>-1</sup>	Volatilization Loss %	$ET_p$ mm·h <sup>-1</sup>
35	Blending	11.1	15	0.446
35	Cyclic	39.45	9	0.142
57	Blending	92.57	32	0.68
57	Cyclic	157	22	0.24
<b>N-NH<sub>3</sub> volatilization from soil surface</b>				
Late winter DAE	Application Strategy	N-NH <sub>4</sub> in Irrigation water mg·m <sup>-2</sup>	N-NH <sub>3</sub> volatilization mg·m <sup>-2</sup>	Volatilization Loss %
29-36	Cyclic	2407.82	1.614	6.7·10 <sup>-6</sup>

core at depths of 5, 15 and 25 cm (total of 30 samples, 10 at each of these depths). Due to the small soil volume used in the combustion method, each sample was divided into three subsamples (total of 90 subsamples) that were analyzed for their total N and C content.

In practice,  $N_{application}^I$  was calculated from Equation [3.2] to meet the projected  $N_{plant}^I$  and  $E_{O1}$  during the subsequent time interval. The projected plant uptake for each time interval was determined from potential N uptake curves for crops under optimum growth conditions (Bélanger and Richards, 2000; Gibson et al., 2007; Rahman et al., 2001), and the projected mineralization rate was estimated from literature values (Stenger et al., 2001) or from the previous time step. The blending ratio before each application was determined by matching simultaneously  $I_{application}$  and  $N_{application}^I$ , where  $I_{application} = I_{DWW} + I_{well}$  and  $N_{application}^I = N_{well}^I I_{well} + N_{DWW}^I I_{DWW}$  and the subscripts *DWW* and *well* denote the water source.

Suspended sediments concentration (SSC) of the DWW were measured by centrifuging a known volume at 2040 times gravity for 20 min, decanting the liquid phase and measuring the remaining solid after drying at 60°C for 48 h (ASTM D 3977-97 - Method A). The TDS was assumed to be correlated to the EC ( $1 \text{ dS}\cdot\text{m}^{-1} = 10 \text{ meq}\cdot\text{L}^{-1}$ ) and was measured with an EC meter (M33.1, Agricultural Electronics, Montclair, CA). The concentrations of plant available K (Olsen bicarbonate method) and P (ammonium acetate method) in the soil profile were determined at the beginning and the end of the 2007 growing season, whereas salt concentrations (EC and TDS) in the root zone were measured before each irrigation event.

The T-Statistic (T-Test) was used to evaluate significant differences ( $P < 0.05$ ) between cyclic and blending application strategies during 2007 (Sigmaplot 11, Systat Software Inc., CA).

## Results and Discussion

Results from triticale (winter 2007) and sorghum (summer 2007) data are discussed below in sections entitled **Management Considerations for Salinity**, **Management Considerations for Organic Nitrogen**, and **Plant Available N, P and K**. These two cereal crops do not form nodules to fix atmospheric N, and  $E_{O1}$  therefore reflects exchange due to mineralization. In contrast, alfalfa (summer 2008) is a legume that forms nodules and may fix atmospheric N. The additional N source from fixation poses additional challenges for efficient NMP implementation that is discussed below in a separate section entitled **Nitrogen Fixation – Alfalfa 2008**.

### **Management Considerations for Salinity**

Water balance information for 2007 winter (A) and summer (B) growing seasons are presented in Table 3.2. Rainfall occurred during winter (total of 28.75 mm) but was absent during summer. The value of  $ET_p$  was lower during winter than during summer. The final water application amounts were adjusted to include a leaching factor of 0.2 for the first 30 days and 0.1 for later times in order to leach excess salts from the root zone and to minimize downward migration of  $\text{NO}_3^-$ . A system malfunction, however, delivered an extra 55.4 mm of well water to the cyclic plot on day 58 of the summer growing season. The total drainage flux (average of the blending and cyclic strategies) below the root zone was 23.9 mm and 56.4 mm throughout the winter and summer growing seasons, respectively.

Figure 3.2 presents the absolute value of soil water pressure head ( $|h|$ ) in the soil profile as a function of day after emergence (DAE) for the blending and cyclic strategies during the 2007 summer growing season. Changes in  $|h|$  were restricted only to the upper 60 cm of the soil profile due to the accurate water mass balance on both plots. In general,  $|h|$  followed the water application events: decreasing after irrigation (soil becomes wetter) and increasing with time between irrigations (soil

**Table 3.2.** Potential and actual evapotranspiration (ET), crop coefficient, rainfall and water application during the growing season of triticale during winter 2007 (A) and sorghum during summer 2007 (B), DAE is day after emergence.

<b>A</b> DAE	potential ET mm	Crop coefficient and leaching factor†	Actual ET mm	Rainfall mm	Water application mm
15-29	100.2	0.5	50.1	7.25	42.9
30-36	30.1	0.5	15.05	0.00	15.0
37-50	84.4	0.9	75.96	4.25	71.7
51-58	36.7	1.1	40.37	4.00	36.3
59-65	39.8	1.2	47.76	13.25	34.6
66-72	40.1	1.2	48.12	0.00	48.0

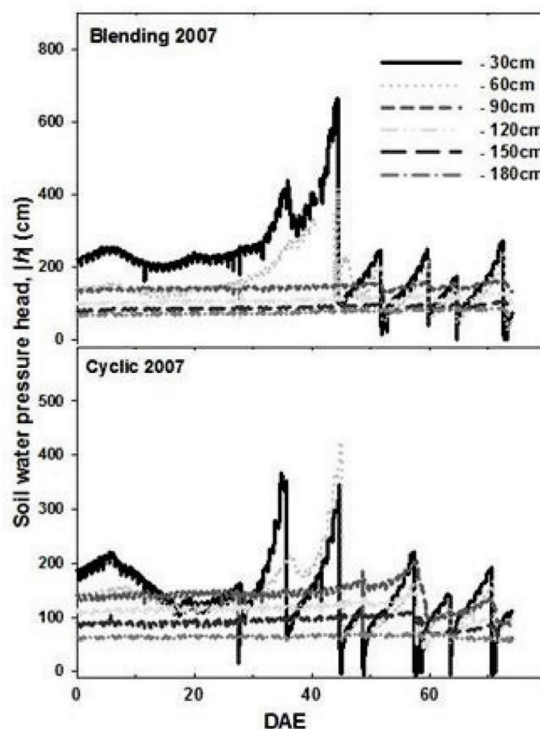
  

<b>B</b> DAE	potential ET mm	Crop coefficient and leaching factor†	Actual ET mm	Rainfall mm	Water application mm
5-28	258.6	0.5	129.3	0	135.1
29-35	86.7	0.75	65.02	0	62.4
36-44	94.0	0.9	84.6	0	90.5
45-49	47.1	1.0	47.1	0	48.5
50-58	86.0	1.0	86.0	0	86.6
59-62	33.5	1.05	35.17	0	35.3
63-70	59.8	1.1	65.78	0	66.6

†Crop coefficient was measured based on water mass balance in the root zone by using weighing lysimeters. The leaching factor was 0.2 during the first 30 days and 0.1 through the rest of the growing season.

becomes drier). Figure 3.2 shows that aerobic conditions were maintained during the majority of the season. The soil water pressure head below the root zone (i.e. <-90 cm) was generally steady throughout the growing season. The system malfunction on the cyclic plot at day 58, however, caused a decrease in  $|h|$  below the root zone (<-60 cm).

The increase in the EC of soil solution ( $EC_w$ ) of the root zone (-30 and -60 cm) over time due to the use of irrigation water with high TDS, a low leaching factor, and concentration of salts by ET is presented in Figure 3.3. The  $EC_w$  of the root zone increased from 1 to 3  $dS \cdot m^{-1}$  for the blending strategy and from 1 to 2.5  $dS \cdot m^{-1}$  for the cyclic strategy (no significant difference in the level of  $P < 0.05$  were found between the final values of  $EC_w$  of each treatment). The extra water application on the cyclic plot produced greater leaching and hence a lower final value of  $EC_w$ . Only minor changes in the electrical conductivity of the soil solution ( $EC_w$ ) were detected below the root zone during the growing seasons (data is not presented), due to the low leaching factor



**Figure 3.2.** The absolute value of the soil water pressure head ( $|h|$ ) in the soil profile as a function of day after emergence (DAE) for the cyclic and blending water application strategies during the sorghum 2007 growing season.

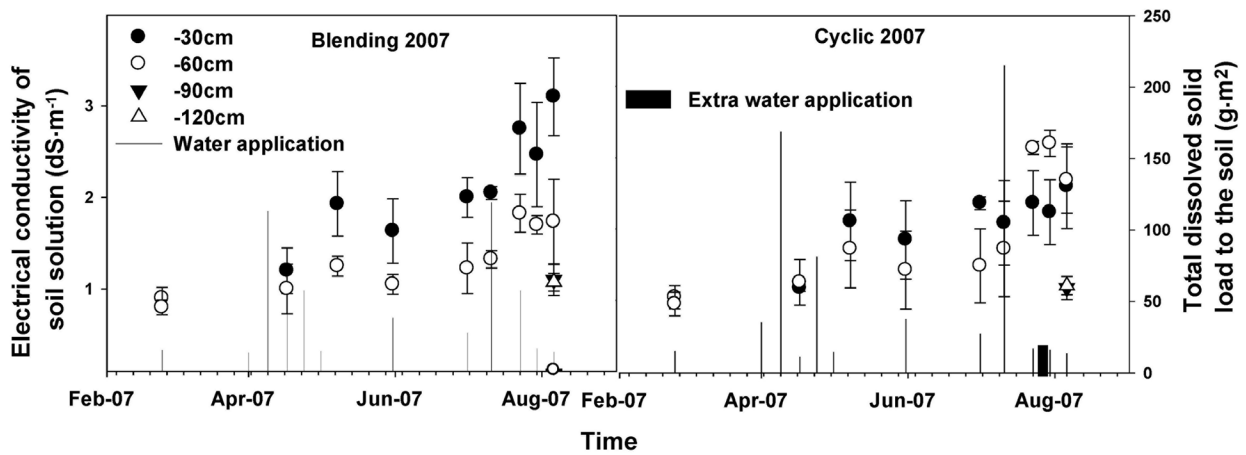


**Figure 3.3.** Electrical conductivity of the soil solution ( $EC_w$ ) over depth and total dissolved solids (TDS) load during 2007 for the blending and cyclic water application strategies.

that was implemented at these sites. The measured values represent the salt load under a conservative NMP approach that applied only a fraction of the total N that was required by the plant with DWW. If 100% of the plant N had been applied by DWW, then the accompanying salts would increase the  $EC_w$  in the root zone to higher levels. High salt levels in the root zone may restrict plant growth, and accordingly water and nutrient uptake. If this reduction in ET is not considered at a NMP site, additional leaching and contaminant migration will occur. An optimum point likely exists between the benefits of nutrient application and the detrimental effects of salt accumulation on crop yield. This point is strongly dependent on the salt tolerance of the crop, suggesting that NMP should use only salt tolerant crops.

Minimizing the potential adverse effects of salts on plant growth is commonly achieved by leaching excess salts below the root zone. The timing of salt leaching may be a crucial management decision in NMPs because organic soil N continues to be converted to inorganic N forms ( $NH_4^+$ ,  $NO_2^-$  and  $NO_3^-$ ) during the fallow season. A pre-irrigation at the beginning of a new growing season, or seasonal rains during the fallow season may result in migration of inorganic N, especially  $NO_3^-$ , below the

root zone towards groundwater (Feng et al., 2005; Woodard et al., 2002).

Figure 3.4 demonstrates this scenario by presenting the concentrations of  $N-(NO_2+NO_3)$  and  $N-NH_4$  in the soil profile at the end (final- after harvesting) and beginning (initial- after seasonal rains and pre-irrigation) of consecutive growing seasons. The graphs of triticale 2007/sorghum 2007 and the sorghum 2007/alfalfa 2008 fallow seasons show that the soil profile at both strategies was depleted from inorganic N at the beginning of the fallow seasons. Conversely, high concentrations of  $N-(NO_2+NO_3)$  were found along the soil profiles at the end of the fallow seasons. No significant difference ( $P < 0.05$ ) between strategies was found in the initial and final values of  $N-NH_4$  and  $N-(NO_2+NO_3)$  in the soil profile. A mass balance of the inorganic N in the profile revealed that 9.67 and 17.95  $g \cdot m^{-2}$  was mineralized for the blending strategy and 3.40 and 19.5  $g \cdot m^{-2}$  for the cyclic strategy during the triticale 2007/sorghum 2007 and the sorghum 2007/alfalfa 2008 fallow periods, respectively. These values are equivalent to mineralization rate of  $2.37E-04 \text{ day}^{-1}$  and  $4.25E-04 \text{ day}^{-1}$  for the blending strategy and  $2.93E-04 \text{ day}^{-1}$  and  $4.72E-04 \text{ day}^{-1}$  for the cyclic strategy. Leaching excess salts is therefore recommended right after harvesting,

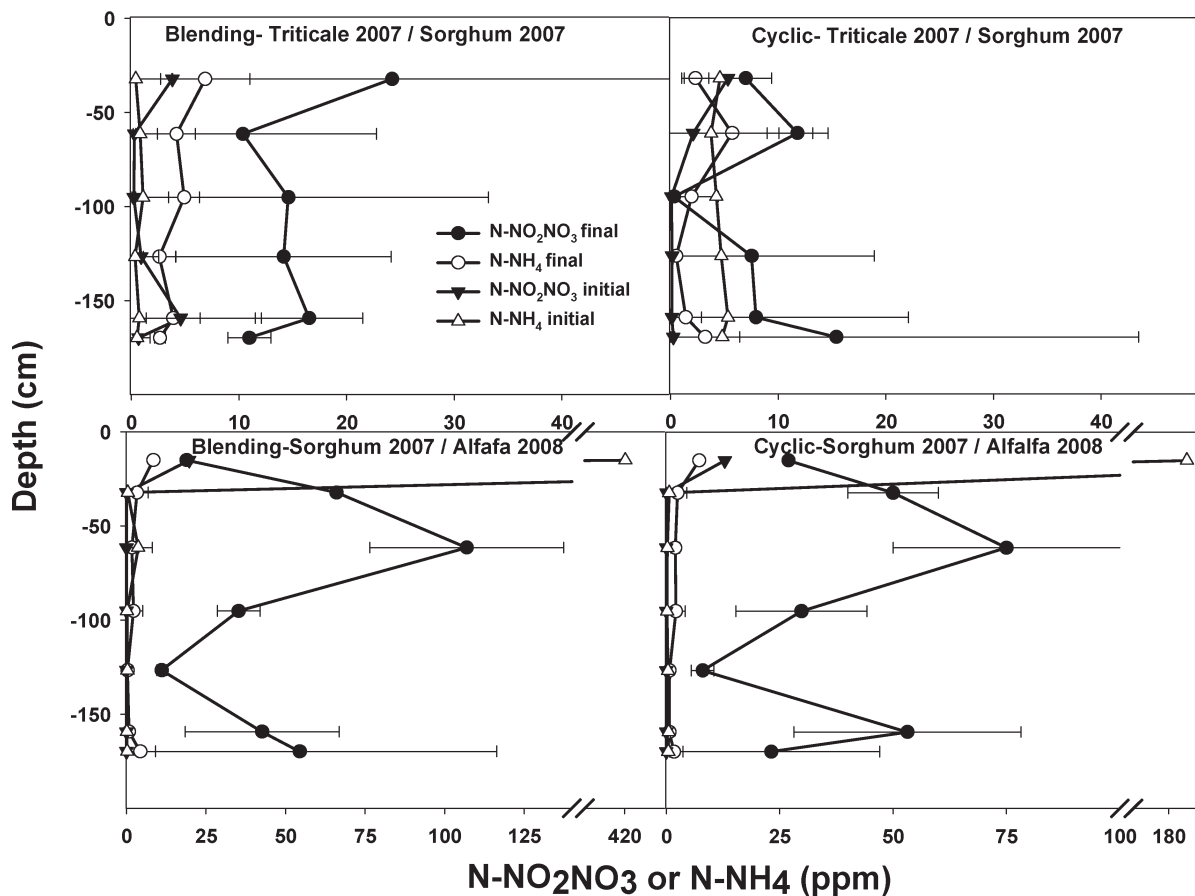


**Figure 3.4.** Nitrogen from ammonium ( $N-NH_4$ ) and nitrogen from combined nitrite and nitrate ( $N-(NO_2+NO_3)$ ) concentration in the soil profile at the end (final) and beginning (initial) of two consecutive growing seasons (triticale 2007/sorghum 2007 and sorghum 2007/alfalfa 2008).

when the inorganic N, and especially  $NO_3^-$  levels are low in the root zone.

#### Management Considerations for Organic Nitrogen

The determination of  $N_{soil}^O$  is hampered due to the inaccuracy of currently available methodologies (i.e. Kjeldahl and Combustion) and the inherent spatial variability of soils and water application systems (Strong et al., 1999; Stenger et al., 2001; Valenzuela-Solano and Crohn, 2006; Watts et al., 2007). Significant variability in  $N_{soil}^O$  was observed at the beginning of the 2008 winter growing season. The average total N (dominated by organic N) was 0.051% for the blending and 0.058% for the cyclic strategies, yet the values varied between 0.03 to 0.12%. This corresponds to total N levels of 121 to 486 g of  $N \cdot m^{-2}$  for the upper

30 cm. The calculated coefficient of variance for the combustion method was 6.95% and from the spatial variability was 19.5%. Hence, when the  $N_{soil}^O$  reservoir plays a dominant role in NMP management, the high uncertainty may lead to an inaccurate application of N. Furthermore, Figure 3.4 suggests that a large  $N_{soil}^O$  reservoir can maximize the potential migration of  $NO_3^-$  below the root zone at the end of the fallow season.

Figure 3.5 shows the effect of the high uncertainty and amount of  $N_{soil}^O$  on NMP implementation (in the absence of N fixation); by presenting three conceptual scenarios representing different ratios of inorganic to organic N sources in the root zone. The values of  $N_{soil}^O$  were assumed to be 333, 1666, and 3333 g of  $N \cdot m^{-2}$  in the top, middle, and lower

figures. Cumulative amounts of potential  $N_{plant}^I$ ,  $E_{OI}$ , and the sum of  $E_{OI}$  and  $N_{application}^I$  as a function of day of the year (DOY) are presented for each  $N_{soil}^O$  level. The year is divided into two growing seasons (winter and summer) and two fallow periods (fall and spring). For winter and summer crops the cumulative amounts of potential  $N_{plant}^I$  were assumed to be 16 and 22 g of  $N \cdot m^{-2}$  and mineralization rates were assumed to be  $2E-04$  and  $3E-04$   $day^{-1}$ , respectively. The error bars reflect the assumed variance (40%) in the mineralization rate. Differences in the predicted cumulative amounts of  $E_{OI}$  are due to differences in the initial organic reservoir.  $N_{application}^I$  is determined from the difference between potential  $N_{plant}^I$  and  $E_{OI}$ , while considering the uncertainty.

For the case of a low  $N_{soil}^O$  reservoir, matching between potential  $N_{plant}^I$  and  $N_{application}^I$  is practical with low deviations due to the minor amounts of  $N_{soil}^O$  and  $N_{application}^I$ . This well controlled NMP condition is similar to fertigation. The second scenario, intermediate  $N_{soil}^O$  reservoir, is representative of our field study during 2007 and requires the consideration of  $E_{OI}$ ,  $N_{soil}^O$  and  $N_{application}^I$ . This second scenario will under apply  $N_{plant}^I$  when uncertainty in the mineralization rate is considered and the  $N_{soil}^O$  reservoir will deplete over time and shift the system to the well controlled NMP condition shown in the upper graph. In the third scenario, the entire  $N_{plant}^I$  is dependent on the  $N_{soil}^O$  pool and mineralization rates. When considering the high uncertainty in  $E_{OI}$ , significant under-application of N is likely with corresponding yield reductions. Consequently, the  $N_{soil}^O$  reservoir will be depleted over time. If uncertainty in the mineralization rate is not considered with scenarios 2 and 3, then yield reduction can be minimized but the risk for N migration below the root zone toward groundwater increases.

Figure 3.5 indicates that the potential migration of N below the root zone can be minimized when  $N_{soil}^O$  is low. The majority of the SSC from the DWW was therefore removed

as part of the NMP implementation with an inclined screen separator, a sedimentation tank and a sand filter. In addition to this NMP consideration, lower SSC in the DWW

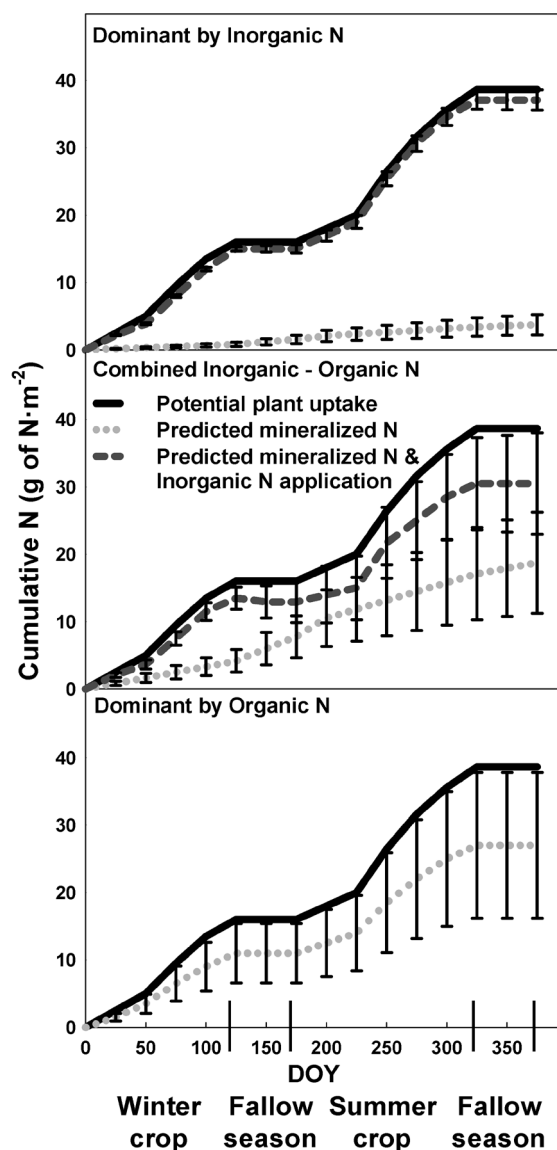


**Figure 3.5.** Three conceptual approaches for nitrogen NMPs based on low (top figure-333 g of  $N \cdot m^{-2}$ ), intermediate (middle figure-1666 g of  $N \cdot m^{-2}$ ), and high (lower figure-3333 g of  $N \cdot m^{-2}$ ) soil organic N reservoirs. Cumulative amounts of potential plant N uptake (16 and 22 g of  $N \cdot m^{-2}$  for winter and summer crops), predicted mineralized N, and the sum of mineralized N and applied inorganic N are presented as a function of the day of the year (DOY). Mineralization rates were  $2E-04$  and  $3E-04$   $day^{-1}$  for winter and summer seasons. The error bars reflect the assumed variance (40%) in the mineralization rate.

allowed us to use a water application system with a high uniformity (micro-sprinkler). The inorganic and organic N species and their distribution in applied DWW during the 2007 winter growing season (triticale) are presented in Figure 3.6. The organic N was relatively constant throughout the growing season (6.12-7.78 mg L<sup>-1</sup>), and the inorganic N fraction increased from 90% to 97% of the total N. Figure 3.6 also indicates that N-NH<sub>4</sub> was the dominant N form in the DWW (Campbell-Mathews et al., 2001; Cameron et al., 2002; Wang et al., 2004). Temporal variability in the fraction and amount of N-NH<sub>4</sub> and N-(NO<sub>2</sub>+NO<sub>3</sub>) in the DWW is due to NH<sub>3</sub> volatilization and nitrification during storage (Bussink and Oenema, 1998). The DWW treatment was found to also have an effect on many chemical properties (Table 3.3). A small reduction in EC was measured and was attributed to adsorption (Rodgers et al., 2005) and removal of suspended solids.

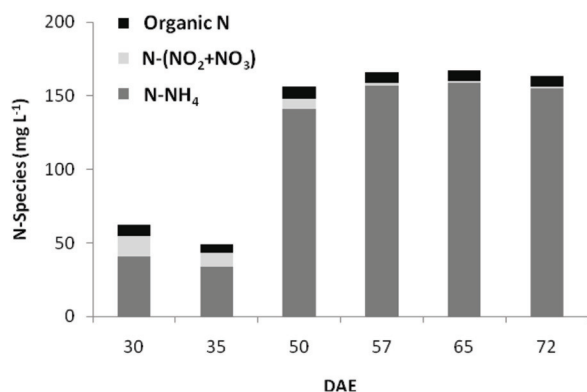


**Figure 3.6.** The composition, distribution, and amount of organic and inorganic N species (mg L<sup>-1</sup>) in dairy wastewater during the triticale 2007 growing season.

### Plant Available N, P, and K

NMPs need to be designed to maintain soil fertility and to minimize the risk of N migration below the root zone. A conservative NMP approach was implemented at our field site for triticale and sorghum during 2007 in an attempt to transition the soil organic reservoir to an optimum value of  $N_{soil}^O$ . During

**Table 3.3.** Salts and macro-nutrients of a raw and treated dairy wastewater (DWW). DWW was sequentially treated by solid separator, sedimentation tank and sand filter.

Category	Component	Raw DWW	Treated DWW
General	EC (dS·m <sup>-1</sup> )	3.7	3.2
	SSC (mg·L <sup>-1</sup> )	1611.4	199.1
	pH	7.57	8.16
Salts (mg·L <sup>-1</sup> )	Na	182.5	149.9
	Ca	378.3	299.3
	Mg	243.1	231.4
	Cl	174.2	175.8
	S-SO <sub>4</sub>	109.1	70.4
	HCO <sub>3</sub>	2163.1	1829.0
Macro-Nutrients (mg·L <sup>-1</sup> )	N-(NH <sub>4</sub> +NO <sub>2</sub> +NO <sub>3</sub> )	157.4	145.2
	Organic N	55.5	6.9
	K	404.9	380.5
	Total P	39.0	27.9

this transition phase, the  $N_{soil}^O$  reservoir was depleted over time in order to minimize the migration of NO<sub>3</sub> below the root zone. Once an optimal value of  $N_{soil}^O$  is achieved then it can be maintained by matching rates of dominant N sources (DWW addition) and sinks (plant uptake).

NMP results for triticale and sorghum during 2007 are summarized in Figure 3.7. Here  $N_{soil}^I$ ,  $N_{soil}^O$  and cumulative values of  $N_{plant}^I$ ,  $E_{OI}$ ,  $N_{drainage}^I$ ,  $N_{application}^I - N_{atmosphere}^I$  in the root zone are presented over time (no significant difference at  $P < 0.05$  level were found between cyclic and blending treatments). Initial low  $N_{soil}^I$  and minor changes in  $N_{drainage}^I$  over time were measured for both cyclic and blending strategies and crops. Average  $N_{application}^I - N_{atmosphere}^I$  for the triticale and sorghum crops were 48% and 28% of the total  $N_{plant}^I$ , hence the dominant N source was  $E_{OI}$  (mineralization). An additional factor influencing  $N_{application}^I$  was the low ET values during winter. Implementation of the cyclic strategy during these low ET conditions could not add sufficient N to match plant requirements for

several weeks, without adding DWW in excess of ET.

Decreases in  $N_{soil}^O$  over time are shown in Figure 3.7 for both triticale and sorghum plots as a result of mineralization. Average mineralization rates were  $1.23E-03 \text{ day}^{-1}$  during the triticale growing season and  $2.54E-03 \text{ day}^{-1}$  during the sorghum growing season. The elevated rates during summer were associated with higher soil temperatures (the average soil temperatures for the winter and summer growing seasons at -15 cm were  $15.6^\circ\text{C}$  and  $24.5^\circ\text{C}$ , respectively) that accelerated the mineralization process (Watts et al., 2007). These mineralization rates are lower than earlier studies using DWW (Feng et al., 2005; Stenger et al., 2001). This is likely due to the low organic content of the applied DWW that was treated, and the fact that most of the organic N in the soil was plant residuals (low C to N ratio). Mineralization continues during fallow periods (Figure 3.4) and this lead to differences in  $N_{soil}^O$  between growing seasons, especially for the long fallow period (241 days) between the harvest of sorghum and emergence of alfalfa. A comparison between measured and calculated (N mass balance) values of  $N_{soil}^O$  at the beginning of winter 2008 revealed no significant difference. The final calculated and measured  $N_{soil}^O$  reservoir at the beginning of winter 2008 was found to be  $267.9 \pm 45.1$  and  $220.2 \pm 44.6$  g for the blending strategy and  $276.6 \pm 39.8$  and  $236.3 \pm 38.9$  g of organic  $\text{N} \cdot \text{m}^{-2}$  for the cyclic strategy.

The typical concentration ratios of N, P and K in the applied DWW were 10:1.93:26.2 (Table 3.3). Direct measurements of P and K contents in plant tissues were not made during the course of the growing season. However, plant uptake rates of N, P, and K by wheat and sorghum have been reported to be 10:1.9:11.5 and 10:1.4:8.75, respectively (Bar-Tal et al., 2004; Vanderlip and Reeves, 1972). If these nutrient uptake ratios are assumed, then P and K will be applied in

excess and accumulated in the root zone when a NMP based on N is implemented to meet crop demand. Excess application of P becomes an environmental concern when surface water runoff and shallow water tables can mobilize the P into surface water bodies (Wang et al., 2004). Yet, arid and semi-arid environments are mostly associated with deep water tables, a high capacity of mineral soils for P adsorption and limited runoff to nearby surface water due to efficient water application.

Figure 3.8 presents concentrations of plant available K and P (phosphorus from phosphate,  $\text{P-PO}_4$ ) in the soil profile at the beginning of the 2007 winter growing season (initial) and the end of the 2007 summer crop season (final) for both blended and cyclic dairy wastewater application strategies. The distributions of K and P exhibited changes primarily in the upper 50 cm of the soil profile, where roots were most active in water and nutrient uptake. The actual deficit  $N_{application}^I$  (Figure 3.7) corresponded to  $5.05 \text{ g of P} \cdot \text{m}^{-2}$ , relative to an estimated  $8.65 \text{ g of P} \cdot \text{m}^{-2}$  taken up by the crop. Therefore, the final soil P content with both strategies is less than the initial content. However, if  $N_{application}^I$  is matched to  $N_{plant}^I$  as the main N sink, P will be applied in excess and accumulate in the soil. Similarly, excess amounts of K in the DWW and the large pool of K in the soil profile causes accumulation of K in the root zone for both cyclic and blending strategies.

#### **Nitrogen Fixation – Alfalfa 2008**

Since no significant differences in cyclic and blended treatments were observed during 2007, only the blended treatment was implemented on alfalfa during 2008. In contrast to triticale (winter 2007) and sorghum (summer 2007) crops discussed above, alfalfa (summer 2008) is a legume and may also obtain N through fixation. The implications of N fixation on efficient NMP implementation will be discussed below.

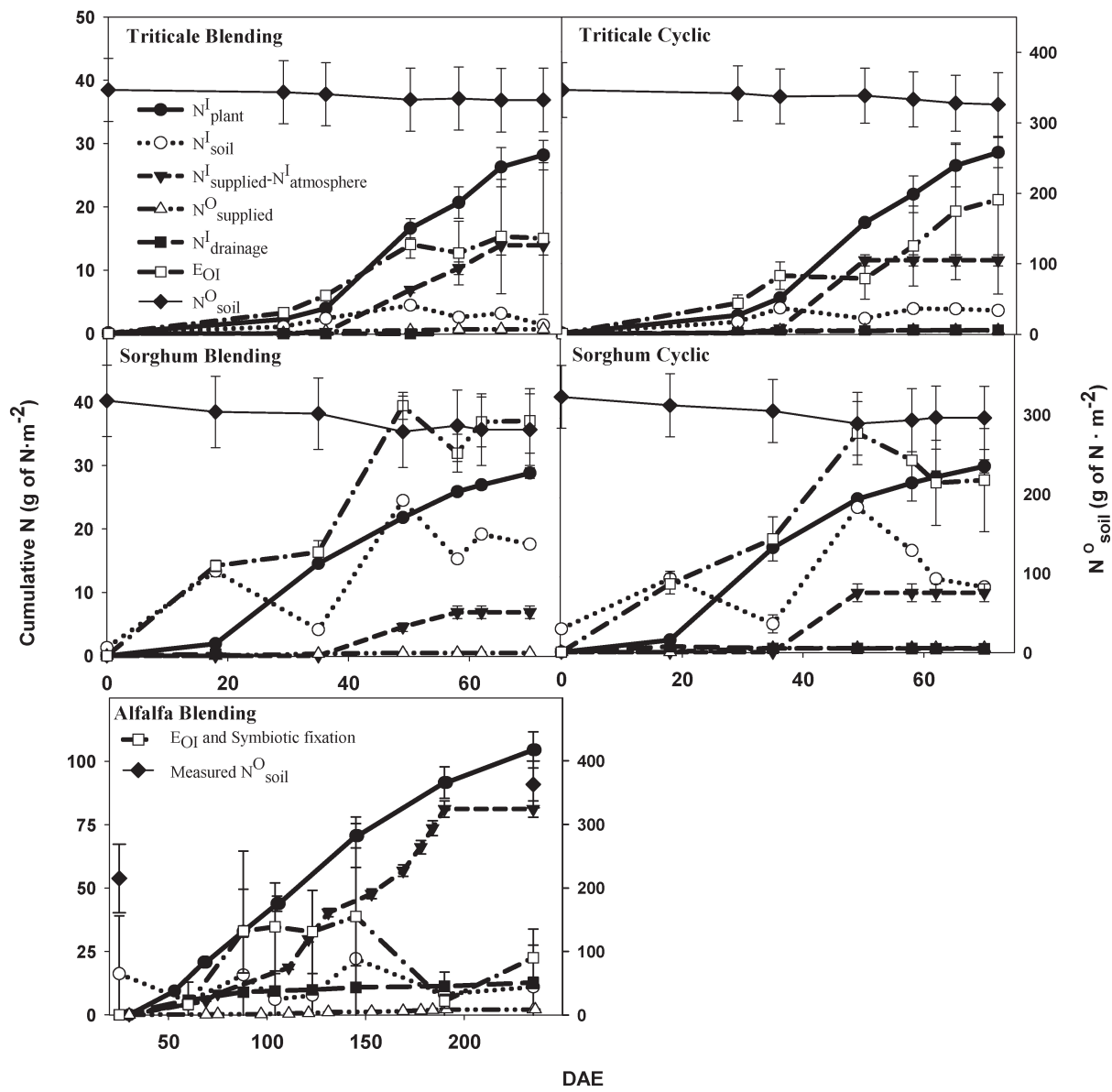


**Figure 3.7:** Soil inorganic and organic N reservoirs ( $N_{soil}^I$  and  $N_{soil}^O$ ) and cumulative values of N uptake by plant ( $N_{plant}^I$ ), exchange to/from organic and inorganic N forms ( $E_{OI}$ ), N loss to drainage ( $N_{drainage}^I$ ), supplied organic N ( $N_{application}^O$ ), and supplied inorganic N minus loss to the atmosphere ( $N_{application}^I - N_{atmosphere}^I$ ) in the root zone are presented over time. Data is presented as g of N·m<sup>-2</sup> for triticale (30 cm root zone), sorghum (60 cm root zone) and the alfalfa (90 cm root zone). Error bars represent measured or calculated standard deviations. The value of  $E_{OI}$  was obtained by closure of the mass balance (Eqs. 3.2 and 3.3), and reflects changes due to mineralization for triticale and sorghum, and mineralization and N fixation for alfalfa.

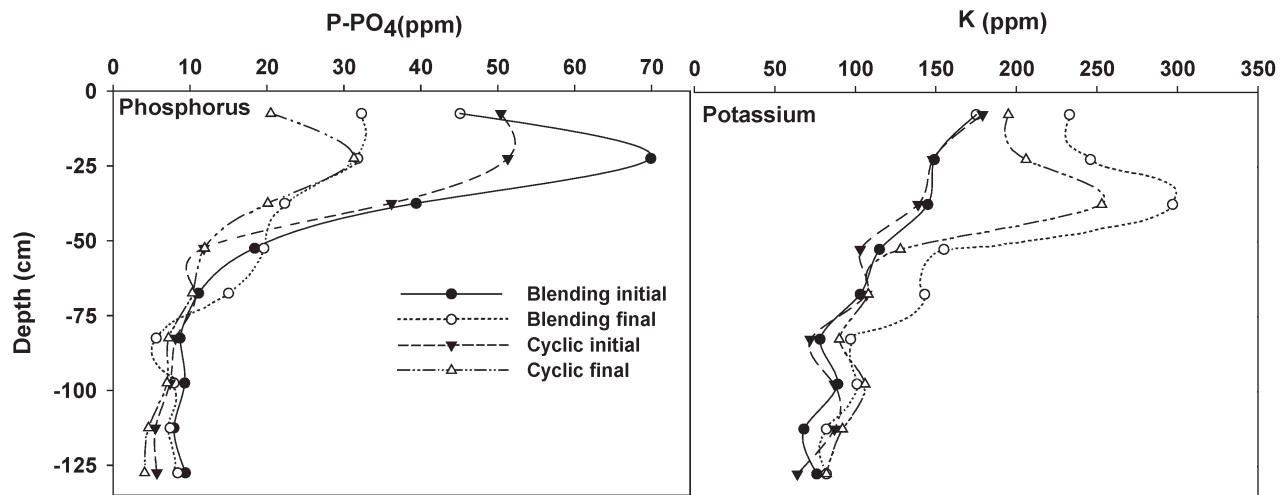


**Figure 3.8.** Plant available phosphorus ( $P-PO_4$ ) and potassium ( $K$ ) in the soil profile at the beginning (initial) of the triticale and end (final) of the sorghum growing seasons in 2007 for the blending and cyclic water application strategies.

Similar to triticale and sorghum data shown in Table 3.2 and Figure 3.2, an efficient water mass balance was implemented for alfalfa during 2008. Dry phytomass, cumulative water application and cumulative  $ET_{actual}$  throughout the five growing cycles of alfalfa in 2008 are presented in Figure 3.9. The error bars represent an estimation of the measuring error associated with the sampling procedure of alfalfa (10%). Dry phytomass ranged between  $325 \text{ g}\cdot\text{m}^{-2}$  at the last growing cycle, to  $750 \text{ g}\cdot\text{m}^{-2}$  at the second growing cycle (ending July 24<sup>th</sup>). The relatively slow growth rate during the last cycle was due to seasonal variation in climate; i.e., the average maximum and minimum air temperatures and solar radiation during this period were relatively low with values of  $23.1^\circ\text{C}$ ,  $3.07^\circ\text{C}$  and  $265.3 \text{ W}\cdot\text{m}^{-2}$ , respectively. In contrast, the low dry phytomass of the first cycle was related to the extensive weed growth that interfered with the normal development of the alfalfa during this period. The ratio between the total water applications ( $1626.7 \text{ mm}$ ) to the total  $ET_{actual}$  ( $1455.5 \text{ mm}$ ) corresponded to a leaching fraction of 11.7%. The calculated crop coefficients,  $K_c$ , were consistent with published data (Allen et al., 1998) and varied between 0.4 after harvesting to 1.2 when full

foliage cover was reached. Similar to 2007 data shown in Figure 3.2, changes in  $lhI$  were restricted only to the upper 60 cm of the soil profile due to the accurate water balance.

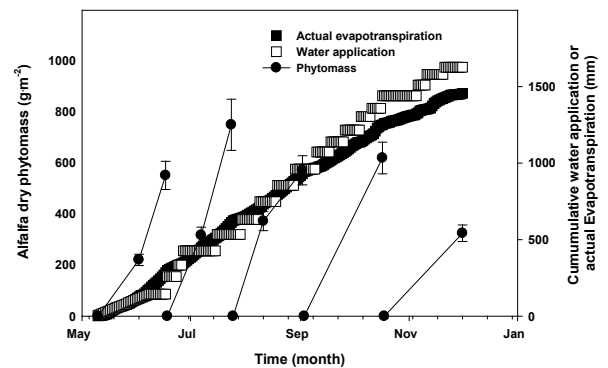


**Figure 3.9.** Dry phytomass, cumulative water application and actual evapotranspiration throughout the five growing cycles of alfalfa in 2008.

The alfalfa 2008 growing season started after a long fallow period (Nov. 2007-April 2008). A total of 25.7 cm of rainfall occurred during the fallow period that leached salts further into the soil profile. Similar to the 2007 data presented in Figure 3.3, the TDS increased over the growing season. The TDS in the soil profile (0 to -170 cm) at the beginning

of the growing season (May 2008) was  $937.7 \pm 338 \text{ g}\cdot\text{m}^{-2}$  and at the end (Dec. 2008) was  $1391.7 \pm 265 \text{ g}\cdot\text{m}^{-2}$ . This increase was pronounced at all depths and especially the upper 30 cm ( $98.8 \text{ g}\cdot\text{m}^{-2}$  versus  $254.3 \text{ g}\cdot\text{m}^{-2}$ ).

Figure 3.7 shows the various components of the N balance that were measured for alfalfa during 2008. Since alfalfa can fix atmospheric N through nodules, the value of  $E_{OI}$  now accounts for the net exchange between organic and inorganic N forms due to both mineralization and atmospheric N fixation. Due to this additional complication, only initial and final values of measured  $N_{soil}^O$  are shown in Figure 3.7 for alfalfa. Recall that a very conservative NMP approach was implemented for triticale and sorghum crops in 2007 that depleted the soil organic N. In contrast, a less conservative NMP strategy was implemented for alfalfa during 2008 due to a greater value of  $N_{plant}^I$ , a deeper root system, and the desire to suppress atmospheric N fixation. Specifically, the cumulative value of  $N_{plant}^I$  was  $104 \text{ g of N}\cdot\text{m}^{-2}$  for alfalfa in comparison to  $60 \text{ g of N}\cdot\text{m}^{-2}$  for both triticale and sorghum. The depth of the root zone, where roots are most active in water and nutrient uptake under irrigated conditions, for alfalfa was approximately 90 cm in comparison to 30 and 60 cm for triticale and sorghum, respectively. A larger root zone allows nutrients to be extracted over a larger area and to implement a more flexible schedule for lagoon water application. In addition, by maintaining a high N concentration in the root zone, we can minimize the need of the plant to seek for alternative N sources and theoretically apply more DWW. The value of  $N_{application}^I - N_{atmosphere}^I$  for the alfalfa was selected to be 76% of the total  $N_{plant}^I$ . This implies that the remaining 24% of  $N_{plant}^I$  comes from mineralization or atmospheric N fixation.

Several implications for the less conservative NMP strategy that was implemented on alfalfa during 2008 are discussed below. First, an increase in measured  $N_{soil}^O$  is shown

in Figure 3.7 for alfalfa. This observation can be attributed to three factors, namely: i) intensive root growth of the alfalfa that increased the total  $N_{soil}^O$ ; ii) the less conservative NMP approach yielded a higher ratio of  $N_{application}^I - N_{atmosphere}^I$  to the total  $N_{plant}^I$ ; and iii) the mechanism of N fixation through nodules reduced the need for mineralized  $N_{soil}^O$ , and induced immobilization of inorganic N. Amounts of N in excess of plant uptake requirements were apparently generated due to these factors. Consequently, 15% of the supplied inorganic N was measured to be steadily drained below the root zone throughout the growing season under the applied leaching factor of 11.7%. Additional research is therefore needed to optimize NMP performance with leguminous crops.

# 4.0

## NMP Results – Indicator Microorganisms

### Background

NMPs implicitly assume that pathogenic microorganisms in CAFO lagoon water will be retained and inactivated/degraded in the root zone, so that food and water supplies are protected. This assumption has not yet been thoroughly tested. The objective of this work was to test the hypothesis that fecal indicator microorganisms (*Enterococcus*, total *E. coli*, fecal coliforms, and somatic coliphage) will be retained and die-off in the root zone of a NMP application site. To this end, the fate of indicator microorganisms at a field NMP site was monitored during winter and summer growing seasons. Additional information was obtained in well controlled laboratory experiments in order to: (i) identify mechanisms that controlled the fate of the indicator microorganisms at the NMP site, and (ii) to develop recommendations for improved NMP performance. Specifically, batch experiments were conducted to quantify the survival characteristics of the indicator microorganisms. Small-scale packed column experiments were conducted to study the influence of the soil matrix on transport and retention behavior. Finally, a large undisturbed column experiment was conducted to assess the influence of soil structure on indicator microorganism transport and survival under a worst case scenario of ponded infiltration and redistribution.

### Materials and Methods

#### **NMP Field Site**

The experimental field site is located in San Jacinto, CA (33°50'22" N, 117°00'46" W), next to a dry river bed and has a shallow perched water table at a depth of -220 cm. The experiments were conducted on a 6x6 m plot that was described in detail

in Chapters 2 and 3. Soil cores were periodically collected from the NMP plot boundaries for microbial analysis as described below.

Before initiating the NMP, extensive field and laboratory studies were conducted to characterize the soil hydraulic properties, the water flow behavior, and the transport of a conservative solute tracer on these plots. Detailed information is provided in Segal et al. (2008 and 2009) and in Chapter 2.

For accurate NMP implementation it was necessary to conduct a treatment on the dairy wastewater using an inclined screen, a sedimentation tank, and sand filtration. This treatment significantly decreased the organic load of the wastewater and thus increased the proportion of plant available inorganic N relative to organic N, which was necessary for efficient management of the NMP (Segal et al. 2010). The indicator microbial composition of the dairy wastewater before and after this treatment was measured as part of this work. Detailed information on the NMP design and implementation is provided in Segal et al. (2010) and in Chapter 3.

#### **Analysis and Sampling for Indicator Microorganisms**

Representative viral (somatic coliphage) and bacterial (total *E. coli*, fecal coliforms, and *Enterococcus*) indicator microorganisms were monitored at the NMP application site and in laboratory experiments discussed below. These microbes are commonly associated with fecal contamination and are typically found in high concentrations in animal wastes (Havelaar, 1986; Bradford et al., 2008). Somatic coliphage, such as  $\phi X174$ , are very persistent bacterial viruses that resemble pathogenic viruses in their fate and behavior

(Schijven and Hassanizadeh, 2000), but are harmless to humans and can be prepared and quantified easily. Total *E. coli* and *Enterococcus* are frequently used as indicators of bacterial pathogens that are found in the intestinal tract of humans and warm-blooded animals.

The concentration of indigenous somatic coliphage in aqueous samples was determined using the double agar overlay Method 1601 (USEPA, 2001b) with bacterial host *Escherichia coli* CN-13 (ATCC 700609). In brief, 1 mL of log phase host culture and 1 mL sample was added to borosilicate test tubes (Thermo Fisher Scientific, Waltham, MA) containing 4 mL of trypticase soy agar (TSA) (BD Diagnostic Systems, Sparks, MD) supplemented with 1% nalidixic acid (NA) (Sigma-Aldrich, St. Louis, MO). The mixture was poured onto sterilized 100 × 15 mm plastic petri plates (Thermo Fisher Scientific, Waltham, MA) and allowed to solidify for 15 min, after which, they were inverted and incubated for 16 h at 36°C ± 1.0°C. The number of plaque forming units (PFU) in the plates was determined by counting the plaque density under a darkfield colony counter (Leica, Buffalo, NY). All coliphage assays were run in duplicate and diluted as necessary.

Aqueous concentrations of total *E. coli*, fecal coliforms, and *Enterococcus* were determined using the conventional spread plating method (Clesceri et al., 1989). A 100 µl sample was plated on Chromagar ECC (CHROMagar Microbiology, Paris, France) plates for total *E. coli*, on mFC agar (BD Diagnostic Systems, Sparks, MD) plates for fecal coliforms, and on KF agar (EM Science, Gibbstown, NJ) plates for *Enterococcus*. The plates were inverted and incubated at 37°C for total *E. coli* (24 h) and *Enterococcus* (24-48 h), and at 44.5°C for fecal coliform (24 h). The bacterial colony forming units (CFU) were then counted. All bacterial assays were run in duplicate and diluted as necessary.

Dairy wastewater samples were analyzed directly according to the procedures outlined above. Soil samples were collected and weighed under field and oven dried conditions. For microbial analysis, a 10 g sample of the field soil from each depth increment was placed in a 50 mL sterile polypropylene centrifuge tube (Thermo Fisher Scientific, Waltham, NJ), 20 mL of phosphate buffered solution or de-ionized water was added, and the solution was gently mixed on a Eberbach shaker (Eberbach corporation, Ann Arbor, Michigan) for 30 min, and then the soil solution was allowed to settle for 5 min. This solution was subsequently analyzed for microbial concentrations using the outlined procedures, and the concentrations were corrected for the amount of soil and solution in each depth increment. Results from column transport and batch survival experiments discussed below demonstrate that reasonable mass balance and microbe recovery was achieved when using this protocol with soil from the field plot and the considered indicator microorganisms.

For laboratory transport experiments that utilized spiked concentrations of indicator microorganisms the following protocols were followed. Stock bacteria, *E. coli* (ATCC 11775); *Enterococcus faecalis* (ATCC 19433), and somatic coliphage,  $\phi X174$  (ATCC 13706-B1) were grown 24 h prior to the laboratory experiments. *E. coli* was propagated in trypticase soy broth (TSB) (BD Diagnostic Systems, Sparks, MD) and *Enterococcus faecalis* was grown in LB broth (FisherBiotech, Fair Lawn, NJ). Both bacterial strains were incubated overnight at 37°C ± 1.0°C. The somatic coliphage host, *E. coli* (ATCC 13706) was incubated in TSB for 18 h at 37°C ± 1.0°C. Bacteriophage  $\phi X174$  was then added into the broth culture of host bacteria and allowed to propagate overnight. The host, *E. coli*, was removed from the suspension, containing bacteriophage  $\phi X174$ , by centrifugation at 17329 × g for 10 min. The other bacteria were harvested from the growth broth,

and washed twice in PBS and centrifuged at  $17329 \times g$  before using them in the transport experiments.

### Laboratory Experiments

**Batch** – Batch experiments were conducted to assess the survival characteristics of the indicator microorganisms. Experiments were conducted by placing 7.5 g of field soil into a 20 ml glass scintillation vial. Two conditions were studied to determine the influence of biotic factors on the survival of the indicator microorganisms. One set of experiments employed native soil and wastewater, and the other used sterilized (autoclaved) soil and wastewater spiked with indicator microorganisms. Lagoon water (0.43 ml) and deionized water were added to the vials to achieve a water saturation of 80%. The porosity of the soil in the vials was estimated from the soil volume and mass to be 0.43. The deionized water and wastewater were then thoroughly mixed with the soil using a metal spatula, and the vial was capped (a pin hole was used for aeration) and wrapped in aluminum foil. The vials were subsequently stored at 25°C and analyzed for indicator microorganism concentrations at desired times. Separate vials were used for each time (0, 6, 10, 24, 48, 80, 144, and 168 h). Hence, a total of 8 vials were independently analyzed for native and sterilized batch experiments.

Microorganism death/inactivation is typically assumed to follow a simple first-order decay model (Yates et al., 1987; Schijven and Hassanizadeh, 2000). However, virus inactivation and bacterial growth in soils have been observed to exhibit more complex survival behavior than the simple first-order decay model. The following model was proposed by Sim and Chrysikopoulos (1996) to account for observed time dependent inactivation:

$$\frac{dC_T}{dt} = -\lambda_o \exp(-\alpha t) C_T \quad [4.1]$$

where  $C_T$  [ $N L^{-3}$ ]; where N is the number of microorganisms, and L denotes units of

length], is the total microorganism concentration, t [T, denotes units of time] is time,  $\lambda_o$  [ $T^{-1}$ ] is the initial rate of die-off/inactivation, and  $\alpha$  [ $T^{-1}$ ] is the resistivity coefficient to die-off/inactivation. The solution to Equation [4.1] is given as (Sim and Chrysikopoulos, 1996):

$$\frac{C_T}{C_{Ti}} = \exp\left(\frac{\lambda_o}{\alpha} [\exp(-\alpha t) - 1]\right) \quad [4.2]$$

where  $C_{Ti}$  [ $N L^{-3}$ ] is the initial total microorganism concentration. The parameters  $\lambda_o$  and  $\alpha$  will be fitted herein to measured batch survival data using a nonlinear least squares optimization routine.

**Packed Column** - Packed soil column experiments were conducted using top soil from the field site to assess the transport potential of *Enterococcus*, somatic coliphage, and *E. coli* under well controlled conditions. Sterilized field soil and wastewater that was spiked with indicator microorganisms were used for this purpose.

Kontes Chromaflex chromatography columns (Kimble / Kontes, Vineland, NJ) made of borosilicate glass (15 cm long and 4.8 cm inside diameter, equipped with an adjustable adapter at the top) were used in the transport studies. The columns were packed dry with oven-dried soil from the surface of the NMP site. Well water from the field was slowly pumped upward through the vertically oriented columns at a steady flow rate for several pore volumes (PV) to saturate the column. A peristaltic pump (Cole-Parmer, Vernon Hills, IL) was used for this purpose. Microorganism transport experiments were subsequently conducted by pumping tracer solution at a steady rate through the column for several PV, after which a three-way valve was used to switch to the well water for several additional PV. Effluent samples were continuously collected in  $16 \times 150$  mm borosilicate test tubes (Thermo Fisher Scientific, Waltham, NJ) using an auto sampler (Isco, Inc., Lincoln, NE).

Following completion of the transport experiments, the concentration of indicator microorganisms in the effluent and retained in the soil was determined using the previously outlined protocols.

**Undisturbed Column** - To study the influence of soil structure on the transport and survival of indigenous indicator microorganisms in wastewater a larger undisturbed soil column (length was 65 cm and the internal diameter was 24 cm) was taken from the field site just outside of the plot. This column was also used in water flow and bromide transport experiments, and details on the collection, handling, instrumentation, hydraulic properties, and solute transport characteristics of this column are provided in the literature (Segal et al. 2009). In brief, the soil core was encased in an acrylic cylinder that was pushed into the soil with a hydraulic piston and then dug out. The bottom of the column was placed on a ceramic plate with a bubbling pressure of 100 kPa and a hanging water column was used to control the water pressure and to collect effluent samples. The soil surface boundary condition was selected to mimic a worst case transport scenario of ponded infiltration in which saturated conditions enable water flow and pathogen transport through macropores and soil structure. In this case, wastewater was instantaneously added to the soil surface to a depth of 7 cm and allowed to infiltrate into the profile. Following application and infiltration of the wastewater, 2 cm diameter and 65 cm long soil cores were collected vertically from the column surface at selected times and analyzed for concentrations of indicator microbes. The sample locations were subsequently plugged with a similar sized PVC tube that was capped. This experiment was conducted at 25°C in a temperature controlled room.

## Results and Discussion

### NMP Field Site

The sequential treatment (inclined screen separator, sedimentation tank and sand filter)

of the dairy wastewater at the field site had a large effect on many microbial properties. Table 4.1 provides representative information on the concentration of indicator microorganisms before and after this treatment. The treatment produced almost a 2 log decrease in the concentration of the various indicator microorganisms. Concentrations of indicator microorganisms in the treated wastewater, however, still significantly exceeded the recommended U.S. standards for unrestricted irrigation (USEPA, 2004). If pathogenic microorganisms behave similarly to indicators, then care must be taken in using dairy wastewater as a source for irrigation water. To protect surface and groundwater supplies it is therefore essential that pathogenic microorganisms in the dairy wastewater be removed by treatment, or be retained and inactivated/degraded in the root zone of NMP sites.

**Table 4.1.** Representative concentrations of indicator microorganisms in raw and treated dairy wastewater, and the percent removal by treatment. Treatment included solid separator, sedimentation tank and sand filter.

Indicator	Raw	Treated	% Removal
<i>Enterococcus</i> (cfu ml <sup>-1</sup> )	1.56E+06	6.10E+04	96.1
fecal coliform (cfu ml <sup>-1</sup> )	2.47E+05	6.00E+03	97.6
somatic coliphage (pfu ml <sup>-1</sup> )	7.50E+03	5.00+02	93.3
total <i>E. coli</i> (cfu ml <sup>-1</sup> )	9.30E+04	3.00E+03	96.8

Water mass balance information for the winter triticale and the summer sorghum growing seasons are presented in Table 4.2 as a function of day after emergence (DAE). The accurate water application quantities (well water + lagoon water) relative to the actual

plant evapotranspiration (ET) restricted changes in water pressure to the upper 60 cm of the soil profile (Segal et al., 2010). Hence, the amounts of drainage below the root zone (Table 4.2) were very small throughout the winter and summer growing seasons and most of this drainage occurred with well water application (57.6 and 86.9% during winter and summer, respectively). This finding indicates that there exists little potential for advective transport of the indicator microorganisms below the root zone under these NMP management conditions. If the indicator microorganisms survive in the root zone, however, they may still be transported below the root zone when water in excess of ET is applied to this NMP site such as during the fallow period with high precipitation events or during pre-irrigations to leach salts. Hence, pathogen survival in the root zone may pose a risk to food and water resources at NMP sites.

Figure 4.1a-d present plots of the concentration of *Enterococcus*, fecal coliform, somatic coliphage, and total *E. coli* in soil ( $S, N\ g^{-1}$ ) as a function of depth at several different DAE during the winter triticale growing season, respectively. Table 4.2 also includes the amount of well water and dairy wastewater that was applied to the NMP study site. Irrigation water was applied at the end of the intervals provided in Table 4.2, except for the first interval in which the irrigation water was applied periodically throughout the interval. Low concentrations of total *E. coli*, fecal coliform, and somatic coliphage were initially present in the surface soil of the NMP site. The *Enterococcus* concentrations, however, were initially more abundant. After wastewater addition on DAE 36, the concentrations of the indicator microorganisms in the soil core increased dramatically. The highest concentrations occurred near the soil surface (top

**Table 4.2.** Actual evapotranspiration (ET), rainfall, well water application, wastewater application, and drainage amounts during the winter (triticale) and summer (sorghum) growing seasons as a function of day after emergence (DAE).

<b>Winter</b> DAE	Actual ET mm	Rainfall mm	Well Water mm	Waste Water mm	Drainage <sup>1</sup> mm
15-29	40.1	7.2	42.9	0.0	10.0
30-36	13.5	0.0	0.0	15.0	1.5
37-50	68.4	4.2	0.0	71.7	7.6
51-58	36.5	4.1	36.3	0.0	4.1
59-65	43.0	13.2	0.0	34.5	4.8
66-72	43.2	0.0	48.0	0.0	4.8

<b>Summer</b> DAE	Actual ET mm	Rainfall mm	Well Water mm	Waste Water mm	Drainage <sup>1</sup> mm
5-28	104.0	0.0	135.0	0.0	26.0
29-35	58.5	0.0	62.0	0.0	6.5
36-44	76.2	0.0	0.0	91.51	8.5
45-49	42.4	0.0	48.6	0.0	4.7
50-58	77.4	0.0	86.6	0.0	8.6
59-62	31.7	0.0	35.3	0.0	3.5
63-70	59.1	0.0	66.7	0.0	6.6

<sup>1</sup>- Value estimated from water balance

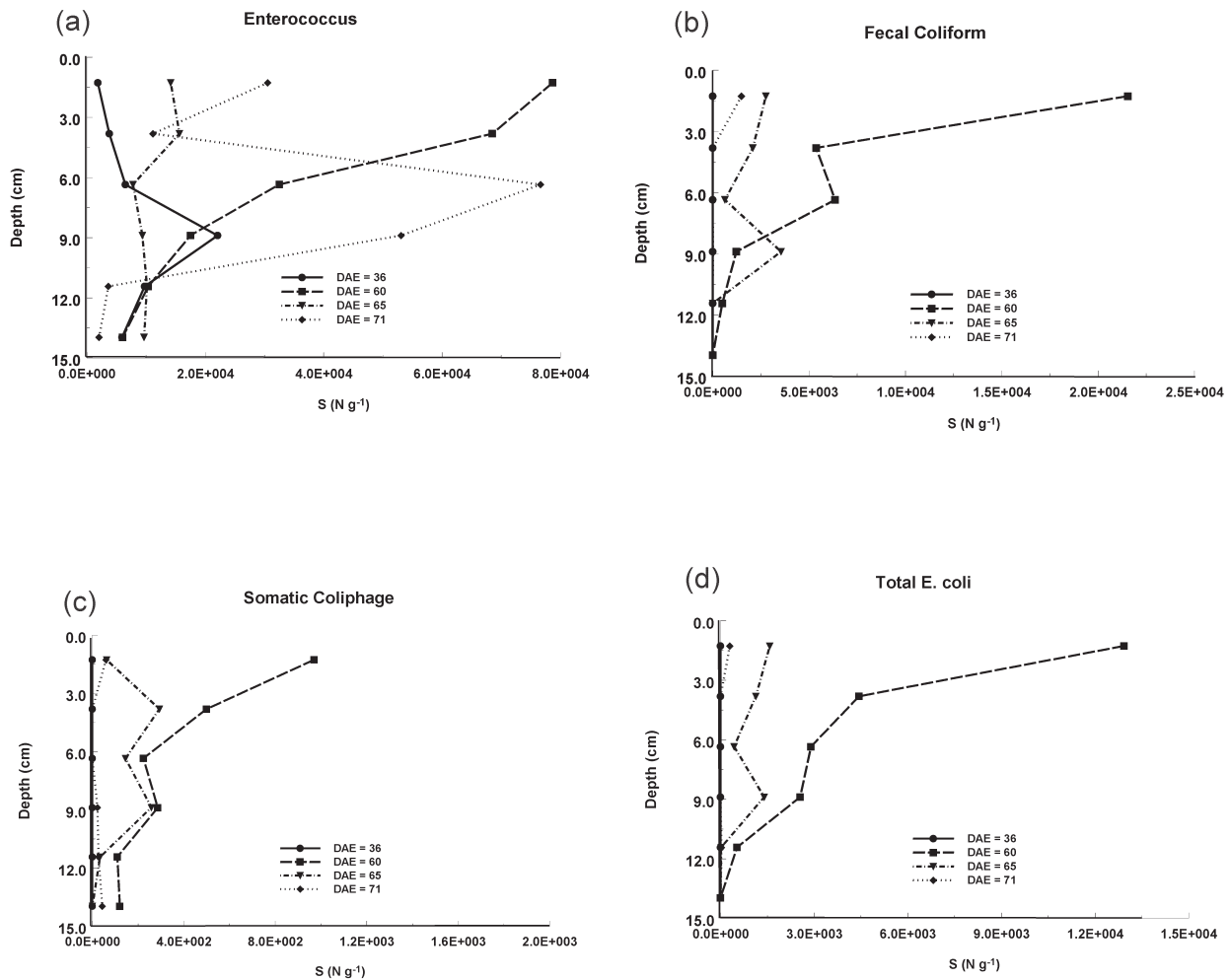


**Figure 4.1.** Plots of the concentration of *Enterococcus* (Figure 4.1a), fecal coliform (Figure 4.1b), somatic coliphage (Figure 4.1c), and total *E. coli* (Figure 4.1d) in soil ( $S$ ,  $N\ g^{-1}$ ) as a function of depth at several different days after emergence (DAE) during the winter triticale growing season at the NMP field site.

4-6 cm) and then rapidly decreased with soil depth. Over time concentrations of the indicator microorganisms at the soil surface tended to decrease, and by DAE 71 approached the low levels that were found before wastewater application (DAE 36).

Similar NMP experiments were conducted during the summer on sorghum. Soil cores were periodically collected from the field site during the summer season and analyzed for indicator microorganism concentrations. Similar to the winter crop, only low levels of *Enterococcus* were found in the surface soil at the beginning and end of the summer season.

A more detailed NMP experiment was initiated the following summer growing season (alfalfa, *Medicago sativa*, was the crop) to better understand the transport and fate of the indicator microorganisms. In this case, the sampling frequency (initial, and times=0, 14, 62, 134, and 206 h after wastewater application) and number of soil cores (composite of 3 cores) were much higher after a single wastewater application event. In addition, the gravimetric water content with depth was measured at selected times after wastewater application. Initial concentrations in soil were low for the somatic coliphage and total *E.*

*coli* ( $C_T$  was 0 CFU cm<sup>-3</sup>). Conversely, initial concentrations for *Enterococcus* ( $C_T$  was 5E4 CFU cm<sup>-3</sup>) and fecal coliform ( $C_T$  was 1.3E4 CFU cm<sup>-3</sup>) in soil were higher. Approximately 10.5 cm of wastewater was applied to the field site at an average rate of 0.95 cm h<sup>-1</sup>. Changes in the water content occurred over depth and time (Figure 4.2a) as a result of infiltration, redistribution, and then evapotranspiration in the root zone (top 60 cm of soil). Figure 4.2b-e present plots of the normalized concentration of *Enterococcus*, fecal coliform, somatic coliphage, and total *E. coli* in soil ( $S/C_T$ ; cm<sup>3</sup> g<sup>-1</sup>) as a function of depth at selected sampling times after wastewater application. Here the concentrations of a given microorganism in soil were normalized by  $C_T$  for the entire soil core taken at time=0 h, i.e., denoted as  $C_{T_0}$ . The concentration of indicator microorganisms in the soil was high at time = 0 h, and reflected initial conditions, transport during wastewater infiltration, and retention of the indicator microorganisms in the soil. At later sampling times (greater than or equal to 14 h) infiltration has ceased; redistribution and evapotranspiration of water depletes water from the root zone (Figure 4.2a). In general, the concentration of the indicator microorganisms in the soil cores is controlled at earlier sampling times (t=14 and 62 h) by initial conditions and microbe retention, and at later times (t=134 and 206) by microbe survival and/or inactivation. Microbe retention tends to be highest at the soil surface and to rapidly decrease with soil depth. Survival of fecal coliforms, somatic coliphage, and total *E. coli* was apparently short lived under these NMP conditions, with concentrations in soil approaching low background levels within 134 h after wastewater application. This result is at least partly due to the high summer soil temperature which averaged 22.6°C at a depth of 7 cm during this experiment. Cooler temperatures that were measured during the winter growing season (20.3°C at a depth of 7 cm) are expected to enhance microorganism survival (Reddy et al., 1981; Yates et al., 1987) shown

in Figure 4.1. Conversely, final concentrations of *Enterococcus* in soil were more pronounced than the other indicator microbes. This may occur as a result of differences in survival or due to differences in the initial concentration in these microbes in the soil ( $C_T$  was 5E4 and 1.3E4 CFU cm<sup>-3</sup> for *Enterococcus* and fecal coliform, respectively) and wastewater ( $C_i$  in the wastewater was 8.9E04 and 1.7E3 CFU ml<sup>-1</sup> for *Enterococcus* and fecal coliform, respectively).

A more quantitative determination of the transport and survival of the indicator microorganisms at the NMP site was not attempted due to the relatively low initial concentration levels of these microbes in the irrigation water and our analytical detection limits, potential spatial variability in microbe concentrations in the field, incomplete control of the lower water flow boundary conditions, and transients in water content that were induced by infiltration, redistribution, and ET. Laboratory experiments that are described below were initiated to overcome many of these limitations.

#### **Laboratory Experiments**

Figure 4.3 presents results from the batch survival experiments conducted under sterile (Figure 4.3a) and native (Figure 4.3b) conditions at 80% water saturation for the various indicator microorganisms. A semi-log plot of  $C_T/C_{T_0}$  as a function of time is shown in this figure. The considered bacterial indicator microorganisms had much greater die-off under native than sterile conditions. This indicates that biotic factors such as predation and competition in native soil and wastewater had a significant influence on the survival of the considered bacterial indicator microorganisms. Other researchers have reported similar observations and this literature has been reviewed by Van Veen et al. (1997). Conversely, the somatic coliphage exhibited similar survival/inactivation under both sterile and native conditions, suggesting that abiotic factors controlled die-off/inactivation for this coliphage. The native condition is expected

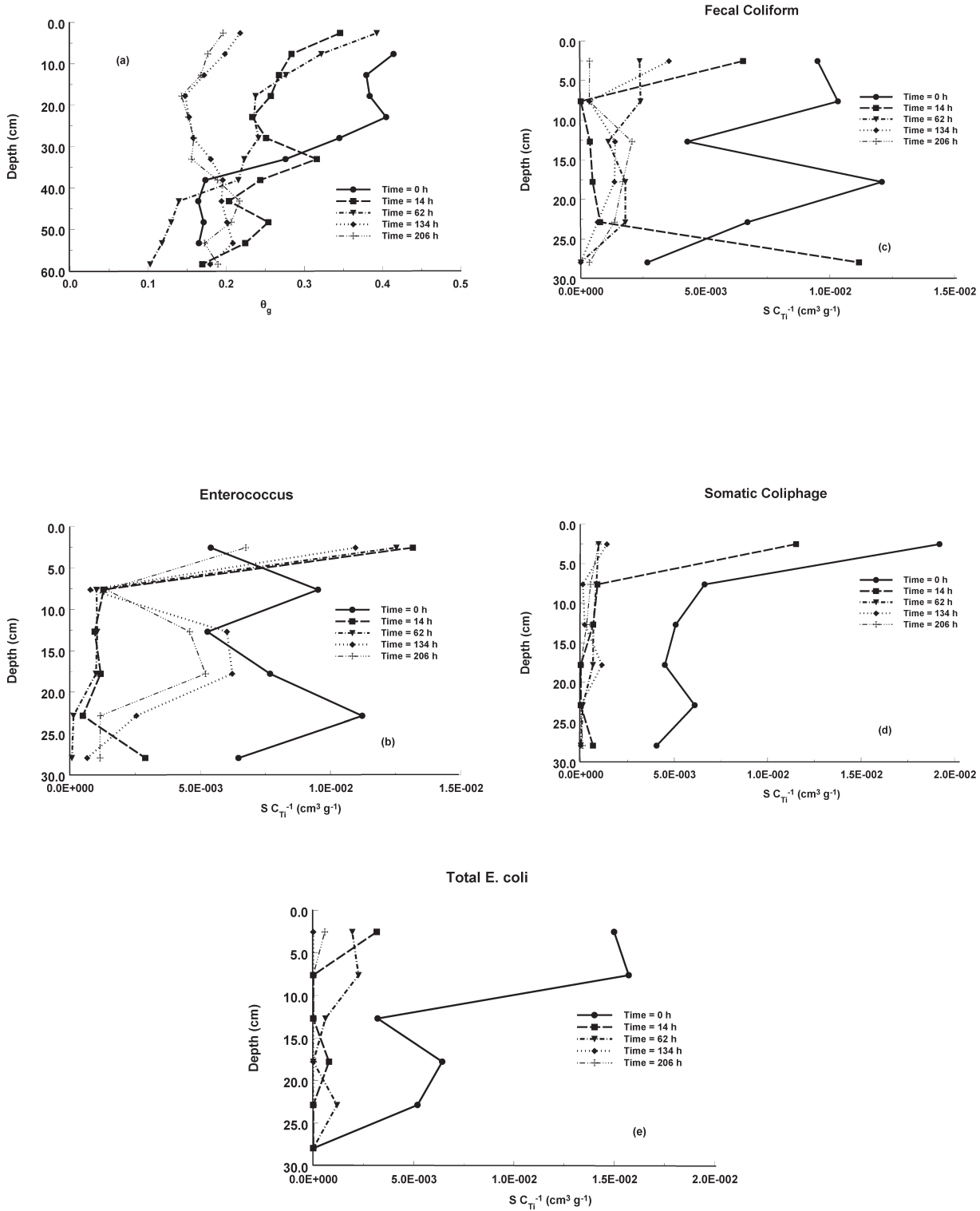


**Figure 4.2.** Plots of the gravimetric water content ( $\theta_g$ ) (Figure 4.2a), and the normalized concentration of Enterococcus (Figure 4.2b), fecal coliform (Figure 4.2c), somatic coliphage (Figure 4.2d), and total E. coli (Figure 4.2e) in soil ( $S/C_{Ti}$ ) as a function of depth at selected sampling times (initial, and times=0, 14, 62, 134, and 206 h after wastewater application) during the summer alfalfa growing season at the NMP field site. Microbial concentrations were determined from a composite of 3 soil cores at the indicated depth and time, and normalized by the total concentration of a given microorganism measured in the entire core at time=0 ( $C_{Ti}$ ).

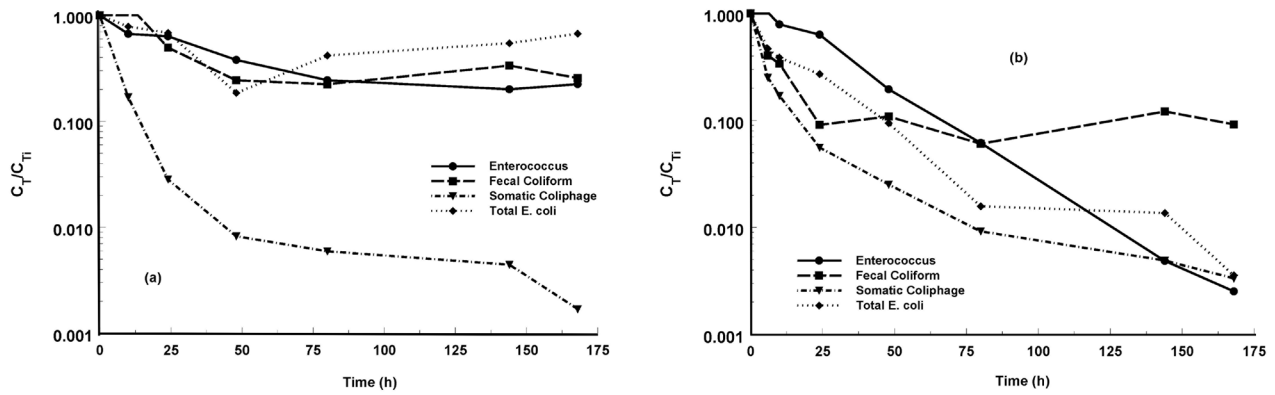


**Figure 4.3.** A semi-log plot of the relative total concentration ( $C_T/C_{Ti}$ ) as a function of time in batch survival experiments under sterile (Figure 4.3a) and native (Figure 4.3b) conditions at 80% water saturation for the various indicator microorganisms.

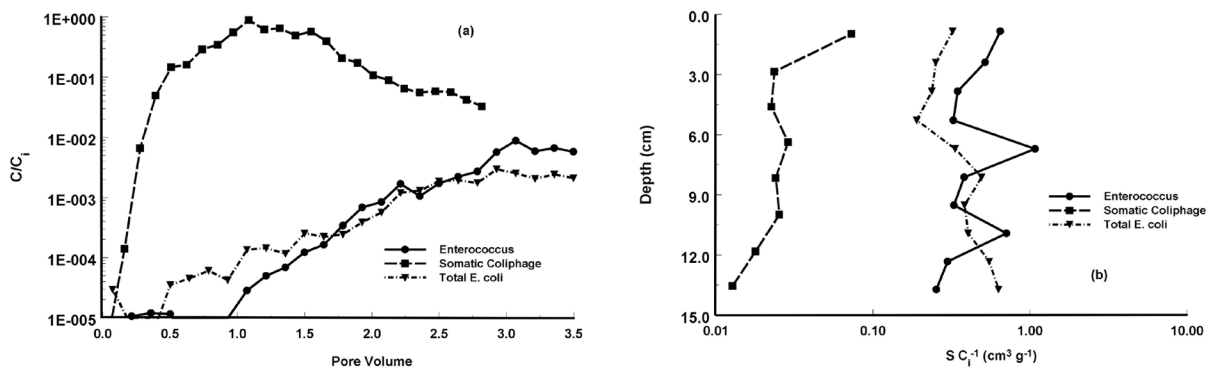
to be most representative of field conditions at the NMP site. Table 4.3 therefore provides a summary of the fitted die-off/inactivation rates (Equation 4.2) and the standard error coefficient on these parameters for the various indicator microorganisms under native conditions at 80% water saturation. The P values for statistical significance of the correlation coefficients were less than 0.00002. It is interesting to note that fecal coliforms had a lower die-off rate than *Enterococcus* under native conditions (Figure 4.3b and Table 4.3). This finding implies that the observed differences in final concentrations of these microbes in soil shown in Figure 4.2 was likely due to differences in the initial concentrations of these organisms in soil and wastewater. Packed soil column experiments were conducted using sterilized soil (sandy loam) from the root zone of the NMP field site to better understand the transport of the indicator microorganisms. The tracer solution consisted of sterilized (autoclaved) wastewater spiked with a known concentration of specific microorganisms, and sterilized well water was employed as the resident and eluant solutions.

Figure 4.4a presents breakthrough curves for *Enterococcus*, total *E. coli*, and  $\phi X174$  in the packed soil column. Relevant experimental

**Table 4.3.** Fitted parameters ( $\lambda_o$  and  $\alpha$ ) from the time dependent decay model (Equation 4.2) for the various indicator microorganisms under native conditions at 80% water saturation. The goodness of model fit is quantified by the coefficient of linear regression ( $R^2$ ) on natural log transformed data, and standard error coefficient of the fitted model parameters is provided in brackets.

Indicator	$\lambda_o$ ( $h^{-1}$ )	$\alpha$ ( $h^{-1}$ )	$R^2$
<i>Enterococcus</i>	3.52E-02 (1.31E-03)	3.54E-11 (4.32E-04)	0.992
fecal coliform	1.90E-01 (4.03E-02)	7.81E-02 (1.86E-02)	0.933
somatic coliphage	1.61E-01 (2.05E-02)	2.95E-02 (4.65E-03)	0.973
total <i>E. coli</i>	7.29E-02 (1.22E-02)	1.25E-02 (3.55E-03)	0.963

conditions are provided in the figure caption. The coliphage  $\phi X174$  exhibited much greater transport potential (87.1%) than the bacteria *Enterococcus* (0.6%) or *E. coli* (0.3%). This is likely due to differences in the size and surface chemistry of these microorganisms. In particular,  $\phi X174$  is much smaller than *Enterococcus* or *E. coli* (0.5-2 microns). Straining is therefore expected to play a more dominant role in retention of the bacterial



**Figure 4.4.** Breakthrough curves (Figure 4.4a) and retention profiles (Figure 4.4b) for *Enterococcus*, total *E. coli*, and  $\phi X174$  in a column experiment packed with sterilized field soil. In Figure 4.4a log relative concentrations ( $C/C_i$ ; where  $C$  is the aqueous concentration and  $C_i$  is the initial concentration in the influent suspension) are plotted as a function of pore volumes. In Figure 4.4b log relative concentrations in soil, ( $S/C_i$ ), is plotted as a function of distance away from the inlet. Relevant experimental conditions include the following parameters: porosity=0.50, column length=14.4 cm, tracer pulse duration=112.5 min, and the Darcy water velocity=3.36  $cm h^{-1}$ .

cells than the coliphage based on size considerations (Bradford et al., 2003). It is interesting to note that the breakthrough curve for both *Enterococcus* and *E. coli* exhibited a similar shape and magnitude in the relative concentrations, with initially low effluent concentrations that slowly increased with time. This observation suggests the potential for low but persistent amounts of bacteria transport that were likely due to slow release of cells from the solid phase, i.e., detachment, hydrodynamic shearing, or diffusion from low velocity regions (Bradford and Torkzaban, 2008).

After recovery of the breakthrough curve, the soil in the column was excavated to recover the remaining cells in the column. Figure 4.4b presents the microorganism retention profiles for *Enterococcus*, total *E. coli*, and  $\phi X174$  in the packed soil column. Consistent with the breakthrough curve information the total amounts of microbes recovered in the soil were 7.8, 83, and 109% for  $\phi X174$ , *E. coli*, and *Enterococcus*, respectively. Reasonable mass balance was achieved in this packed column experiment (83 to 109%). Batch results shown in Figure 4.3a indicate that little death or growth of the

indicator microorganisms was likely to occur during the column experiments (<6.25 h). Hence, the mass balance information supports our methodology for determining microorganism concentrations in the field. It should also be mentioned that the collected retention profiles for the microorganisms were not log-linear with depth; i.e., the rate of retention was not first-order. The observed nonmonotonic shape of the retention profiles for the bacteria cells likely reflected the release and continued slow migration of cells through the soil. Other researchers have reported nonmonotonic profiles for bacteria in porous media and this shape has been reported to be sensitive to the soil grain size, the system hydrodynamics, and the sampling time (Tong et al., 2005; Bradford et al., 2006b). In contrast, the retention profile for  $\phi X174$  shows enhanced retention near the column inlet that decreased with distance. In the literature this type of depth dependent retention has been attributed to straining (Bradford et al., 2006a) as well as chemical heterogeneity of the microorganisms (Li et al., 2004; Tufenkji and Elimelech, 2005).

Collectively, Figures 4.4a and 4.4b demonstrate the complexity of microorganism

transport and retention behavior in soil from the NMP site. In this work we do not attempt to quantify and simulate the exact retention mechanisms, as this would require additional experiments and model development that are beyond the scope of this manuscript. In addition, application of laboratory retention information collected under saturated conditions to predict transport of the microorganisms at the NMP site is complicated by the sensitivity of microorganism retention to water content, transients, and fluid velocity. The interested reader is referred to the following literature that discusses current challenges in modeling microorganism retention in porous media (Bradford and Toride, 2007; Bradford and Torkzaban, 2008).

Wastewater application under ponded infiltration conditions represents a worst case scenario for microorganism transport, because more conductive pore spaces and soil structure are water filled under saturated conditions. An additional transport experiment was therefore conducted on an undisturbed column from the NMP site (core length was 65 cm and the internal diameter was 24 cm), with wastewater instantaneously added to the soil surface to a depth of 7 cm. Figure 4.5 presents plots of the normalized concentration of the indicator microorganisms in soil as a function of depth at a sampling time of 24 h. In this case, the infiltrate front has already passed through the column and water is slowing redistributing (data not shown). High concentrations of the indicator microorganisms occur near the soil surface and then tend to rapidly decrease with depth. This mainly reflects microbe retention behavior. Figure 4.5 also indicates the presence of isolated low concentrations of bacterial indicators at several deeper depths (27.94 and 53.34 cm). The concentrations at these locations likely reflect the influence of soil structure or low levels of bacteria release and migration as previously identified in Figure 4.4.

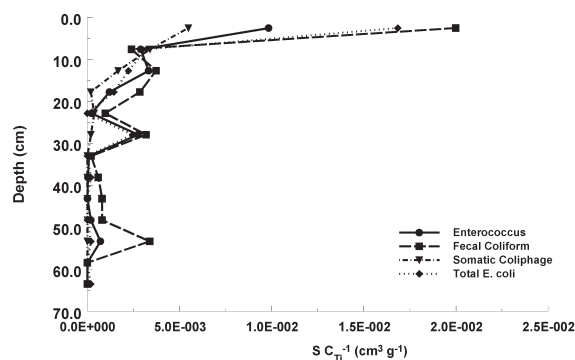


**Figure 4.5.** Plots of the normalized concentration of the indicator microorganisms in soil ( $S/C_T$ ) as a function of depth at a sampling time of 24 h after ponded infiltration of wastewater ceased on the undisturbed soil core from the NMP site. Here the concentration in soil is normalized by the total concentration of a given microorganism measured in the entire core at time = 0 ( $C_T$ ).

It should be mentioned that analysis of the column effluent and soil at the column outlet from the undisturbed core did not reveal any indicator microorganisms for all core sampling times (24, 48, 96, and 176 h). Soil cores taken at later sampling times primarily reflected the influence of indicator microorganism survival and may be analyzed in a similar fashion to the batch survival experiments by plotting the log of  $C_T/C_T$  for the entire core as a function of time in Figure 4.6. Survival information obtained from batch experiments under native conditions and 80% water saturation were generally consistent with results shown in Figure 4.6. After 176 h the batch and undisturbed column values of  $C_T/C_T$  were 0.003 and 0.006 for *Enterococcus*, and 0.003 and 0.005 for somatic coliphage, respectively. The total concentrations of fecal coliform and total *E. coli* in the undisturbed column could only be detected up to 96 and 48 h, respectively, but were similar in magnitude to native batch experiments at these times (compare with Figure 4.3b).

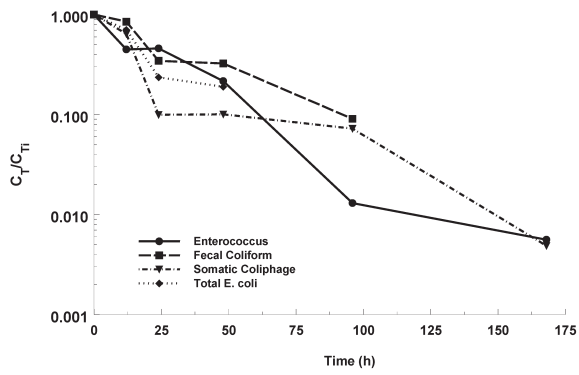


**Figure 4.6.** A semi-log plot of the relative total concentration ( $C_T/C_{T0}$ ) of the various indicator microorganisms as a function of time in the ponded infiltration undisturbed soil column experiment. Here the total concentration in soil is normalized by the total concentration of a given microorganism measured in the entire core at time = 0 ( $C_{T0}$ ).

## 5.0

# Laboratory Studies Investigating Mechanisms of Colloid Retention

### Background

Recent experimental and theoretical research has indicated that the pore structure and the solid-water-air triple point can play an important role in colloid and microorganism retention under unfavorable attachment conditions (Cushing and Lawler, 1998; Bradford et al., 2002, 2003, 2004, 2005, 2006abcd; Li et al., 2004, 2006ab; Tufenkji et al., 2004; Bradford and Bettahar, 2005 and 2006; Foppen et al., 2005). Pore spaces occurring at grain contacts and triple points provide optimum locations for colloids that are weakly associated with the solid water interface (SWI) or the air-water interface (AWI) to be retained because of reduced hydrodynamic forces, size limitations, and adhesive interactions from multiple interfaces (Hoek and Agarwal, 2006). Enhanced retention of colloids in the smallest regions of the soil pore space formed adjacent to grain-grain contacts and the triple point has been referred to as straining (Cushing and Lawler, 1998; Bradford and Torkzaban, 2008).

Most published research on straining has focused on the role of physical factors such as the relative size of the colloid to the median grain diameter, and little attention has been given to the potential interrelated influence of solution chemistry and hydrodynamics on straining. Attachment under unfavorable conditions is known to be highly dependent on solution chemistry (e.g., Li et al., 2004; Tufenkji and Elimelech, 2004 and 2005a), and system hydrodynamics (Wang et al., 1981; Tan et al., 1994; Kretzschmar et al., 1997; Compere et al., 2001; Li et al., 2005). Under unfavorable attachment conditions, hydrodynamic forces may be sufficient to overcome weak adhesive interactions (Bergandahl and Grasso, 1999; Torkzaban et al., 2007). In this case, attached colloids may be lifted

from the solid surface and detach, or they may roll, skip or slide down gradient on the SWI and/or AWI to locations where the hydrodynamic shear is less significant. It is logical to anticipate that some of these mobilized colloids will be retained in small pore spaces formed at grain-grain contacts and the triple point. One can therefore expect that solution chemistry and hydrodynamic forces will play an important interrelated role in straining.

The objective of this research is to investigate the role of solution chemistry and system hydrodynamics on colloid transport and straining. Negatively charged latex microspheres and quartz sands were used in batch experiments and packed column studies that encompassed a range of solution ionic strength, Darcy water velocity, grain sizes, and water saturation. All experiments were conducted using electrolyte solution buffered to a pH of 10 to ensure highly unfavorable attachment conditions. Data analysis and interpretation was aided through interaction energy calculations, mass balance computation, mathematical modeling, and experimental determination of breakthrough curves and deposition profiles. Details on the saturated colloid transport experiments and results are given in Bradford et al. (2007), whereas Torkzaban et al. (2008a) discusses findings from the unsaturated colloid transport experiments. Only an abbreviated discussion is provided below.

### Materials and Methods

#### Colloids

Yellow-green fluorescent latex microspheres (Molecular Probes, Eugene, OR) were used as model colloid particles in the experimental studies (excitation at 505 nm, and emission at 515 nm). Two sizes of microspheres were used in the transport experiments,

1.1 and 3.0  $\mu\text{m}$ . The uniformity of the colloid size was verified using a Horiba LA 930 (Horiba Instruments Inc., Irvine, CA 92614) laser scattering particle size and distribution analyzer and by inspections of suspensions under an epi-fluorescent microscope. The microspheres had carboxyl surface functional groups, a density of  $1.055 \text{ g cm}^{-3}$ , and are reported as hydrophilic by the manufacturer. The initial influent concentration ( $C_i$ ) for the 1.1 and 3.0  $\mu\text{m}$  colloids for the experiments was  $2.7 \times 10^{10}$  and  $1.3 \times 10^9 N_c \text{ L}^{-1}$  (where  $N_c$  denotes number of colloids), respectively. Several experiments with the 1.1  $\mu\text{m}$  colloids were also conducted at a lower initial concentration of  $C_i = 6.8 \times 10^8 N_c \text{ L}^{-1}$ .

### **Sand**

Aquifer material used for the column experiments consisted of various sieve sizes of Ottawa sand (U.S. Silica, Ottawa, IL). The porous media were selected to encompass a range in grain sizes, and are designated by their median grain size ( $d_{50}$ ) as: 360, 240, and 150  $\mu\text{m}$ . Specific properties of the 360, 240, and 150  $\mu\text{m}$  sands include: the coefficient of uniformity ( $d_{60}/d_{10}$ ; here 10 and 60% of the sand mass is finer than  $d_{10}$  and  $d_{60}$ , respectively) of 1.88, 3.06, and 2.25; and intrinsic permeabilities of  $6.37 \times 10^{-11}$ ,  $1.12 \times 10^{-11}$ , and  $4.68 \times 10^{-12} \text{ m}^2$ , respectively. Ottawa sands typically consist of 99.8%  $\text{SiO}_2$  (quartz) and trace amounts of metal oxides, have spheroidal shapes, and contain relatively rough surfaces. An estimate of the pore-size distribution for these sands can be obtained by using Laplace's equation of capillarity and measured capillary pressure - saturation curves presented by Bradford and Abriola (2001).

### **Electrolyte Solution Chemistry**

The background electrolyte solutions utilized in the column studies consisted of deionized water with a buffered pH of 10 achieved with 1.7 mM  $\text{NaHCO}_3$  and 1.7 mM  $\text{Na}_2\text{CO}_3$  (Cherrey et al., 2003). This solution chemistry was chosen to create a stabilized

mono-dispersed suspension with the selected colloids. In particular, at a pH of 10 quartz and iron oxides possess a net negative charge (Tipping, 1981; Redman et al., 2004), and any attractive electrostatic interactions between the colloids and porous media is expected to be minimized at this pH. The ionic strength (IS) of the eluant, resident, and tracer solutions in the transport experiments was varied between 6-106 mM using this same pH 10 solution by changing the amounts of added NaCl, KCl, or NaBr. Unless specifically indicated, the concentrations of resident, tracer, and eluant solutions were maintained over the course of an experiment.

### **DLVO Calculations**

Derjaguin, Landau, Verwey and Overbeek (DLVO) theory (Derjaguin and Landau, 1941; Verwey and Overbeek, 1948) was used to calculate the total interaction energy (sum of London-van der Waals attraction and electrostatic double-layer repulsion) for our 1.1 and 3  $\mu\text{m}$  colloids upon close approach to quartz surfaces (assuming sphere-plate interactions) for the various solution chemistries (pH=10, and IS=6-106 mM). In these calculations, constant-potential electrostatic double layer interactions were quantified using the expression of Hogg et al. (1966) and zeta potentials in place of surface potentials. Retarded London-van der Waals attractive interaction force was determined from the expression of Gregory (1981) utilizing a value of  $4.04 \times 10^{-21} \text{ J}$  for the Hamaker constant (Bergendahl and Grasso, 1999) to represent our polystyrene latex-water-quartz system. The zeta potential of the quartz at pH 10 and for IS ranging from 6 to 106 mM was estimated using results presented in Elimelech et al. (2000) and Redman et al. (2004). Zeta potentials for our 1.1 and 3  $\mu\text{m}$  colloids in the various solution chemistries that were used in the DLVO calculations were calculated from experimentally measured electrophoretic mobilities using a ZetaPals instrument (Brookhaven Instruments Corporation, Holtsville, NY).

### **Batch Experiments**

Batch experiments were conducted by placing 10 g of sand and 10 ml of a known initial concentration of colloid suspension into a polypropylene centrifuge tubes with the temperature kept at approximately 20°C. Three different ionic strength solutions (6, 30, 60 mM) buffered at pH 10 were used for making the colloid suspension. The suspension and sand were allowed to equilibrate for 2 h by gently rotating the tubes end over end (15 rpm) on a tube rotator (Fisher Scientific, San Diego, CA). The 2-h equilibration time was chosen to mimic the duration of the column experiments. A control experiment without colloids was also run for measuring the background concentration of colloids introduced from the sand. The initial and final concentrations of colloids in the suspension were determined using a spectrophotometer (Perkin Elmer LC95 UV/VIS spectrometer, Irvine, CA) after setting the tube to rest for a few minutes. All experiments were performed in duplicate.

### **Column Experiments**

Procedures and protocols for the saturated packed column glass (15 cm long and 4.8 cm inside diameter, equipped with an adjustable adapter at the top) experiments are reported in detail by Bradford et al. (2002 and 2007), whereas details on the unsaturated column (10 cm long and 5 cm inside diameter) experiments are provided in Torkzaban et al. (2008a). The columns were wet packed (water level kept above the sand surface) with the various sands. For saturated systems, the colloid suspension was pumped upward through the vertically oriented columns at a steady flow rate, after which a three-way valve was used to switch to the background solution.

The unsaturated column experiment was designed to accurately establish steady state flow and uniform saturation conditions. In this case, the sand in the column was drained to the desired water saturation level by reducing the inflow water rate to the hydraulic conductivity corresponding to that saturation.

Simultaneously, the pressure head at the bottom of the column was gradually reduced until unit hydraulic gradient conditions were achieved (the only driving force for water flow was gravity), which implies a constant capillary pressure and saturation along the column. After establishing a specified saturation and water chemistry, colloid transport experiments were initiated by introducing a colloid suspension and then rinsing with background electrolyte.

Effluent samples from the column experiments were collected and analyzed for colloid concentration using a Turner Quantech Fluorometer (Barnstead/ThermoLyne, Dubuque, IA) or a spectrometer (Perkin Elmer LC95 UV/VIS spectrometer, Irvine, CA). The average of three measurements were used to determine each colloid concentration (reproducibility was typically within 1% of  $C_i$ ).

Following completion of the colloid transport experiments, the spatial distribution of retained colloids in each packed column was determined. The sand was carefully excavated into tubes containing excess eluant solution of the same IS and pH that was used in the transport experiment. The tubes were slowly shaken to liberate reversibly retained colloids. The concentration of the colloids in the excess aqueous solution was then measured with the fluorometer. The volume of solution and mass of sand in each tube was determined from mass balance.

A colloid mass balance was conducted at the end of each column experiment using effluent concentration data and the final spatial distribution of retained colloids in the sand. The calculated number of colloids in the effluent and retained in the sand was normalized by the total number of injected particles into a column.

### **Colloid Transport Model for Saturated and Unsaturated Systems**

The HYDRUS-1D code (Šimůnek et al., 2009) was used to simulate colloid transport and retention in the column experiments. Details

are given by Torkzaban et al. (2008a). In brief, the model includes provisions for transport by advection and dispersion, and two-site kinetic colloid retention/release with various time and depth dependent blocking functions. Colloid retention and release parameters for given conditions (e.g., ionic strength, water velocity and saturation, porous medium size, and colloid size) were obtained by nonlinear least squares optimization to the experimental data.

## Results and Discussion

Details on the experimental results are presented in Bradford et al. (2007) and Torkzaban et al. (2008a). In this section we focus our discussion on the interpretation and implications of these findings.

Experimental evidence in this study demonstrated that attachment to the SWI was not the dominant mechanism responsible for colloid retention. The first piece of indirect evidence was from the batch experiments in which no significant colloid attachment to the sand was observed. Additionally, the experimental protocol for determining the deposition profiles was based upon the rapid release of colloids into solutions, and high recoveries were not consistent with the low detachment rates that were observed in the column experiments. If the colloids were irreversibly attached to the SWI, they should have remained on the grain surface even after suspending the sand in the same solution that was used for the transport experiments. The next piece of evidence is the fact that colloid retention occurred in the column, even under conditions when DLVO calculations indicate the presence of a substantial energy barrier to colloid – SWI interaction. Finally, the colloid deposition profiles resulting from the column experiments were not consistent with first-order attachment-detachment model predictions (e.g., non-exponential).

Non-exponential deposition profiles in saturated conditions have been attributed to charge variability of the porous media

(Johnson and Elimelech, 1995), heterogeneity in colloid surface charge characteristics (Bolster et al., 1999; Li et al., 2004), and deposition of colloids in a secondary energy minimum (Redman et al., 2004; Tufenkji and Elimelech, 2005b). These factors may have been involved; however, these mechanisms cannot fully explain the experimental data. The experiments were conducted in a solution at a pH 10, which should minimize any effect of charge heterogeneity on the sand surface because the isoelectric points of most metal oxides fall below this pH (Elimelech et al., 2000). The results of our batch experiments and DLVO calculations do not support the existence of any significant heterogeneity on the grain or colloid surfaces. Furthermore, the colloids may be held in the secondary minima; however, this cannot explain the observed depth and sand size dependent deposition. Therefore, another retention mechanism must also be involved.

Retention of colloids under unsaturated conditions has also been attributed to partitioning at the AWI and/or film straining (e.g. Wan and Wilson 1994a; Wan and Tokunaga 1997; Sayers and Lenhart, 2003a; Lenhart and Sayers, 2002). However, attachment to the AWI is not believed to play a significant role in the reported unsaturated experiments, as both the AWI and colloids were negatively charged even in the highest ionic strength solution. It has been well documented that hydrophilic-negatively charged colloids are unlikely to attach to the negatively charged AWI (e.g. Wan and Tokunaga 2002; Crist et al. 2004, 2005; Torkzaban et al. 2006a, 2006b).

It is also unlikely that film straining is playing a major role in the reported colloid retention as the 1.1  $\mu\text{m}$  latex colloids are too large to be bound within a thin-film. These thin water films have calculated thicknesses around 50 nm during steady-state water flow – over an order of magnitude thinner than the diameter of the colloids used in this current study. Moreover, film straining is theoretically independent of solution ionic strength

and flow velocity (Wan and Tokunaga, 1997). In contrast, notably more colloid retention is observed in higher ionic strength solutions and for lower water velocities.

Straining of colloids provides a plausible explanation and mechanism for the observed colloid deposition behavior. Colloids can become trapped in small pores where the flow velocity is reduced. These nearly immobile regions include the small pores formed by narrow wedges that are defined by grain-to-grain contacts, dead-end pores, and the three-phase contact line of the solid-water-air interface (in case of unsaturated conditions). It is proposed that colloids are weakly associated with the SWI interface via the secondary energy minimum; hence, they are subject to fluid drag forces that can translate and/or funnel the colloids to the low velocity regions of the pore structure or “straining sites”. Earlier studies have observed similar trends by fluorescent microscopy and x-ray microtomography that colloids accumulate in the narrow region of the pore spaces near the contacts of irregularly shaped sand grains under unfavorable attachment conditions (Bradford et al., 2005, Li et al., 2006a, and Bradford et al., 2006b). In these studies, pore-space constrictions apparently served as locations for colloid retention by straining, whereas few colloids appeared to be immobilized far from the grain-to-grain contacts. Colloid retention in the pore network is further supported by Hoek and Agarwal (2006) who reported that DLVO forces act on colloids up to 5 times more in small pores than with a single flat surface. Straining, as the mechanism of colloid retention, is also supported by mass balance calculations and the fact that once the sand is resuspended in the solution and the pore structure eliminated, the colloids return to solution.

As noted previously, colloids that are weakly associated with the SWI via the secondary energy minima experience significant hydrodynamic forces (e.g., fluid drag, lift forces)

due to fluid flow. The shear force acting on the colloid surface held in the secondary energy minimum is different than that acting on the colloid surface in the bulk fluid. Consequently, at close range to the SWI the colloids experience a combination of forces (hydrodynamic forces, electrical double-layer repulsion, and London-van der Waals) which creates a torque and hence rotation on the surface (Bergendahl and Grasso 2000; Cushing and Lawler 1998). It is therefore hypothesized that colloids associated with secondary energy minima can be translated to regions of low velocity where there are no significant hydrodynamic forces present and they can remain attached even by a weak attraction force. Based on this argument, more colloids will be retained in a secondary energy minimum as ionic strength is increased and these colloids will subsequently be funneled to the straining sites. It is believed that colloids retained in straining sites can aggregate together depending upon the solution chemical conditions as it has been observed by Bradford et al. (2005), Li et al. (2006), and Bradford et al. (2006b). This hypothesis can also explain the observed decrease in colloid retention with increasing fluid velocity. In this case, enhanced hydrodynamic forces may overcome the electrostatic and van der Waals interactions and detach colloids from the grain surface. It is also possible that the extent of stagnation regions decreases as the water velocity increases. This is consistent with our observations and modeling results presented by Cushing and Lawler (1998).

It was anticipated that the magnitude of straining would be enhanced with decreasing sand size and water saturation level due to a greater amount of low velocity regions. Both of these expected trends were verified by our experimental observations. The extent of retention of colloids increased with ionic strength and soil grain size for all of the various saturation levels tested (Figure 5.1). With decreasing soil grain size, the peak effluent concentration was lower, indicating a greater

removal of colloids. This is especially true for the higher ionic strength conditions when very little breakthrough of colloids occurred. Comparison of the breakthrough curves for all of the ionic strength conditions reveals a decrease in peak effluent concentrations with water content. All these results provide substantial direct and indirect evidence that straining is an important removal mechanism for the CML colloids in the Ottawa sands investigated.

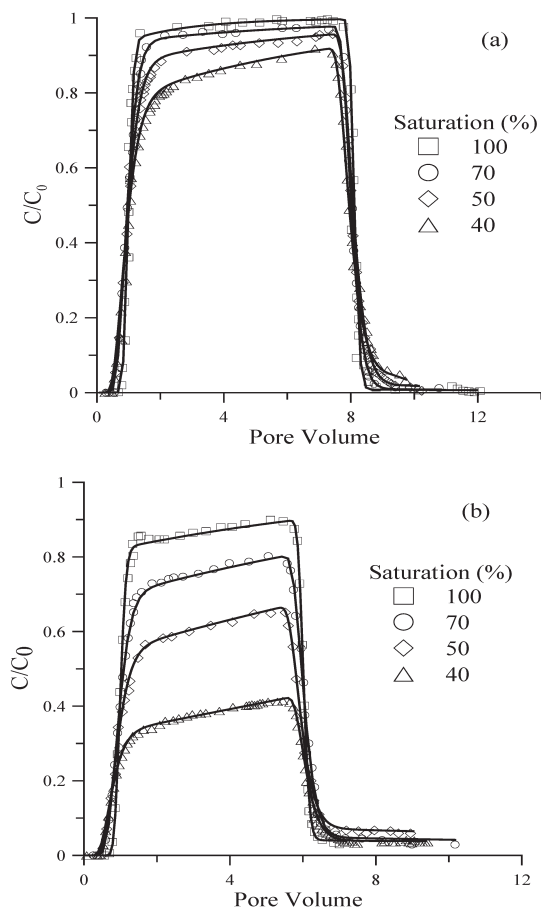


**Figure 5.1.** Observed and simulated breakthrough curves of colloids for various saturation levels in 360  $\mu\text{m}$  sand at an ionic strength of 6 mM (Figure 5.1a) and 30 mM (Figure 5.1b)

The comparison of experimental and modeled results also suggests that straining is the underlying mechanism in colloid deposition in both the saturated and unsaturated systems tested. The concentration of retained colloids

enumerated after the column experiments was found to exhibit hyper-exponential spatial distribution through the length of the column. This indicates the deposition coefficient was depth-dependent, a trend that has previously been associated with straining (e.g., Bradford et al., 2002, 2003, and 2006a).

All the observations discussed above provide convincing evidence that straining was the primary mechanism of colloid retention in our column experiments. The straining rate in a given porous medium is apparently a complicated mechanism, coupled with such parameters as pore size distribution, hydrodynamics, solution chemistry and water content. Specific findings are highlighted below.

- Straining increases in magnitude with increasing ionic strength due to an increased force (secondary energy minimum) and number of colloids that are funneled to and retained in small pores formed adjacent to grain-grain junctions.
- Straining increases in magnitude with water content due to an increase in the extent of stagnant regions of flow within the pore structure in lower water content.
- Increasing the flow rate of a system tends to decrease the amount of straining as a result of the increased fluid drag force that acts on weakly-attached colloids on the SWI and also decreased flow stagnation regions.
- The shape of the colloid deposition profile is highly sensitive to the physical (grain size, water content, and flow rate) and chemical (solution IS and pH) properties of a system due to the interrelation of these parameters on colloid straining.

Additional research is required to better understand and quantify the coupling of physical and chemical processes that influence colloid straining in saturated and unsaturated porous media. This information is believed to be essential for predicting colloid transport and fate in many natural environments.

## 6.0

# Mathematical Models to Simulate Pathogen and Nutrient Fate

### Background

Most models for microorganism retention in porous media have been based on filtration theory (Yao et al., 1971, Rajagopalan and Tien, 1976). These models have typically only considered the average pore-water velocity in the porous medium and a single first-order attachment rate coefficient which predicts that the profile of retained colloids in porous media will decrease exponentially with distance. Under unfavorable attachment conditions, these models have commonly been found to be inadequate to predict the amount of retention, the shape of the deposition profile, and the dependence of colloid retention on velocity, solution chemistry, and grain and colloid size (Bradford et al., 2003, 2006a, 2007; Tufenkji and Elimelech, 2005ab; Tong et al., 2005; Li and Johnson, 2005; Li et al., 2005; Johnson et al., 2007; Torkzaban et al., 2007 and 2008a).

Recent research has demonstrated that colloid and microorganism retention in porous media does not solely depend on the strength of the adhesive interaction (Bradford et al., 2007 and 2009; Bradford and Torkzaban, 2008b; Johnson et al., 2007; Torkzaban et al., 2007 and 2008; Duffadar and Davis, 2008; Shen et al., 2008; Kim et al., 2009ab). Findings suggest that colloid retention in porous media is a strongly coupled process that depends on the chemistry of the aqueous and solid phases, as well as the pore structure and surface roughness, the colloid size and concentration, and water velocity. In particular, it has been reported that weakly associated colloids with the solid-water interface via the secondary minimum or nanoscale heterogeneity may experience significant hydrodynamic forces due to fluid flow that may result in rolling, sliding, skipping, or detachment of colloids

on/from the collector surface (Bradford and Torkzaban, 2008b; Torkzaban et al., 2007 and 2008b; Duffadar and Davis, 2008). Some of these weakly associated colloids can be translated and/or funneled by fluid drag force to low velocity regions in small pore spaces and “eddy zones” which occur near some grain-grain contacts and surface roughness locations where they can be retained (Bradford and Torkzaban, 2008b; Torkzaban et al., 2007 and 2008b). Indeed, recent experimental evidence by Kuznar and Elimelech (2007) demonstrates that weakly interacting colloids can be translated along the collector surface via hydrodynamic forces and be retained in regions near the rear stagnation point.

The above literature indicates that, under unfavorable attachment conditions, colloid retention will be enhanced in the low velocity regions of the porous medium. It is therefore not surprising that models that consider only the average pore water velocity and a single attachment coefficient have been found to be inadequate to predict colloid retention behavior in many instances. Below, we discuss alternative model formulations that can be used to account for different colloid retention mechanisms in the various regions of the pore space. Specific model formulations that will be discussed include: a combined physical-chemical nonequilibrium model (Leij and Bradford, 2009), the dual permeability model (Bradford et al., 2009), and the stochastic stream tube model (Bradford and Toride, 2007). A brief description of the applications, implications, and limitations of these models to characterize colloid/microorganism transport and retention will be discussed. Although specific examples are provided below for colloid transport in homogeneous porous media, these same

models are well designed to simulate colloid transport in the field.

### Physical Chemical Nonequilibrium (PCNE) Model

The two governing equations for transport of a colloid in a porous medium with mobile and immobile regions of water are defined as:

$$\theta_m \frac{\partial C_m}{\partial t} + \theta_{im} \frac{\partial C_{im}}{\partial t} + \rho_b \frac{\partial S}{\partial t} = \theta_m D_m \frac{\partial^2 C_m}{\partial z^2} - \theta_m v_m \frac{\partial C_m}{\partial z} \quad [6.1]$$

$$\theta_{im} \frac{\partial C_{im}}{\partial t} + \rho_b \frac{\partial S_{im}}{\partial t} = \alpha(C_m - C_{im}) \quad [6.2]$$

where  $\theta$  is the volumetric water content, the subscripts  $m$  and  $im$  refer to the mobile and immobile region,  $C$  is colloid concentration in aqueous phase [N/L<sup>3</sup>],  $S$  is solid phase concentration of colloid from either the mobile or immobile region per mass of dry soil [N/M],  $\rho_b$  is dry soil bulk density [M/L<sup>3</sup>],  $D$  is dispersion coefficient [L<sup>2</sup>/T],  $v$  is pore-water velocity [L/T],  $\alpha$  is a physical nonequilibrium (PNE) coefficient for mass transfer between mobile and immobile region [1/T],  $z$  is depth [L], and  $t$  is time [T].

The aqueous phase consists of mobile and immobile regions. The solid phase of the soil is either in contact with the mobile or immobile aqueous region, colloid may be retained or released from the solid phase. Without considering the actual mechanism for colloid retention, the following equalities hold:

$$\begin{aligned} \theta_m + \theta_{im} &= \theta, & \theta_m v_m &= \theta v \\ \theta_m D_m &= \theta D, & S_m + S_{im} &= S \end{aligned} \quad [6.3a,b,c,d]$$

The chemical nonequilibrium (CNE) component is introduced by further distinguishing between equilibrium (type 1) and kinetic (type 2) retention:

$$S_m = S_{m,1} + S_{m,2}, \quad S_{im} = S_{im,1} + S_{im,2} \quad [6.4a,b]$$

Colloid retention on type-1 sites is an equilibrium process described by:

$$S_{m,1} = K_{m,1} C_m, \quad S_{im,1} = K_{im,1} C_{im} \quad [6.5a,b]$$

with  $K$  as a “distribution” constant expressed as volume of aqueous phase (either the “mobile” or “immobile” region) per mass of dry soil [L<sup>3</sup>/M]. Retention on type-2 sites is governed by a first-order rate equation:

$$\frac{\partial S_{m,2}}{\partial t} = \beta_m (K_{m,2} C_m - S_{m,2}), \quad [6.6a,b]$$

$$\frac{\partial S_{im,2}}{\partial t} = \beta_{im} (K_{im,2} C_{im} - S_{im,2})$$

The retention rate is proportional to the difference in (eventual) equilibrium and actual solid phase concentration with  $\beta$  as the proportionality constant [1/T]. These coefficients are likely to be different for retention from the mobile and immobile regions. For both regions a ratio of “equilibrium” to “total” sites may be defined. At equilibrium these follow from the solid phase concentrations or the distribution coefficients according to:

$$f_m = \frac{S_{m,1}}{S_m} = \frac{K_{m,1}}{K_m}, \quad [6.7a,b]$$

$$f_{im} = \frac{S_{im,1}}{S_{im}} = \frac{K_{im,1}}{K_{im}}$$

The total concentration, which is given as mass per volume of bulk soil, is defined as:

$$C_T = \theta_m C_m + \theta_{im} C_{im} + \rho_b (S_m + S_{im}) \quad [6.8]$$

At equilibrium, the total concentration is given by:

$$\begin{aligned} C_T &= \theta R C_m \\ &\text{with } R = 1 + \rho_b K / \theta \\ &\text{and } K = K_m + K_{im} \end{aligned} \quad [6.9]$$

where  $R$  is a retardation factor.

The system of mathematical equations that needs to be solved is as follows:

$$\begin{aligned} \theta_m \frac{\partial C_m}{\partial t} + \theta_{im} \frac{\partial C_{im}}{\partial t} + \rho_b \left( f_m K_m \frac{\partial C_m}{\partial t} + \frac{\partial S_{m,2}}{\partial t} + f_{im} K_{im} \frac{\partial C_{im}}{\partial t} + \frac{\partial S_{im,2}}{\partial t} \right) \\ = \theta_m D_m \frac{\partial^2 C_m}{\partial z^2} - \theta_m v_m \frac{\partial C_m}{\partial z} \end{aligned} \quad [6.10a]$$

$$\theta_{im} \frac{\partial C_{im}}{\partial t} + \rho_b \frac{\partial S_{im}}{\partial t} = \alpha(C_m - C_{im}) \quad [6.10b]$$

$$\frac{\partial S_{m,2}}{\partial t} = \beta_m [(1 - f_m) K_m C_m - S_{m,2}] \quad ,$$

$$\frac{\partial S_{im,2}}{\partial t} = \beta_{im} [(1 - f_{im}) K_{im} C_{im} - S_{im,2}]$$

[6.10c,d]

The problem will be rewritten with only  $C_m$  as dependent variable. The selected mathematical conditions involve a zero initial condition and a time-dependent input  $C_o(t)$ :

$$C_m(\mathbf{z}, 0) = 0 \quad [6.11]$$

$$C_m(0, t) = C_o(t) \quad , \quad C_m(\infty, t) = 0 \quad [6.12a,b]$$

The advection-dispersion equation was adapted to separately account for physical and chemical nonequilibrium during transport of solutes and colloids in porous media. In the resulting physical-chemical nonequilibrium (PCNE) model the aqueous phase is partitioned into an immobile and a mobile aqueous region. Based on equilibrium or nonequilibrium interaction of colloids with the solid phase, four types of solid domains may be distinguished.

An analytic solution for the PCNE model described above was obtained by Leij and Bradford (2009). Expressions for the first three time moments of the solutions are presented in Table 6.1. These may be used to elucidate the impact of transport parameters on the mean, variance, and skewness of breakthrough curves. There are several reasons to have analytical tools available to quantify PNCE transport. Analytical methods are useful to verify numerical methods, elucidate the role of different model parameters, and to approximately quantify transport such as for longer time or spatial scales. The derived analytical tools for the PCNE model also offer the flexibility to independently quantify the impact of a “chemical” and “physical” nonequilibrium process on colloid transport.

The sensitivity of the breakthrough curves to model parameters was illustrated by Leij and Bradford (2009) for different types of non-equilibrium using the analytical solution for the PCNE model. The simplest cases involve the dependency of the curve on the PNE parameter  $\theta_m/\theta$  and the CNE parameters  $f_m$  and  $f_{im}$  in the presence of physical nonequilibrium. The curves exhibit the characteristic features of earlier breakthrough and more tailing with increased nonequilibrium. However, the shape of the curves is not very sensitive to the parameter values. On the other hand, the shape of the curve will change with different combinations of the PCNE parameters  $\alpha$  and  $\beta$ . The additional parameters in the PCNE allow greater flexibility to generate different types of breakthrough curves. The moment results of Table 6.1 were used to predict contours of mean, variance, and skewness of the colloid breakthrough curve as a function of either  $\log \alpha$  and  $\log k_{im,a}$  or  $\theta_{im}$  and  $\log k_{im,a}$ . This information illustrates the utility of having a model with independent physical and chemical nonequilibrium terms.

Colloid transport will be affected by physical nonequilibrium because pores are not (readily) accessible and by chemical nonequilibrium due to (different) attachment and detachment rates. These nonequilibrium phenomena are intertwined because attachment/detachment rates depend on the flow regime. The PCNE model, with its ability to independently model physical and chemical nonequilibrium, was therefore applied to four colloid breakthrough experiments by Bradford et al. (2002). It should be noted that independently quantifying physical and chemical nonequilibrium processes will become more useful for transport in natural porous media where non-equilibrium phenomena may no longer be ignored.

#### **Dual-Permeability Model**

Dual-permeability models have commonly been used to study preferential and non-equilibrium flow and solute transport in

**Table 6.1.** Expressions for the second- and third-order moments for breakthrough after a Dirac delta input according to physical nonequilibrium (PNE), chemical nonequilibrium (CNE), and PCNE models. The first-order moment is equal to  $Rz/v$  for all the models.

Model	Moment	Expression
PNE	$M_2$	$z \left[ \frac{R^2}{v^3} (2D + vz) + \frac{2\theta_{im}^2 R_{im}^2}{\alpha \theta v} \right]$
CNE	$M_2$	$z \left[ \frac{R^2}{v^3} (2D + vz) + \frac{2R_2}{\beta v} \right]$
PCNE	$M_2$	$z \left\{ \frac{R^2}{v^3} (2D + vz) + \frac{2}{\theta v} \left[ \frac{\theta_{im}^2 R_{im}^2}{\alpha} + \frac{\theta_{im} R_{im,2}}{\beta_{im}} + \frac{\theta_m R_{m,2}}{\beta_m} \right] \right\}$
PNE	$M_3$	$z \left[ \frac{R^3}{v^5} (12D^2 + 6Dvz + v^2 z^2) + \frac{6\theta_{im}^2 R_{im}^2}{\alpha \theta v} \left( \frac{R}{v^2} (2D + vz) + \frac{\theta_{im} R_{im}}{\alpha} \right) \right]$
CNE	$M_3$	$z \left[ \frac{R^3}{v^5} (12D^2 + 6Dvz + v^2 z^2) + \frac{6R_2}{\beta v} \left( \frac{R}{v^2} (2D + vz) + \frac{1}{\beta} \right) \right]$
PCNE	$M_3$	$z \left[ \frac{R^3}{v^5} (12D^2 + 6Dvz + v^2 z^2) + \frac{6}{\theta v} \left[ \frac{\theta_{im}^2 R_{im}^2}{\alpha} \left( \frac{R}{v^2} (2D + vz) + \frac{\theta_{im} R_{im}}{\alpha} \right) + \frac{\theta_{im} R_{im,2}}{\beta_{im}} \left( \frac{R}{v^2} (2D + vz) + \frac{1}{\beta_{im}} + \frac{2\theta_{im} R_{im}}{\alpha} \right) + \frac{\theta_m R_{m,2}}{\beta_m} \left( \frac{R}{v^2} (2D + vz) + \frac{1}{\beta_m} \right) \right] \right]$

structured soils and fractured rocks (Šimůnek et al., 2003; Gerke, 2006; Šimůnek and van Genuchten, 2008). In this case, the dual-permeability model partitions the pore space into two regions that have fast (fracture) and slow (matrix) rates of advective and dispersive transport of solutes. In contrast to previous work, Bradford et al. (2009) used the dual-permeability model described herein to simulate the different colloid retention mechanisms that occur in fast (larger pore spaces - region 1) and slow (small pore spaces, dead end pores, and grain-grain contact points - region 2) velocity regions of homogeneous porous media. The dual-permeability model

has not been previously used to gain insight into enhanced colloid retention processes in low velocity regions of homogeneous porous media. The approach is somewhat analogous to multiphase flow and transport models that partition the pore space to regions accessible for the wetting (small pore spaces) and non-wetting (large pore spaces) phases. The small pore spaces in the dual-permeability model are assumed to maintain continuity by slow flow adjacent to the solid phase, in crevice sites near grain-grain contacts, and in small pores in the same way as the wetting phase in multiphase systems.

As indicated in the Background section, colloids that collide with solid surfaces in fast regions of the pore space experience different hydrodynamic forces than colloids in slow regions. The higher hydrodynamic forces in region 1 act to remove colloids from the solid surface, thus causing region 1 to be associated with lower rates of colloid retention. Colloid exchange in the aqueous phase may occur to and from “slow” water (region 2). In addition, in this work we also consider the potential for colloid exchange on the solid phase from fast to slow regions due to either rolling or sliding of colloids on the solid surface. The governing equations for water flow in the dual-permeability model are well known and are available in the literature (Gerke and van Genuchten, 1993a,b; Šimůnek and van Genuchten, 2008). The corresponding one-dimensional dual-permeability equations for local scale colloid transport and retention are as follows:

$$\frac{\partial(\theta_{w1}C_1)}{\partial t} = -\frac{\partial J_1}{\partial z} + \frac{\Gamma_s}{1-w} - \theta_{w1}k_1C_1 + \rho_{b1}k_{det1}s_1 \quad [6.13]$$

$$\frac{\partial(\theta_{w2}C_2)}{\partial t} = -\frac{\partial J_2}{\partial z} - \frac{\Gamma_s}{w} - \theta_{w2}k_2C_2 + \rho_{b2}k_{det2}s_2 \quad [6.14]$$

$$\frac{\partial(\rho_{b1}s_1)}{\partial t} = \theta_{w1}k_1C_1 - \rho_{b1}k_{det1}s_1 - \frac{\rho_{b1}k_{12}s_1}{1-w} \quad [6.15]$$

$$\frac{\partial(\rho_{b2}s_2)}{\partial t} = \theta_{w2}k_2C_2 - \rho_{b2}k_{det2}s_2 + \frac{\rho_{b1}k_{12}s_1}{w} \quad [6.16]$$

$$\Gamma_s = \omega(1-w)\theta_{w1}(C_2 - C_1) \quad [6.17]$$

where  $z$  [L] is distance,  $t$  [T] is time,  $C_1$  and  $C_2$  [ $N_c L^{-3}$ ;  $N_c$  denotes the number of colloids] are the liquid phase concentrations of colloids in regions 1 and 2,  $s_1$  and  $s_2$  [ $N_c M^{-1}$ ] are the solid phase concentrations of colloids in regions 1 and 2,  $\theta_{w1}$  and  $\theta_{w2}$  are the volumetric water contents in regions 1 and 2 [-],  $\rho_{b1}$  and  $\rho_{b2}$  are the bulk densities in regions 1 and 2 [ $M L^{-3}$ ],  $k_1$  and  $k_2$  [ $T^{-1}$ ] are the first order colloid

retention rate coefficients in regions 1 and 2,  $k_{det1}$  and  $k_{det2}$  [ $T^{-1}$ ] are the first order detachment coefficients in regions 1 and 2,  $J_1$  and  $J_2$  [ $N_c L^{-2} T^{-1}$ ] are the total solute fluxes (sum of the advective and dispersive flux) for colloids in regions 1 and 2,  $\omega$  [ $T^{-1}$ ] is a coefficient for colloid exchange between liquids in regions 1 to 2,  $k_{12}$  [ $T^{-1}$ ] is a coefficient for transfer of colloids from solid phase region 1 to 2, and  $w$  is the ratio of the volume of region 2 to the total volume (volume of region 1 + volume of region 2). The term  $\Gamma_s$  [ $N L^{-3} T^{-1}$ ] accounts for aqueous phase mass exchange of colloids between regions 1 and 2.

Equations [6.13]-[6.17] were written in terms of local scale mass balances of regions 1 and 2. To formulate the equations in terms of the total pore space, the mass balance equations for regions 1 and 2 need to be multiplied by  $(1-w)$  and  $w$ , respectively. The relationship between several variables at the local scale and total pore space is provided below. Under steady-state flow conditions, the total water flux ( $q_t$ ;  $LT^{-1}$ ) is defined as:

$$q_t = (1-w)q_1 + wq_2 \quad [6.18]$$

where  $q_1$  ( $LT^{-1}$ ) and  $q_2$  ( $LT^{-1}$ ) are the local scale water fluxes in regions 1 and 2, respectively. Expressions for the total water content and bulk density are written in an analogous manner as Equation [6.18]. The total flux concentration of colloids ( $C_t$ ,  $N_c L^{-3}$ ) is given as (Šimůnek and van Genuchten, 2008):

$$C_t = \frac{wq_2C_2 + (1-w)q_1C_1}{wq_2 + (1-w)q_1} \quad [6.19]$$

and the total solid phase colloid concentration ( $s_t$ ,  $N_c M^{-1}$ ) as:

$$s_t = \frac{w\rho_{b2}s_2 + (1-w)\rho_{b1}s_1}{w\rho_{b2} + (1-w)\rho_{b1}} \quad [6.20]$$

The dual-permeability model outlined above has been implemented into the HYDRUS-1D computer model (Šimůnek et al., 2007; and Šimůnek and van Genuchten, 2008). The

code employs the Galerkin-type linear finite element method for spatial discretization of the governing differential equations, and a finite difference method to approximate temporal derivatives. A Crank-Nicholson finite difference scheme was used to solve the outlined transport equations sequentially (with equations for region 1 solved first). Complete details about the numerical techniques are provided in the HYDRUS-1D technical manual (Šimůnek et al., 2007). For the simulations discussed below, a third-type boundary condition was used at the inlet, and a concentration gradient of zero was fixed at  $z$  equal to the outlet depth. The initial concentration of the simulation domain was zero.

Bradford et al. (2009) performed a sensitivity analysis with the dual-permeability model parameters. Simulation results indicated that low amounts of advective transport to low velocity regions of the pore space had a dramatic effect on the shape of the retention profile, especially near the inlet boundary (Figure 6.1). The total water flow rate was also shown to have a significant influence on the shape of the colloid retention profile near the inlet boundary (Figure 6.2). In this case, higher water velocities were found to produce less colloid retention near the inlet boundary because greater amounts of colloids bypassed the low velocity regions. Both of these predictions are consistent with experimental observations that have been reported in the literature. Away from the inlet boundary, colloid retention was controlled by the deposition rate in the higher velocity region, and the aqueous and solid phase exchange rates. Example figures are shown below.

Published colloid transport and retention data that were obtained for unfavorable attachment conditions for a range of colloid and sand sizes, water velocities, and solution chemistries were described using the dual-permeability model. Fitted model parameters exhibited systematic trends with grain size, velocity, and solution chemistry. The

dual-permeability model provided a plausible interpretation for the experimental observations, and a reasonable approximation of the pore-scale physics controlling colloid retention under unfavorable attachment conditions.

### Stochastic Stream Tube Model

The CXTFIT program (Toride et al., 1995) served as the foundation for our stochastic modeling effort. This code includes the analytical solution for the one-dimensional advective dispersion equation with one-site kinetic chemical nonequilibrium deposition subject to various initial and boundary conditions. This model formulation is equivalent to the well-known first-order attachment and detachment model that is commonly employed to describe colloid transport and deposition (e.g., Harvey and Garabedian, 1991; Corapcioglu and Choi,

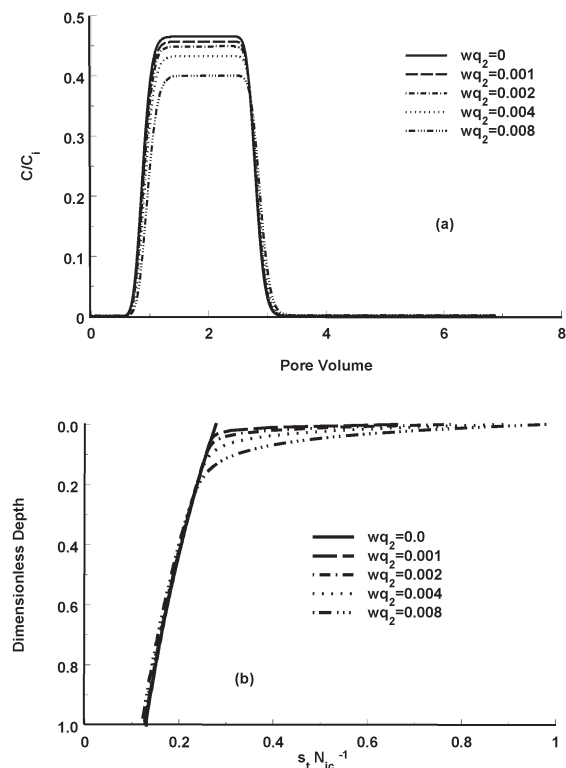


**Figure 6.1.** Plots of simulated breakthrough curves (Figure 6.1a) and retention profiles (Figure 6.1b) when  $q_t$  was equal to  $0.0918 \text{ cm min}^{-1}$  and the value of  $wq_2$  was 0, 0.001, 0.002, 0.004, and  $0.008 \text{ cm min}^{-1}$ .

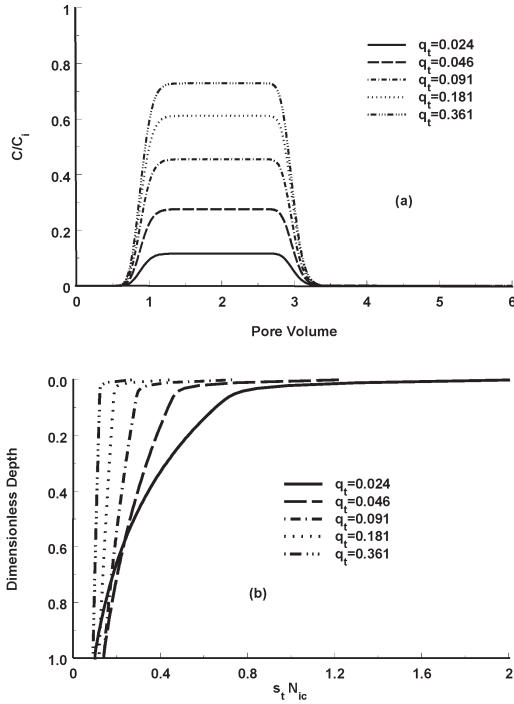


**Figure 6.2.** Plots of the simulated breakthrough curves (Figure 6.2a) and retention profiles (Figure 6.2b) when  $wq_2$  was  $0.001 \text{ cm min}^{-1}$  and  $q_t$  was equal to 0.024, 0.046, 0.091, 0.181, and 0.361  $\text{cm min}^{-1}$ . Other model parameters are provided in the manuscript text.

1996; Bolster et al., 1999; Schijven and Hassanizadeh, 2000). This analytical solution was used in conjunction with the stochastic stream tube model in CXTFIT to explore colloid transport and deposition. Details are provided in Bradford and Toride (2007).

The value of first-order deposition coefficient ( $k_d$ ) is typically assumed to be constant in colloid transport models. In the stochastic modeling approach, parameters may be defined by probability density functions. If  $k_d$  is considered to be stochastic, we assume a log-normal probability density function (PDF) that is defined as:

$$F(k_d) = \frac{1}{k_d \sigma_d \sqrt{2\pi}} \exp\left[-\frac{Y_d^2}{2}\right] \quad [6.21]$$

where  $\sigma_d$  is the standard deviation of the log-normal probability density function, and

$Y_d$  is the normalized log-transformed variable defined as:

$$Y_d = -\frac{\ln(k_d) - \mu_d}{\sigma_d} \quad [6.22]$$

Here  $\mu_d$  is the mean value of the log-normal probability density function defined as  $\mu_d = \ln(\langle k_d \rangle) - 0.5\sigma_d^2$ , where  $\langle k_d \rangle$  is the ensemble average of  $k_d$ . The subscript  $d$  is used on  $\sigma_d$ ,  $Y_d$ , and  $\mu_d$  to identify parameters associated with the deposition coefficient. Subscripts  $r$  and  $v$  are used in a similar fashion to identify parameters associated with the release coefficient and the pore water velocity, respectively.

If both  $k_d$  and  $k_r$  are assumed to be log-normal stochastic parameters that are correlated, then a joint probability density function is defined as:

$$F(k_d, k_r) = \frac{1}{2\pi\sigma_d\sigma_r k_d k_r \sqrt{1-\rho_{dr}^2}} \exp\left[-\frac{Y_r^2 - 2\rho_{dr}Y_r Y_d + Y_d^2}{2(1-\rho_{dr}^2)}\right] \quad [6.23]$$

The parameter  $\rho_{dr}$  is the correlation coefficient between  $Y_d$  and  $Y_r$  and is defined as:

$$\rho_{dr} = \langle Y_d Y_r \rangle = \int_0^\infty \int_0^\infty Y_r Y_d F(k_d, k_r) dk_d dk_r \quad [6.24]$$

When  $Y_d$  and  $Y_r$  are perfectly correlated then  $\rho_{dr} = 1$ , when they are uncorrelated  $\rho_{dr} = 0$ , and when they are perfectly inversely correlated  $\rho_{dr} = -1$ .

The mean aqueous and solid phase colloid concentrations at a given depth and time can also be determined for two log-normally distributed parameters  $k_d$  and  $k_r$  as:

$$\langle C(z, t) \rangle = \int_0^\infty \int_0^\infty C(z, t; k_d, k_r) F(k_d, k_r) dk_d dk_r \quad [6.25]$$

and

$$\langle S(z, t) \rangle = \int_0^\infty \int_0^\infty S(z, t; k_d, k_r) F(k_d, k_r) dk_d dk_r \quad [6.26]$$

where  $C(z, t; k_d, k_r)$  and  $S(z, t; k_d, k_r)$  are the aqueous and solid phase colloid

concentrations determined from the analytical solution of the advective dispersion equation with one-site kinetic chemical nonequilibrium. The variance in solid phase colloid concentrations is given as  $\langle S(z,t)S(z,t) \rangle - \langle S(z,t) \rangle^2$  when using the two parameter stochastic model. Alternatively, if  $k_d$  and  $v$  are stochastic and  $k_r$  is constant, Equation [6.23–6.26] can be rewritten by replacing  $k_r$  and  $v$ .

Simulation results presented in Bradford and Toride (2007) indicate that variations in the deposition coefficient and the average pore water velocity can both produce hyper-exponential deposition profiles. Bimodal formulations for the PDF were also able to produce hyper-exponential profiles, but with much lower variances in the deposition coefficient. The shape of the deposition profile was found to be very sensitive to the correlation of deposition and release coefficients, and to the correlation of pore water velocity and deposition coefficient (example simulations are shown below in Figure 6.3). Application of the developed stochastic model to a particular set of colloid transport and deposition data indicated that chemical heterogeneity of the colloid population could not fully explain the observed behavior. Alternative interpretations were therefore proposed based on variability of the pore size and the water velocity distributions.

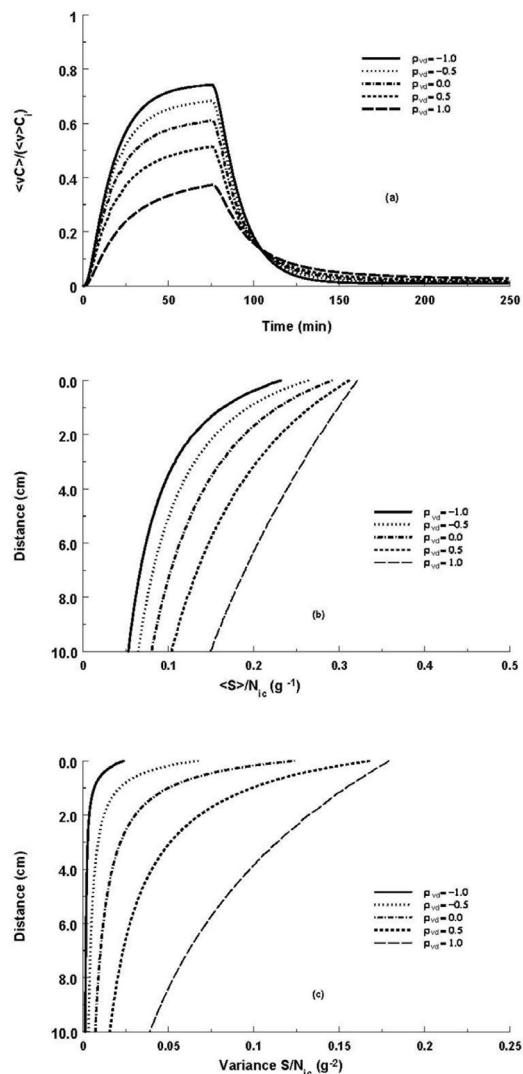


**Figure 6.3.** (a) Plot of the relative flux concentration,  $\langle vC \rangle / (\langle v \rangle C_i)$ , at a depth of 10 cm as a function of time when  $v$  and  $k_d$  are both stochastic parameters and values of  $\rho_{vd} = -1, -0.5, 0, 0.5,$  and  $1$ . (b, c) Corresponding normalized solid phase colloid concentration,  $\langle S \rangle / N_{ic}$ , and associated variance after 250 min with depth, respectively. Model parameters that were employed in these simulations were  $D = 0.0313 \text{ cm}^2 \text{ min}^{-1}$ ,  $\langle v \rangle = 0.313 \text{ cm min}^{-1}$ ,  $\langle k_d \rangle = 0.03 \text{ min}^{-1}$ ,  $k_r = 0.001 \text{ min}^{-1}$ ,  $\sigma_v = 1$ , and  $\sigma_d = 1$ .

# 7.0

## Summary and Conclusions

Concentrated animal feeding operations generate large volumes of manure-contaminated water that are typically stored in lagoons before land application. In Chapter 1 we review the current level of understanding on the environmental impact and sustainability of concentrated animal feeding operation (CAFO) wastewater reuse in agriculture. Specifically, we address the source, composition, application practices, environmental issues, transport pathways, and potential treatments that are associated with nutrients and pathogens in CAFO wastewater.

When applied to land at agronomic rates, CAFO lagoon water has the potential to be a valuable fertilizer and soil amendment that can improve the physical condition of the soil for plant growth and reduce the demand for high quality water resources. However, excess amounts of nutrients, organics with high biochemical oxygen demand, salts, heavy metals, pathogenic microorganisms, and pharmaceutically active compounds (antibiotics and hormones) in CAFO lagoon water can all adversely impact soil and water quality, as has been well documented in the literature. The current regulatory framework is based on nutrient management plans (NMPs) to ensure that lagoon water is applied to agricultural lands at agronomic rates to meet the nutrient demands of crops. Other lagoon water contaminants are implicitly assumed to be retained, inactivated, or degraded in the root zone. Additional studies are needed to thoroughly test these hypotheses.

Potential problems and weaknesses associated with the implementation of NMPs were identified in Chapter 1. One problem for proper NMP implementation is due to differences in the nutrient composition of lagoon water and the nutrient uptake rates by plants. A

second more critical issue concerns the accurate estimation and delivery of water to meet plant water demands. Potential errors in water balance may occur as a result of inaccuracies in estimates of potential evapotranspiration (PET), due to not accounting for all sources of plant available water, spatial variability of soil hydraulic properties and evapotranspiration (ET), nonuniform irrigation water application, and preferential water flow that bypasses the root zone. If water in excess of PET is applied (due to irrigation inefficiency or unforeseen natural causes) to or preferential water flow occurs at specific locations on a NMP site, lagoon water contaminants may also be transported below the root zone towards groundwater resources. Of special concern are contaminants that have limited ability to sorb to solid surfaces such as nitrate, or contaminants that can be associated with the mobile colloidal fraction of soil solution. Water in excess of PET will also lead to potential surface water contamination issues, especially for contaminants that are associated with sediments in runoff water such as phosphorus. If water application (from all water sources) is less than or equal to PET and preferential flow does not occur, then all lagoon water contaminants should remain in the root zone. In this case, potential environmental problems may occur due to accumulation of salts and/or survival of pathogens.

Mitigation of the environmental risks associated with the reuse of CAFO lagoon water on agricultural lands may require planning to prevent contamination, as well as various lagoon water treatments before use in NMPs. Prevention measures may include the wise choice of locations for CAFOs, proper manure management and modification of animal diets to minimize specific contaminants (e.g., pathogens). Potential treatments to CAFO

lagoon water include: use of solid-liquid separators; optimization of the design of lagoon water storage basins to remove sediment loads and nutrients (aerobic compared to anaerobic); and the adaptation of various municipal wastewater treatments such as chemical flocculants and/or soil treatments.

A nutrient management plan (NMP) was implemented in a semi-arid environment on a triticale and sorghum rotation during 2007 and on alfalfa during 2008, where nitrogen (N) was assumed to be the primary environmental concern. Chapter 2 discusses extensive research that was conducted to characterize flow and transport properties at this site. Chapters 3 and 4 discuss results pertaining to nutrients and indicator microorganisms, respectively. The NMP field site was designed to accurately measure the water and N mass balances in the root zone and to determine the fate of N, phosphorus (P), potassium (K) and other salts. Cyclic and blending dairy wastewater (DWW) application strategies, varying in nutrient application timing, were investigated during 2007. Only minor differences were found between these two strategies, therefore the key findings discussed below were valid for both conditions.

This NMP study was initiated under the conditions of high levels of soil organic N, which may be representative of historic manure and DWW application at many sites. Such conditions require that the soil organic N reservoir be taken into account in the N mass balance and this may induce difficulties in conservative NMP implementation that is protective of the environment due to: i) difficulties in estimation of mineralization rates and its spatial variability; ii) delayed availability of the organic N for plant uptake; iii) DWW can only be applied to meet a fraction of plant N uptake; and iv) continuous mineralization and potential nutrient leaching during fallow periods.

Based on these insights we implemented a conservative NMP in 2007 that depleted the

soil organic reservoir. This was achieved by applying only a fraction of the plant N uptake with DWW and using DWW that was treated to remove most of the suspended solids content (SSC). One advantage of lowering the SSC of DWW is the ability to irrigate using water application systems with high water use efficiency (sprinkler or drip). The outcome of this transition was an accurate application of plant available inorganic N that minimized the migration of nutrients below the root zone. After the soil organic reservoir is depleted, the total amount of DWW that can be applied per crop is expected to increase.

In contrast, a more aggressive NMP (higher N application rates) implemented in 2008 demonstrated potential problems associated with the use of treated DWW to grow alfalfa. Specifically, the soil organic N reservoir increased and leaching of nitrate below the root zone (15%) increased during the multi-cut alfalfa growing season, in spite of the much larger plant uptake of N by alfalfa than the cereal rotation in 2007. These observations were attributed to fixation of atmospheric N, increased root density, and applying a higher fraction of plant N uptake with DWW.

The precise water application in conjunction with the high content of salts in the DWW caused salt accumulation in the root zone over time. The measured values represent the salt load under a conservative NMP approach that applied only a fraction of the total N that was required by the plant with DWW. If 100% of the plant N had been applied by DWW, then the accompanied salts would increase the  $EC_w$  in the root zone to higher levels. High salt levels in the root zone may restrict plant growth, and accordingly water and nutrient uptake. If this reduction is not considered at NMP sites, additional leaching and contaminant migration may occur. An optimum point likely exists between the benefits of nutrient application and the detrimental effects of salt accumulation on crop yield. This point is strongly dependent on the salt tolerance of the

crop, suggesting that NMPs should use only salt tolerant crops.

The leaching timing of excess of salts below the root zone is a crucial aspect in NMP design. In this study, the soil profile was found to be depleted from inorganic N at the end of the 2007 growing seasons, yet mineralization of organic N was observed to continue during fallow periods, and high levels of N-(NO<sub>2</sub>+NO<sub>3</sub>) (nitrogen from the sum of nitrite and nitrate) were found in the soil profile at the beginning of the sorghum 2007 and alfalfa 2008 seasons. This fallow period poses a greater contamination risk to ground water due to planned (pre-irrigation) or natural (precipitation) water application in excess of ET. In order to minimize nutrient leaching, pre-irrigations should be scheduled at the end of the growing season.

A comprehensive measurement of N mass balance in the root zone requires information on both organic N (soil reservoir) and inorganic N (DWW) sources. During the growing seasons, the major N sink was plant uptake and losses to the atmosphere during irrigation. Atmospheric losses may be minimized by applying DWW during times that are associated with low potential ET (i.e. early morning), or through drip systems that minimize the exposure of DWW to the atmosphere.

Differences in the concentration ratios of N, P, and K between DWW and plant uptake may lead to accumulation of P and K in the root zone. However, the conservative NMP implemented in this study applied only a fraction of the plant N uptake with DWW because it accounted for the organic N reservoir in the soil. Similarly, in 2007 the P in DWW was applied in deficit to plant uptake, and this resulted in a depletion of soil P. In contrast, K was applied in excess and needed to be leached with the salts.

Additional longer term research is needed on both cereal and legume crops to optimize NMPs, the soil organic reservoir, and irrigation methods to simultaneously: (i) Prevent

excessive nitrate leaching even after multiple years of implementation and through crop rotations; (ii) Maximize the plant uptake of N in DWW per unit land; (iii) Provide economic returns on the forage harvest; and (iv) Prevent excessive salt build up.

NMPs implicitly assume that pathogenic microorganisms in the lagoon water will be retained and die-off in the root zone. To test this assumption with regard to groundwater protection, the transport and fate of indicator microorganisms were monitored during winter and summer growing seasons at the NMP field site. These results are discussed in detail in Chapter 4.

In order to efficiently implement the NMP the dairy wastewater was treated (screen, sedimentation tank, and sand filter) to minimize the organic load in the wastewater. This treatment also produced close to a 2-log reduction in concentrations for *Enterococcus*, fecal coliform, total *E. coli*, and somatic coliphage. When well-water and treated wastewater were applied to the field site to meet ET and plant nutrient requirements, little advective transport of the indicator microorganisms occurred below the root zone (60 cm). The remaining concentrations of these indicator microorganisms in the root zone died-off during the winter and summer growing seasons. These observations support the hypothesis that a well-designed and implemented NMP at this site will protect groundwater supplies from microorganism contamination.

Additional experiments were conducted in the laboratory to better quantify microorganism transport and survival in the field soil. Batch survival experiments revealed much more rapid die-off rates for the bacterial indicator microorganisms in native than in sterilized soil, suggesting that the biotic factors played a dominant role in survival behavior. Saturated column experiments with packed field soil, demonstrated much greater transport potential for somatic coliphage than bacterial indicators (*Enterococcus* and total *E. coli*). Retention

rates for the indicator microorganisms were not log-linear with depth (not first-order with respect to concentration), demonstrating the complexity of the microorganism transport behavior. A worst case transport scenario of ponded infiltration on a large undistributed soil column from the field was also investigated. Concentrations of the indicator microorganisms were not detected in the column outflow and in the soil at a depth of 65 cm. The remaining concentrations of the indicator microorganisms in the column rapidly decreased toward low concentrations within 1 week at a temperature of 25°C. Both of these observations were consistent with field NMP results and conclusions.

Results from field and laboratory experiments demonstrate that the fate of microorganisms at NMP sites will depend on both transport and survival characteristics. Although transport and survival of microorganisms in NMP soils were shown to be complicated and are likely to be site specific, a few recommendations for NMP implementation can be developed. The transport potential of microorganisms can be significantly reduced by minimizing water leaching below the root zone and surface water runoff. This can be achieved by: (i) precise estimation of ET rate; (ii) uniform application of wastewater; and (iii) selecting water application timing and quantities based on considerations of soil permeability and ET. Special caution is warranted in coarse textured and structured soils and during water flow transients where enhanced microorganism transport potential has been reported in the literature (Natsch et al., 1996; Bradford et al., 2003; and Saiers et al., 2003). Survival characteristics of microorganisms are also likely to be site specific, but may be quantified through relatively simple batch type experiments that mimic natural conditions. Timing of water application should allow for adequate die-off of microorganisms before leaching the root zone by irrigation or natural precipitation. Finally, the potential for groundwater contamination

will increase with shorter travel times and distances. The water table depth is therefore another important consideration for environmentally protective NMPs. Implementation of these NMP recommendations will undoubtedly be technically challenging, and may not be economically feasible in some instances. Nevertheless, these recommendations provide guidance to minimize the potential risks of pathogen contamination of water resources at NMP sites.

In Chapter 5 we discuss experimental and theoretical studies that were undertaken to explore the coupling of physical and chemical mechanisms of colloid retention under unfavorable attachment conditions (pH=10). Negatively charged latex microspheres (1.1 and 3  $\mu\text{m}$ ) and quartz sands (360, 240, and 150  $\mu\text{m}$ ) were used in packed column studies that encompassed a range in suspension ionic strengths (6-106 mM), Darcy water velocities (0.1-0.45  $\text{cm min}^{-1}$ ), and water saturations (40-100%). Derjaguin-Landau-Verwey-Overbeek (DLVO) calculations, moment analysis, and batch results suggest that attachment of colloids to the solid-water and air-water interfaces was not a significant mechanism of deposition for the selected experimental conditions. Breakthrough curves and hyperexponential deposition profiles were strongly dependent on the solution chemistry, the system hydrodynamics, and the colloid and collector grain size. A mathematical model, accounting for time- and depth-dependent straining, produced a reasonably good fit for both the breakthrough curves and final deposition profiles. Greater deposition occurred for increasing ionic strength, lower flow rates and water saturations, and larger ratios of the colloid to the median grain diameter. Increasing the solution ionic strength is believed to increase the adhesive force and number of colloids in the secondary minimum of the DLVO interaction energy profile. These weakly associated colloids can be funneled to small pore spaces formed adjacent to grain-grain junctions and the air-water-solid triple

point. For select systems, the ionic strength of the eluant solution was decreased to 6 mM following the recovery of the breakthrough curve. In this case, only a small portion of the deposited colloids was recovered in the effluent and the majority was still retained in the sand. These observations suggest that the extent of colloid removal by straining is strongly coupled to solution chemistry.

Experimental research has demonstrated that much greater microorganism retention is possible in the smallest regions of the pore space that are associated with lower flow rates. We have therefore developed models that are based upon physical and chemical nonequilibrium (PCNE), dual permeability, and stochastic stream tube formulations. This research is discussed in Chapter 6. Although specific examples were provided for colloid transport in homogeneous porous media, these same models are well designed to simulate microorganism transport and retention in the field at NMP sites.

The PCNE model partitions the pore space into “mobile” and “immobile” flow regions with first-order mass transfer between these two regions (i.e., “physical” nonequilibrium or PNE). Partitioning between the aqueous and solid phases can either proceed as an equilibrium or a first-order process (i.e., “chemical” nonequilibrium or CNE) for both the mobile and immobile regions. An analytical solution for the PCNE model was obtained using iterated Laplace transforms. The PCNE model allows greater flexibility to describe experimental breakthrough curves and retention profiles than the traditional CNE model. Expressions for moments and transfer functions were developed to facilitate the analytical use of the PCNE model.

The dual-permeability model accounts for different rates of advective and dispersive transport, as well as first-order colloid retention and release in fast and slow velocity regions of the pore space. The model also includes provisions for the exchange

of colloids from fast to slow regions in the aqueous phase and/or on the solid phase. A sensitivity analysis performed with the dual-permeability model parameters indicated that low rates of advective transport to low-velocity regions had a pronounced influence on colloid retention profiles, especially near the inlet.

The stochastic model for colloid transport and retention is based on the conventional advective dispersion equation that accounts for first-order kinetic deposition and release of colloids. One or two stochastic parameters can be considered in this model, including the deposition coefficient, the release coefficient, and the average pore water velocity. In the case of one stochastic parameter, the probability density function (PDF) is characterized using lognormal, bimodal log-normal, or a simple two species/region formulation. When two stochastic parameters are considered, then a joint log-normal PDF is employed. Simulation results indicated that variations in the deposition coefficient and the average pore water velocity can both produce hyperexponential deposition profiles. Bimodal formulations for the PDF were also able to produce hyperexponential profiles, but with much lower variances in the deposition coefficient.

### **Quality Assurance**

This project was designed to evaluate and select basic options, and/or to perform preliminary assessment of unexplored areas with regard to NMPs. A quality assurance plan was followed in all experimental phases of this study. The data was obtained using standard physical, chemical, and/or microbiological laboratory measurements, analytical procedures, bench studies, and field evaluations outlined in this report. The data presented in this report met the project’s data quality requirements. Conclusions and recommendations made in this report are supported by this data, and are scientifically, but not legally defensible. Caution is warranted when extrapolating this information and findings to other conditions.

# 8.0

## References

- Abdul-Jabbar, A.S., Sammis, T.W., and Lugg, D.G. 1982. Effect of moisture level on the root pattern of alfalfa. *Irrig. Sci.* 3:197-207.
- Ahammed, M.M. and Chaudhuri, M. 1999. A low-cost home water filter. *J. Water. SRT - Aqua.* 48:263-267.
- Allen, R.G., Pereira, L.S., Raes, D., and Smith, M. 1998. Crop evapotranspiration-guidelines for computing crop water requirements. FAO - *Food and Agriculture Organization of the United Nations, Irrigation and drainage paper* 56.
- Arai, Y. and Sparks, D.L. 2007. Phosphate reaction dynamics in soils and soil components: a multiscale approach. *Adv. Agron.* 94:135-179.
- ASAE. 1999. Manure production and characteristics. AS Data: AS D384.1. St. Joseph, MI. *American Society of Agricultural Engineers.*
- Ayers, R.S. and Westcot, D.W. 1989. Water quality for agriculture, FAO Irrigation and Drainage Paper 29, Rev. 1, FAO, Rome, Italy.
- Bales, R.C., Li, S., Maguire, K.M., Yahya, M.T., and Gerba, C.P. 1993. MS-2 and poliovirus transport in porous media: hydrophobic effects and chemical perturbations. *Water Resour. Res.* 29:957-963.
- Barker, J.C. and Zublena, J.P. 1996. Livestock manure nutrient assessment in North Carolina. In: Proc. 7th International Symposium on Agriculture and Food Processing Wastes, ASAE. pp. 98-106.
- Bar-Tal, A., Yermiyahu, U., Beraud, J., Keinan, M., Rosenberg, R., Zohar, D., Rosen, V., and Fine, P. 2004. Nitrogen, phosphorus, and potassium uptake by wheat and their distribution in soil following successive, annual compost applications. *J. Environ. Qual.* 33:1855-1865.
- Bélanger, G., and Richard, J.E. 2000. Dynamics of biomass and N accumulation of alfalfa under three N fertilization rates. *Plant and Soil.* 219:177-185
- Benner, S.G., Blowes, D.W., Gould, W.D., Herbert Jr., R.B., and Ptacek, C.J. 1999. Geochemistry of a permeable reactive barrier for metals and acid mine drainage. *Environ. Sci. Technol.* 33:2793-2799.
- Bergendahl, J., and Grasso, D. 1999. Prediction of colloid detachment in a model porous media: thermodynamics. *AIChE J.* 45:475-484.
- Bergendahl, J., and Grasso, D. 2000. Prediction of colloid detachment in a model porous media: hydrodynamics. *Chem. Eng. Sci.* 3:1523-1532.
- Black, A.S., Sherlock, R.R., Smith, N.P., Cameron, K.C., and Goh, K.M. 1985. Effect of form of nitrogen, season and urea application rate on ammonia volatilization from pastures. *New Zealand J. Agric. Res.* 28:469-474.
- Blumenthal, J.M., and Russelle, M.P. 1996. Subsoil nitrate uptake and symbiotic dinitrogen fixation by alfalfa. *Agron. J.* 88:909-915.
- Bodvarsson, G.S., Ho, C.K., and Robinson, B.A. 2003. Yucca Mountain Project, special issue. *J. Contam. Hydrol.* 62-63:1-750.
- Bohn, H., McNeal, B., and O'Connor, G. 1985. *Soil chemistry.* 2<sup>nd</sup> Ed. Wiley, New York, NY.
- Bolster, C.H., Mills, A.L., Hornberger, G.M., and Herman, J.S. 1999. Spatial distribution of deposited bacteria following miscible displacement experiments in intact cores. *Water Resour. Res.* 35:1797-1807.
- Bouwer, H. 2002. Integrated water management for the 21<sup>st</sup> century: problems

- and solutions. *J. Irrig. Drain. Engrg.* 128:193-202.
- Bradford, S.A., and Abriola, L.M. 2001. Dissolution of residual tetrachloroethylene in fractional wettability porous media: incorporation of interfacial area estimates. *Water Resour. Res.* 37:1183-1195.
- Bradford, S.A. and Schijven, J. 2002. Release of *Cryptosporidium* and *Giardia* from dairy calf manure: impact of solution salinity. *Environ. Sci. Technol.* 36:3916-3923.
- Bradford, S.A., Yates, S.R., Bettahar, M., and Šimůnek, J. 2002. Physical factors affecting the transport and fate of colloids in saturated porous media. *Water Resour. Res.*, 38(12), 1327, doi:10.1029/2002WR001340.
- Bradford, S.A., Bettahar, M., Šimůnek, J., van Genuchten, M.T. 2004. Straining and attachment of colloids in physically heterogeneous porous media. *Vadose Zone J.* 3:384-394.
- Bradford, S.A., Šimůnek, J., Bettahar, M., Tadassa, Y.F., van Genuchten, M.T., and Yates, S.R. 2005. Straining of colloids at textural interfaces. *Water Resour. Res.* 41:W10404, doi:10.1029/2004WR003675.
- Bradford, S.A., Šimůnek, J., Bettahar, M., van Genuchten, M.T., and Yates, S.R. 2003. Modeling colloid attachment, straining, and exclusion in saturated porous media. *Environ. Sci. Technol.* 37:2242-2250.
- Bradford, S.A., and Bettahar, M. 2005. Straining, attachment, and detachment, of *Cryptosporidium* oocysts in saturated porous media. *J. Environ. Qual.* 34:469-478.
- Bradford, S.A., and Bettahar, M. 2006. Concentration dependent colloid transport in saturated porous media. *J. Contam. Hydrol.* 82:99-117.
- Bradford, S.A., Šimůnek, J., Bettahar, M., van Genuchten, M.T., and Yates, S.R. 2006a. Significance of straining in colloid deposition: evidence and implications. *Water Resour. Res.* 42:W12S15.
- Bradford, S.A., Šimůnek, J., and Walker, S.L. 2006b. Transport and straining of *E. coli* O157:H7 in saturated porous media. *Water Resour. Res.*, 42:W12S12.
- Bradford, S.A., Tadassa, Y.F., and Pachepsky, Y. 2006c. Transport of *Giardia* and manure suspensions in saturated porous media. *J. Environ. Qual.*, 35:749-757.
- Bradford, S.A., Tadassa, Y.F., and Jin, Y. 2006d. Transport of coliphage in the presence and absence of manure suspension. *J. Environ. Qual.* 35:1692-1701.
- Bradford, S.A., and Toride, N. 2007. A stochastic model for colloid transport and deposition. *J. Environ. Qual.* 36:1346-1356.
- Bradford, S.A., Torkzaban, S., and Walker, S.L. 2007. Coupling of physical and chemical mechanisms of colloid straining in saturated porous media. *Water Res.*, 41:3012-3024.
- Bradford, S.A., Segal, E., Zheng, W., Wang, Q., and Hutchins, S.R. 2008. Reuse of concentrated animal feeding operation wastewater on agricultural lands. *J. Environ. Qual.* 37: S97-S115.
- Bradford, S.A. and Torkzaban, S. 2008. Colloid transport and retention in unsaturated porous media: a review of interface-, collector-, and pore-scale processes and models. *Vadose Zone J.* 7:667-681.
- Bradford, S.A., Torkzaban, S., Leij, F.J., Šimůnek, J., and van Genuchten, M.T. 2009. Modeling the coupled effects of pore space geometry and velocity on colloid transport and retention. *Water Resour. Res.* 45:W02414. doi:10.1029/2008WR007096.
- Brock, E.H., Ketterings, Q.M., and Kleinman, P.J.A. 2007. Measuring and predicting the phosphorus sorption capacity of manure-amended soils. *Soil Sci.* 172(4):266-278.
- Burkholder, J., Libra, B., Weyer, P., Heathcote, S., Kolpin, D., Thorne, P.S., and Wichman, M. 2007. Impacts of waste from concentrated animal feeding operations on water quality. *Environ. Health Perspect.* 115:308-312.

- Burns, J.C., Westerman, P.W., King, L.D., Cummings, G.A., Overcash, M.R., and Goode, L. 1985. Swine lagoon effluent applied to 'Coastal' bermudagrass: I. Forage yield, quality, and element removal. *J. Environ. Qual.* 14:9-14.
- Bussink, D.W., and Oenema, O. 1998. Ammonia volatilization from dairy farming systems in temperate areas: a review. *Nutrient Cycling Agroecosyst.* 51:19-33.
- Campbell-Mathews, M., Frate, C. Harter, T., and Sather, S. 2001. Lagoon water composition, sampling, and field analysis. *Proceedings of the 2001 California Plant and Soil Conference*, Fresno, CA. pp 43-51B.
- Cameron, K.C., Rate, A.W., Carey, P.L., and Smith, N.P. 1995. Fate of nitrogen in pig effluent applied to a shallow stony pasture soil. *NZ J. Agric. Res.* 38:533-542.
- Cameron, K.C., Di, H.J., Reijnen, B.P.A., and Li, Z. 2002. Fate of nitrogen in dairy factory effluent irrigated onto land. *NZ J. of Agric. Res.* 45:207-216.
- Callaway, T.R., Elder, R.O., Keen, J.E., Anderson, R.C., and Nisbet, D.J. 2003. Forage feeding to reduce preharvest *Escherichia coli* populations in cattle, a review. *J. Dairy Sci.* 86:852-860.
- Centers for Disease Control and Prevention. 1998. Surveys of waterborne disease outbreaks compiled by the Center for Disease Control and Prevention from 1986 to 1998. *Morbidity and Mortality Weekly Reports*. Atlanta, GA, CDC.
- Chang, C. and Entz, T. 1996. Nitrate leaching losses under repeated cattle feedlot manure applications in southern Alberta. *J. Environ. Qual.* 25:145-153.
- Chang, C., Sommerfeldt, T.G., and Entz, T. 1991. Soil chemistry after eleven annual applications of cattle feedlot manure. *J. Environ. Qual.* 20:475-480.
- Chastain, J.P., Vanotti, M.B., and Wingfield, M.M. 2001. Effectiveness of liquid solid separation for treatment of flushed dairy manure: a case study. *Appl. Eng. Agric.* 17:343-354.
- Chen, G. and Flury, M. 2005. Retention of mineral colloids in unsaturated porous media as related to their surface properties. *Colloids Surf. A: Physicochem. Eng. Aspects.* 256:207-216.
- Cherrey, K.D., Flury, M., and Harsh, J.B. 2003. Nitrate and colloid transport through coarse Hanford sediments under steady state, variably saturated flow. *Water Resour. Res.* 39:1165. doi:10.1029/2002WR001944.
- Choi, H. and Corapcioglu, M.Y. 1997. Transport of a non-volatile contaminant in unsaturated porous media in the presence of colloids. *J. Contam. Hydrol.* 25:299-324.
- Chu, Y., Jin, Y., Flury, M. and Yates, M.V. 2001. Mechanisms of virus removal during transport in unsaturated porous media. *Water Resour. Res.* 37:253-263.
- Clesceri, L.S., Greenberg, A.E., and Trussell, R.R. 1989. Standard methods for the examination of water and wastewater. *American Public Health Association*, Washington, D.C.
- Compere, F., Porel, G., and Delay, F. 2001. Transport and retention of clay particles in saturated porous media: influence of ionic strength and pore velocity. *J. Contam. Hydrol.* 49:1-21.
- Corapcioglu, M.Y., and Choi, H. 1996. Modeling colloid transport in unsaturated porous media and validation with laboratory column data. *Water Resour. Res.* 32:3437-3449.
- Correll, D.L. 1998. The role of phosphorus in the eutrophication of receiving waters: a review. *J. Environ. Qual.* 27:261-266.
- Corwin, D.L., and Lesch, S.M. 2005a. Apparent soil electrical conductivity measurements in agriculture. *Computers and Electronics in Agriculture.* 46:11-43.
- Corwin, D.L. and Lesch, S.M. 2005b. Characterizing soil spatial variability with apparent soil electrical conductivity. I. Survey protocols. *Computers and Electronics in Agriculture.* 46:103-133.

- Craun, G.F., and Calderon, R. 1996. Microbial risks in groundwater systems: Epidemiology of waterborne outbreaks. *In: Under the microscope: Examining microbes in groundwater.* Denver, CO, *Am. Water Works Assoc. Res. Foundation.*
- Crist, J.T., McCarthy, J.F., Zevi, Y., Baveye, P., Throop, J.A., and Steenhuis, T.S. 2004. Pore-scale visualization of colloid transport and retention in partly saturated porous media. *Vadose Zone J.* 3:444-450.
- Crist, J.T., Zevi, Y., McCarthy, J.F., Throop, J.A., and Steenhuis, T.S. 2005. Transport and retention mechanisms of colloids in partially saturated porous media. *Vadose Zone J.* 4:184-195.
- Cumbie, D.H. and McKay, L.D. 1999. Influence of diameter on particle transport in a fractured shale saprolite. *J. Contam. Hydrol.* 37(1-2):139-157.
- Cushing, R.S. and Lawler, D.F. 1998. Depth filtration: fundamental investigation through three-dimensional trajectory analysis. *Environ. Sci. Technol.* 32:3793-3801.
- de Jonge, L.W., Kjaergaard, C., and Moldrup, P. 2004. Colloids and colloid facilitated transport of contaminants in soils: an introduction. *Vadose Zone J.* 3:321-325.
- de Rooij, G.H. 2000. Modeling fingered flow of water in soils owing to wetting front instability: a review. *J. Hydrol.* 231-232:277-294.
- DeNovio, N.M., Saiers, J.E., and Ryan, J.N. 2004. Colloid movement in unsaturated porous media: recent advances and future directions. *Vadose Zone J.* 3:338-351.
- Derjaguin, B.V., and Landau, L.D. 1941. Theory of the stability of strongly charged lyophobic sols and of the adhesion of strongly charged particles in solutions of electrolytes. *Acta Physicochim. USSR* 14:733-762.
- Dobias, B. Coagulation and flocculation. MerceL Dekker, Inc. [v. 47]. 1993. New York, NY. *Surfactant Science Series.*
- Duffadar, R.D., and Davis, J.M. 2008. Dynamic adhesion behavior of micrometer scale particles flowing over patchy surfaces with nanoscale electrostatic heterogeneity. *J. Coll. Interface Sci.* 326:18-27.
- Elimelech, M., Nagai, M., Ko, C.-H., and Ryan, J.N. 2000. Relative insignificance of mineral grain zeta potential to colloid transport in geochemically heterogeneous porous media. *Environ. Sci. Technol.* 34:2143-2148.
- Evans, D.D., Nicholson, T.J., and Rasmusson, T.C. 2001. Flow and transport through unsaturated fractured rock. 2nd ed. AGU, Washington, DC, *Geophysical Monograph* 42.
- Evans, R.O., Westerman, P.W., and Overcash, M.R. 1984. Subsurface drainage water quality from land application of swine lagoon effluent. *Trans. ASABE* 27:473-480.
- Feng, G.L., Letey, J., Chang, A.C., and Campbell-Mathews, M. 2005. Simulating dairy liquid waste management options as a nitrogen source for crops. *Agric. Ecosyst. Environ.* 110:219-229.
- Foppen, J.W.A., Mporokoso, A., and Schijven, J.F. 2005. Determining straining of *Escherichia coli* from breakthrough curves. *J. Contam. Hydrol.* 76:191-210.
- Gagliardi, J.V. and Karns J.S. 2000. Leaching of *Escherichia coli* O157:H7 in diverse soils under various agricultural management practices. *Appl. Environ. Microbiol.* 66:877-883.
- Gagliardi, J.V. and Karns, J.S. 2002. Persistence of *Escherichia coli* O157:H7 in soil and on plant roots. *Environ. Microbiol.* 4(2):89-96.
- Gerba, C.P. 1996. What are the current microbiological and public health issues in drinking water? *In: Under the microscope: Examining microbes in groundwater.* Denver, CO. *Am. Water Works Assoc. Res. Foundation.*
- Gerba, C.P., and Smith Jr., J.E. 2005. Sources of pathogenic microorganisms and their fate during land application of wastes. *J. Environ. Qual.* 34:42-48.

- Gerke, H.H., and van Genuchten, M. T. 1993a. A dual-porosity model for simulating the preferential movement of water and solutes in structured porous media. *Water Resour. Res.* 29:305-319. doi:10.1029/92WR02339.
- Gerke, H.H., and van Genuchten, M.T. 1993b. Evaluation of a first-order water transfer term for variably saturated dual-porosity flow models. *Water Resour. Res.* 29:1225-1238. doi:10.1029/92WR02467.
- Gerke, H.H. 2006. Preferential flow descriptions for structured soils. *J. Plant Nutrition Soil Sci.* 169:382-400. doi:10.1002/jpln.200521955.
- Gerritson, J. and Bradley, S.W. 1987. Electrophoretic mobility of natural particles and cultured organisms in freshwaters. *Limnol. Oceanogr.* 32(5):1049-1058.
- Gibson, L.R., Nance, C.D., and Karlen, D.L. 2007. Winter triticale response to nitrogen fertilization when grown after corn or soybean. *Agron. J.* 99:49-58.
- Ginn, T.R. 2002. A travel time approach to exclusion on transport in porous media. *Water Resour. Res.* 38(4):1041.
- Ginn, T.R., Wood, B.D., Nelson, K.E., Schiebe, T.D., Murphy, E.M., and Clement, T.P. 2002. Processes in microbial transport in the natural subsurface. *Adv. Water Res.* 25:1017-1042.
- Gleick, P.H. The world's water. 2000. Washington, DC. *Island Press*.
- Gregory, J. 1981. Approximate expressions for retarded van der Waals interaction. *J. Colloid Interface Sci.* 83:138-145.
- Gu, B., Phelps, T.J., Liang, L., Dickey, M.J., Roh, Y., Kinsall, B.L., Palumbo, A.V., and Jacobs, G.K. 1999. Biogeochemical dynamics in zero-valent iron columns: implication for permeable reactive barriers. *Environ.Sci.Technol.* 33:2170-2177.
- Guber, A.K., Shelton, D.R., and Pachepsky, Y.A. 2005a. Effect of manure on *Escherichia coli* attachment to soil. *J. Environ. Qual.* 34:2086-2090.
- Guber, A.K., Shelton, D.R., and Pachepsky, Y.A. 2005b. Transport and retention of manure-borne coliforms in soil. *Vadose Zone J.* 4:828-837.
- Hanselman, T.A., Graetz, D.A., and Wilkie, A.C. 2003. Manure-borne estrogens as potential environmental contaminants: a review. *Environ. Sci. Technol.* 37:5471-5478.
- Hao, X. and Chang, C. 2003. Does long-term heavy cattle manure application increase salinity of a clay loam soil in semi-arid southern Alberta? *Agric. Ecosyst. Environ.* 94:89-103.
- Harter, T., Wagner, S., and Atwill, E.R. 2000. Colloid transport and filtration of *Cryptosporidium parvum* in sandy soils and aquifer sediments. *Environ. Sci. Technol.* 34:62-70.
- Harvey, R.W., and Garabedian, S.P. 1991. Use of colloid filtration theory in modeling movement of bacteria through a contaminated sandy aquifer. *Environ. Sci. Technol.* 25:178-185.
- Harvey, R.W. and Harms. H. 2001. Transport of microorganisms in the terrestrial subsurface: In situ and laboratory methods. In: *Manual of Environmental Microbiology*, 2<sup>nd</sup> Edition: ASM Press. Washington, DC. pp. 753-776.
- Havelaar, A.H. 1986. F-specific bacteriophages as model viruses in water treatment processes. Univ. of Utrecht, Utrecht, The Netherlands.
- Hawke, R.M., and Summers, S.A. 2006. Effects of land application of farm dairy effluent on soil properties: a literature review. *NZ J of Agric. Res.* 49:307-320.
- Herzig, J.P., Leclerc, D.M., and LeGoff, P. 1970. Flow of suspension through porous media: application to deep filtration. *Ind. Eng. Chem.* 62(5):129-157.
- Hillel, D. 1998. *Environmental soil physics*. Academic Press.
- Hoek, E.M.V., and Agarwal, G.K., 2006. Extended DLVO interactions between spherical particles and rough surfaces. *J. Colloid Interface Sci.* 298:50-58.

- Hogg, R., Healy, T.W., and Fuerstenau, D.W. 1966. Mutual coagulation of colloidal dispersions. *Trans. Faraday Soc.* 62:1638-1651.
- Hunt, P.G., Szogi, A.A., Humenik, F.J., Rice, J.M., Matheny, T.A., and Stone, K.C. 2002. Constructed wetlands for treatment of swine wastewater from an anaerobic lagoon. *Trans. ASAE.* 45:639-647.
- Hutchins, S.R., White, M.V., Hudson, F.M., and Fine, D.D. 2007. Analysis of lagoon samples from different concentrated animal feeding operations for estrogens and estrogen conjugates. *Environ. Sci. Technol.* 41:738-744.
- Hutson, S.S., Barber, N.L., Kenny, J.F., Linsey, K.S., Lumia, D.S., and Maupin, M.A. 2004. Estimated use of water in the United States in 2000. *USGS Circ. 1268.* U.S. Geological Survey, Reston, VA.
- Ibekwe, A.M., Grieve, C.M., and Lyon, S.R. 2003. Characterization of microbial communities and composition in constructed dairy wetland wastewater effluent. *Appl. Environ. Microbiol.* 69(9):5060-5069.
- Jin, Y. and Flury, M. 2002. Fate and transport of viruses in porous media. *Adv. Agron.* 35:39-102.
- Jin, Y., Pratt, E., and Yates, M.V. 2000. Effect of mineral colloids on virus transport through saturated sand columns. *J. Environ. Qual.* 29:532-539.
- Johnson, W.P. and Logan, B.E. 1996. Enhanced transport of bacteria in porous media by sediment-phase and aqueous-phase natural organic matter. *Water Res.* 30(4):923-931.
- Johnson, P.R., and Elimelech, M. 1995. Dynamics of colloid deposition in porous media: blocking based on random sequential adsorption. *Langmuir* 11:801-812.
- Johnson, W.P., Tong, M., and Li, X. 2007. On colloid retention in saturated porous media in the presence of energy barriers: The failure of  $\alpha$ , and opportunities to predict  $\eta$ . *Water Resour. Res.* 43:W12S13.
- Jokela, W.E. 1992. Nitrogen fertilizer and dairy manure effects on corn yield and soil nitrate. *Soil Sci. Soc. Am. J.* 56:148-154.
- Jongbloed, A.W. and Lenis, N.P. 1998. Environmental concerns about animal manure. *J. Anim.Sci.* 76:2641-2648.
- Joshi, A. and Chaudhuri, M. 1996. Removal of arsenic from groundwater by iron oxide-coated sand. *J. Environ. Eng. (ASCE).* 122(8):769-771.
- Kätterer, T., Hansson, A-C., and Andrén, O. 1993. Wheat root biomass and nitrogen dynamics-effects of daily irrigation and fertilization. *Plant and Soil* 151: 21-30.
- Kapkiyai, J.J., Karanja, N.K., Qureshi, J.N., Smithson, P.C. and Woomer, P.L. 1999. Soil organic matter and nutrient dynamics in a Kenyan nitisol under long-term fertilizer and organic input management. *Soil Biol. Biochem.* 31:1773-1782.
- Keeney, D.R., and Nelson, D.W. 1982. Nitrogen-inorganic forms. p.643-698. A.L. Page (Eds.) *Methods of soil analysis, part 2. Agron. Monogr.* 9. ASA and SSSA, Madison, WI.
- Kellogg, R.L., Lander, C.H., Moffitt, D.C. and Gollehon, N. 2000. Manure nutrients relative to the capacity of cropland and pastureland to assimilate nutrients spatial and temporal trends for the United States. *USDA National Resources Conservation Service and Economic Research Service.*
- Khilar, K.C. and Fogler, H.S. 1998. Migration of fines in porous media. Dordrecht, The Netherlands. *Kluwer Academic Publishers.*
- Kim, H.N., Bradford, S.A. and Walker, S.L. 2009a. *Escherichia coli* O157:H7 transport in saturated porous media: role of solution chemistry and surface macromolecules. *Environ. Sci. Technol.* 43(12):4340-4347.
- Kim, H.N., Hong, Y., Lee, I., Bradford, S.A. and Walker, S.L. 2009b. Surface characteristics and adhesion behavior of *Escherichia coli* O157:H7: role of extracellular macromolecules. *Biomacromolecules* 10: 2556-2564.

- King, L.D., Westerman, P.W., Cummings, G.A., Overcash, M.R. and Burns, J.C. 1985. Swine lagoon effluent applied to 'coastal' bermudagrass: II. Effects on soil. *J. Environ. Qual.* 14:14-21.
- Kretzschmar, R., Barmettler, K., Grolimund, D., Yan, Y.D., Borkovec, M., and Sticher, H. 1997. Experimental determination of colloid deposition rates and collision efficiencies in natural porous media. *Water Resour. Res.* 33(5):1129-1137.
- Kuznar, Z.A. and Elimelech, M. 2007. Direct microscopic observation of particle deposition in porous media: role of the secondary energy minimum. *Colloids Surf. A: Physicochem. Eng. Aspects* 94:156-162
- Lance, J.C. and Gerba, C.P. 1984. Virus movement in soil during saturated and unsaturated flow. *Appl. Environ. Microbiol.* 47:335-341.
- Lander, C.H., Moffitt, D. and Alt, K. 1998. Nutrients available from livestock manure relative to crop growth requirements. Resource Assessment and Strategic Planning Working Paper 98-1. U.S. Department of Agriculture, Natural Resources Conservation Service.
- Leij, F.J. and Bradford, S.A. 2009. Combined physical and chemical nonequilibrium transport model: Analytical solution, moments, and application to colloids. *J. Cont. Hyd.* 110:87-99.
- Lenhart, J.J., and Saiers, J.E. 2002. Transport of silica colloids through unsaturated porous media: experimental results and model comparisons. *Environ. Sci. Technol.* 36:769-777.
- Li, X., Scheibe, T.D. and Johnson, W.P. 2004. Apparent decreases in colloid deposition rate coefficient with distance of transport under unfavorable deposition conditions: a general phenomenon. *Environ. Sci. Technol.* 38:5616-5625.
- Li, X., and Johnson, W.P. 2005. Non-monotonic variations in removal rate coefficients of microspheres in porous media under unfavorable deposition conditions. *Environ. Sci. Technol.* 39:1658-1665.
- Li, X., Lin, C.L., Miller, J.D., and Johnson, W.P. 2006a. Pore-scale observation of microsphere deposition at grain-to-grain contacts over assemblage-scale porous media domains using X-ray microtomography. *Environ. Sci. Technol.* 40:3762-3768.
- Li, X., Zhang, P., Lin, C.L., and Johnson, W.P. 2005. Role of hydrodynamic drag on microsphere deposition and re-entrainment in porous media under unfavorable conditions. *Environ. Sci. Technol.* 39:4012-4020.
- Li, X., Lin, C.L., Miller, J.D., and Johnson, W.P. 2006b. Role of grain-to grain contacts on profiles of retained colloids in porous media in the presence of an energy barrier to deposition. *Environ. Sci. Technol.* 40:3769-3774.
- Lindeburg, M.R. 2001. Civil engineering reference manual for the PE exam. *Professional Publications, Inc.* Belmont, CA.
- Loge, F.J., Thompson, D.E. and Call, D.R. 2002. PCR detection of specific pathogens in water: A risk-based analysis. *Environ. Sci. Technol.* 36:2754-2759.
- Loughrin, J .H., Szogi, A.A. and Vanotti, M.B. 2006. Reduction of malodorous compounds from liquid swine manure by a multi-stage treatment system. *Appl. Eng. Agric.* 22:867-873.
- Luo, J., Tillman, R.W., and Ball, P.R. 1999. Factors regulating denitrification in a soil under pasture. *Soil Biology and Biochem.* 31:913-927.
- Maas, E.V. and Hoffman, G.J. 1977. Crop salt tolerance - current assessment. *J. Irrig. Drainage Div. ASCE* 103:115-134.
- Maas, E.V. 1984. *The handbook of plant science in agriculture.* CRC Press. Boca Raton, FL.
- Macler, B.A. and Merkle, J.C. 2000. Current knowledge on groundwater microbial pathogens and their control. *Hydrogeol. J.* 8:29-40.
- Mallin, M.A. 2000. Impacts of industrial-scale swine and poultry production on rivers and estuaries. *American Scientist* 88:26-37.

- McCarthy, J.F. and Zachara, J.M. 1989. Subsurface transport of contaminants. *Environ. Sci. Technol.* 23:496-502.
- McDowell-Boyer, L.M., Hunt, J.R. and Sitar, N. 1986. Particle transport through porous media. *Water Resour. Res.* 22:1901-1921.
- Merrill, S.D. and Rawlins, S.L. 1979. Distribution and growth of sorghum roots in response to irrigation frequency. *Agron. J.* 71:738-745
- Mohanty, B.P., Bowman, R.S., Hendrickx, J.M.H., and van Genuchten, M.T. 1997. New piecewise-continuous hydraulic functions for modeling preferential flow in an intermittent-flood-irrigated field. *Water Resour. Res.* 33:2049-2063.
- Moore Jr., P.A., and Reddy, K.R. 1994. Role of Eh and pH on phosphorus geochemistry in sediments of Lake Okeechobee, Florida. *J. Environ. Qual.* 23:955-964.
- MWPS. 1993. MWPS-18: Livestock waste facilities handbook. Midwest Plan Service, Iowa State University. Ames, IA.
- NCSU. 1994. Livestock manure production and characterization in North Carolina. *North Carolina Coop. Ext. Service*, Raleigh, NC.
- National Research Council. 2001. Conceptual models of flow and transport in the fractured vadose zone. *National Academy Press*. Washington, DC.
- Natsch, A., Keel, C., Troxler, J., Zala, M., Von Albertini, N. and Défago, G. 1996. Importance of preferential flow and soil management in vertical transport of a bio-control strain of *Pseudomonas fluorescens* in structured field soil. *Appl. Environ. Microbiol.* 62:33-40.
- Nelson, K.E. and Ginn, T.R. 2001. Theoretical investigation of bacterial chemotaxis in porous media. *Langmuir.* 17:5636-5645.
- Nichols, D.J., Daniel Jr., C.P., Moore, P.A., Edwards, D.R. and Pote, P.H. 1997. Runoff of estrogen hormone 17  $\beta$ -Estradiol from poultry litter applied to pasture. *J. Environ. Qual.* 26:1002-1006.
- Ouyang, Y., Shinde, D., Mansell, R.S. and Harris, W. 1996. Colloid-enhanced transport of chemicals in subsurface environments: a review. *Crit. Rev. Environ. Sci. Technol.* 26:189-204.
- Pautler, M.C. and Sims, J.T. 2000. Relationships between soil test phosphorus, soluble phosphorus, and phosphorus saturation in Delaware soils. *Soil Sci. Soc. Am. J.* 64:765-773.
- Penman, H.L. 1948. *Proceedings of the Royal Society of London.*
- Peterson, E.W., Davis, R.K. and Orndorff, H.A. 2000. 17 $\beta$ -estradiol as an indicator of animal waste contamination in mantled karst aquifers. *J. Environ. Qual.* 29:826-834.
- Pieper, A.P., Ryan, J.N., Harvey, R.W., Amy, G.L., Illangasekare, T.H. and Metge, D.W. 1997. Transport and recovery of bacteriophage PRD1 in a sand and gravel aquifer: Effect of sewage-derived organic matter. *Environ. Sci. Technol.* 31:1163-1170.
- Pimentel, D., Berger, B., Filiberto, D., Newton, M., Wolfe, B., Karabinakis, E., Clark, S., Poon, E., Abbett, E. and Nandagopal, S. 2004. Water resources: agricultural and environmental issues. *Biosci.* 54:909-918.
- Powelson, D.K. and Mills, A.L. 2001. Transport of *Escherichia coli* in sand columns with constant and changing water contents. *J. Environ. Qual.* 30:238-245.
- Rahman, M., Fukai, S, Blamey, F.P.C. 2001. Forage production and nitrogen uptake of forage sorghum and maize as affected by cutting under different nitrogen levels. *Proceedings of the 10<sup>th</sup> Australian Agronomy Conference*, Hobart, Australia.
- Rajagopalan, R., and Tien, C. 1976. Trajectory analysis of deep-bed filtration with the sphere-in-cell porous-media model. *AIChE J.*, 22:523-533. doi:10.1002/aic.690220316.
- Raman, D.R., Williams, E.L., Layton, A.C., Burns, R.T., Easter, J.P., Daugherty, A.S., Mullen, M.D. and Sayler, G.S. 2004. Estrogen content of dairy and swine wastes. *Environ. Sci. Technol.* 38:3567-3573.

- Ray, C., Soong, T.W., Lian, Y.Q. and Roadcap, G.S. 2002. Effect of flood induced chemical load on filtrate quality at bank filtration sites. *J. Hydrol.* 266:235-258.
- Reddy, K.R., Khaleel, R., and Overcash, M.R. 1981. Behavior and transport of microbial pathogens and indicator organisms in soils treated with organic wastes. *J. Environ. Qual.* 10:255-266.
- Redman, J.A., Walker, S.L. and Elimelech, M. 2004. Bacterial adhesion and transport in porous media: role of the secondary energy minimum. *Environ. Sci. Technol.* 38:1777-1785.
- Ritsema, C.J. and Dekker, L.W. 2000. Preferential flow in water repellent sandy soils: principles and modeling implications. *J. Hydrol.* 231/232:308-319.
- Ritsema, C.J., Dekker, V., Hendrickx, J.M.H., and Hamminga, W. 1993. Preferential flow mechanism in a water repellent soil. *Water Resour. Res.* 29:2183-2193.
- Rockhold, M.L., Yarwood, R.R. and Selker, J.S. 2004. Coupled microbial and transport processes in soils. *Vadose Zone J.* 3:368-383.
- Rodgers, M., Healy, M.G., and Mulqueen, J. 2005. Organic carbon removal and nitrification of high strength wastewaters using stratified sand filters. *Water Research* 39:3279-3286.
- Russell, J.B., Diez-Gonzalez, F. and Jarvis, G.N. 2000. Effects of diet shifts on *Escherichia coli* in cattle. *J. Dairy Sci.* 83:863-873.
- Ryan, J.N. and Elimelech, M. 1996. Colloid mobilization and transport in groundwater. *Colloids and Surfaces A: Physicochem. and Eng. Aspects.* 107:1-56.
- Ryan, J.N., Harvey, R.W., Metge, D., Elimelech, M., Navigato, T. and Pieper, A.P. 2002. Field and laboratory investigations of inactivation of viruses (PRD1 and MS2) attached to iron oxide-coated quartz sand. *Env. Sci. Technol.* 36:2403-2413
- Sagripani, J.L., Routson, L.B. and Lytle, C.D. 1993. Virus inactivation by copper or iron ions alone and in the presence of peroxide. *Appl. Environ. Microbiol.* 59:4374-4376.
- Saiers, J.E., Hornberger, G.M., Gower, D.B. and Herman, J.S. 2003. The role of moving air-water interfaces in colloid mobilization within the vadose zone. *Geophys. Res. Lett.* 30:2083.
- Saiers, J.E. and Lenhart, J.J. 2003. Colloid mobilization and transport within unsaturated porous media under transient-flow conditions. *Water Resour. Res.* 39(1):1019.
- Schäfer, A., Harms, H., and Zehnder, A.J.B. 1998. Bacterial accumulation at the air-water interface. *Environ. Sci. Technol.* 32:3704-3712.
- Schäfer, A., Ustohal, P., Harms, H., Stauffer, F., Dracos, T., and Zehnder, A.J.B. 1998. Transport of bacteria in unsaturated porous media. *J. Contam. Hydrol.* 33:149-169.
- Shen, C., Huang, Y., Li, B., and Jin, Y. 2008. Effects of solution chemistry on straining of colloids in porous media under unfavorable conditions. *Water Resour. Res.* 44:W05419, DOI: 10.1029/2007WR006580.
- Scherer, M.M., Richter, S., Valentine, R.L. and Alvarez, P.J. 2000. Chemistry and microbiology of permeable reactive barriers for *in situ* groundwater cleanup. *Crit. Rev. Microbiol.* 26:221-264.
- Schets, F.M., During, M., Italiaander, R., Heijnen, L., Rutjes, S.A., van der Zwaluw, W.K. and de Roda Husman, A.M. 2005. *Escherichia coli* O157:H7 in drinking water from private water supplies in the Netherlands. *Water Res.* 39:4485-4493.
- Schijven, J.F., Hoogenboezem, W., Hassanizadeh, S.M. and Peters, J.H. 1999. Modeling removal of bacteriophage MS2 and PRD1 by dune recharge at Castricum, Netherlands. *Water Resour. Res.* 35:1101-1111.
- Schijven, J.F., Mülschlegel, J.H., Hassanizadeh, S.M., Teunis, P.F. and de Roda Husman, A.M. 2006. Determination of protection zones for Dutch groundwater wells against virus contamination - uncer-

- tainty and sensitivity analysis. *J. Water Health.* 4:297-312.
- Schijven, J.K. and Hassanizadeh, S.M. 2000. Removal of viruses by soil passage: overview of modeling, processes, and parameters. *Crit. Rev. Environ. Sci. Technol.* 30:49-127.
- Segal, E., Shouse, P., Poss, J. A., Crohn, D. M. and Bradford, S. A. 2010. Recommendations for nutrient management plans in a semi-arid environment. *Agric. Ecosyst. Environ.*, 137:317-328.
- Segal, E., Bradford, S.A., Shouse, P., Lazarovitch, N. and Corwin, D.L. 2008. Integration on of hard and soft data to characterize field-scale hydraulic properties for flow and transport studies. *Vadose Zone J.* 7:878-889.
- Segal, E., Shouse, P. and Bradford, S.A. 2009. Deterministic analysis and upscaling of bromide transport in a heterogeneous vadose zone. *Vadose Zone J.* 8:601-610.
- Sen, T.K. and Khilar, K.C. 2006. Review on subsurface colloids and colloid associated contaminant transport in saturated porous media. *Adv. Coll. Interface Sci.* 119:71-96.
- Sharma, M.M., Chang, Y.I. and Yen, T.F. 1985. Reversible and irreversible surface charge modification of bacteria for facilitating transport through porous media. *Coll. Surf.* 16:193-206.
- Sharpe, R.R., and Harper, L.A. 1997. Ammonia and nitrous oxide emissions from sprinkler irrigation applications of swine effluent. *J. Environ. Qual.* 26:1703-1706.
- Sharpley, A.N. 1995. Soil phosphorus dynamics: agronomic and environmental impacts. *Ecol. Engr.* 5:261-279.
- Sharpley, A.N. and Moyer, B. 2000. Phosphorus forms in manure and compost and their release during simulated rainfall. *J. Environ. Qual.* 29:1462-1469.
- Shore, L.S., Correll, D.L. and Chakraborty, P.K. 1995. Relationship of fertilization with chicken manure and concentrations of estrogens in small streams. *In: Animal waste and the land-water interface.* Lewis Publ. Boca Raton, FL. pp. 155-162.
- Shore, L.S., Shemesh, M. and Cohen, R. 1988. The role of o-Estradiol and o-Estrone in chicken manure silage in hyperoestrogenism in cattle. *Aust. Veterinary J.* 65:68.
- Sim, Y., and Chrysikopoulos, C.V. 1996. One-dimensional virus transport in porous media with time-dependent inactivation rate coefficients. *Water Resour. Res.* 32:2607-2611.
- Sims, J.T., Simard, R.R., and Joern, B.C. 1998. Phosphorus loss in agricultural drainage: historical perspective and current research. *J. Environ. Qual.* 27:277-293.
- Šimůnek, J., Jarvis, N.J., van Genuchten, M.Th., and Gardenas, A. 2003. Nonequilibrium and preferential flow and transport in the vadose zone: review and case study. *J. Hydrol.* 272:14-35.
- Šimůnek, J., van Genuchten, M.Th., and Sejna, M. 2007. The HYDRUS-1D software package for simulating the one-dimensional movement of water, heat, and multiple solutes in variably saturated media. HYDRUS Software Ser. 3, 315 pp., *Dept. of Environ. Sci., Univ. of Calif., Riverside.*
- Šimůnek, J., van Genuchten, M. T. and Sejna, M. 2009. The HYDRUS-1D software package for simulating the one-dimensional movement of water, heat, and multiple solutes in variably saturated media, version 4.08, HYDRUS Software Ser. 3, 332 pp., *Dept. of Environ. Sci., Univ. of Calif., Riverside.*
- Šimůnek, J. and van Genuchten, M. T. 2008. Modeling nonequilibrium flow and transport using HYDRUS. *Vadose Zone J.*, 7:782-797, doi:10.2136/vzj2007.0074.
- Sinton, L.W., Noonan, M.J., Finlay, R.K., Pang, L. and Close, M.E. 2000. Transport and attenuation of bacteria and bacteriophages in an alluvial gravel aquifer. *New Zealand J. Mar. Freshwater Res.* 34:175-186.

- Sommerfeldt, T.G., Chang, C. and Entz, T. 1988. Long-term annual manure applications increase soil organic matter and nitrogen, and decrease carbon to nitrogen ratio. *Soil Sci. Soc. Am. J.* 52:1667-1672.
- Sommerfeldt, T.G. and Chang, C. 1985. Changes in soil properties under annual applications of feedlot manure and different tillage practices. *Soil Sci. Soc. Am. J.* 49:983-987.
- Sommerfeldt, T.G. and Chang, C. 1987. Soil-water properties as affected by twelve annual applications of cattle feedlot manure. *Soil Sci. Soc. Am. J.* 51:7-9.
- Steenhuis, T.S., Dathe, A., Zevi, Y., Smith, J.L., Gao, B., Shaw, S.B., DeAlwis, D., Amaro-Garcia, S., Fehrman, R., Ekrem Cakmak, E., Toevs, I.C., Liu, B.M., Beyer, S.M., Crist, J.T., Hay, A.G., Richards, B.K., DiCarlo, D. and McCarthy, J.F. 2006. Biocolloid retention in partially saturated soils. *Biologia 61 (Suppl. 19)* S229-S233.
- Stenger, R., Barkle, G.F., and Burgess, C.P. 2001. Mineralization and immobilization of C and N from dairy farm effluent (DFE) and glucose plus ammonium chloride solution in three grassland topsoils. *Soil Biology and Biochem.* 33:1037-1048
- Strong, D.T., Sale, P.W.G., Helyar, K.R. 1999. The influence of the soil matrix on nitrogen mineralisation and nitrification. IV. Texture. *Australian Journal of Soil Research* 37:329-350.
- Svoboda, I.F. 1995. Nitrogen removal from pig slurry by nitrification and denitrification. ASAE. Proc. 7th Int. Symp. Agric. and Food Proc. Wastes (ISAFPW95) St. Joseph, MI. pp. 24-33.
- Sukias, J.P.S., Tanner, C.C., Davies-Colley, R.J., Nagels, J.W., and Wolters, R. 2001. Algal abundance, organic matter, and physico-chemical characteristics of dairy farm facultative ponds: implications for treatment performance. *New Zealand Journal of Agricultural Research* 44:279-296.
- Tan, Y., Cannon, J.T., Baveye, P., and Alexander, M. 1994. Transport of bacteria in an aquifer sand—experiments and model simulations. *Water Resour. Res.* 30:3243-3252.
- Thorne, P.S. 2007. Environmental health impacts of concentrated animal feeding operations: anticipating hazards – searching for solutions. *Environ. Health Perspect.* 115:296-297.
- Tipping, E. 1981. The adsorption of aquatic humic substances by iron oxides. *Geochimica et Cosmochimica Acta* 45:191-199.
- Tong, M., Li, X., Brow, C.N. and Johnson, W.P. 2005. Detachment-influenced transport of an adhesion-deficient bacterial strain within water-reactive porous media. *Environ. Sci. Technol.* 39:2500-2508.
- Toride, N., Leij, F.J. and van Genuchten, M.Th. 1995. The CXTFIT code for estimating transport parameters from laboratory and field tracer experiments. *Research Rep. No. 137*, U.S. Salinity Lab., ARS, USDA, Riverside, CA.
- Torkzaban, S., Hassanizadeh, S.M., Schijven, J.F. and de Roda Husman, A.M. 2006a. Virus transport in saturated and unsaturated sand columns. *Vadose Zone J.* 5:877-885.
- Torkzaban, S., Hassanizadeh, S.M., Schijven, J.F. and van den Berg, H.H.J.L. 2006b. Role of air-water Interfaces on retention of viruses under unsaturated conditions. *Water Resour. Res.* 42:W12S14.
- Torkzaban, S., Bradford, S.A. and Walker, S.L. 2007. Resolving the coupled effects of hydrodynamics and DLVO forces on colloid attachment to porous media. *Langmuir.* 23:9652-9660, doi:10.1021/la700995e.
- Torkzaban, S., Bradford, S.A. and Walker, S.L. 2008a. Colloid transport in unsaturated porous media: the role of water content and ionic strength on particle straining. *J. Contam. Hydrol.* 96:113-127. doi:10.1016/j.jconhyd.2007.10.006.
- Torkzaban, S., Tazehkand, S.S., Walker, S.L., and Bradford, S.A. 2008b. Transport and fate of bacteria in porous media: Coupled effects of chemical conditions and pore space geometry. *Water Resour. Res.*, 44:W04403.

- Tufenkji, N., Ryan, J.N. and Elimelech, M. 2002. The promise of bank filtration. *Environ. Sci. Technol.* 36:A422-A428.
- Tufenkji, N., Elimelech, M. 2004. Deviation from the classical colloid filtration theory in the presence of repulsive DLVO interactions. *Langmuir.* 20:10818-10828.
- Tufenkji, N., Miller, G., Ryan, J., Harvey, R.W., and Elimelech, M. 2004. Transport of *Cryptosporidium* oocysts in porous media: Role of straining and physico-chemical filtration. *Environ. Sci. Technol.* 38:5932-5938.
- Tufenkji, N., and Elimelech, M. 2005a. Breakdown of colloid filtration theory: role of the secondary energy minimum and surface charge heterogeneities. *Langmuir* 21:841-852.
- Tufenkji, N., and Elimelech, M. 2005b. Spatial distributions of *Cryptosporidium* oocysts in porous media: evidence for dual mode deposition. *Environ. Sci. Technol.* 39:3620-3629.
- Tufenkji, N., Dixon, D.R., Considine, R. and Drummond, C.J. 2006. Multi-scale *Cryptosporidium*/sand interactions in water treatment. *Water Res.* 40:3315- 3331.
- United States Department of Agriculture. 1992. Part 651 (210-AWMFH, 4/92). National engineering handbook: Agricultural waste management field handbook. *USDA*. Washington, DC.
- United States Department of Agriculture. 1996. NRCS. National Engineering Handbook: Agricultural Waste Management Field Handbook. *U.S. Dept. Commerce, NTIS*. Springfield, VA.
- United States Environmental Protection Agency. 1997. National Water Quality Inventory, Report to Congress, EPA 841-R-97-008. Washington, DC, *USEPA*.
- United States Environmental Protection Agency. 1998. Environmental impacts of animal feeding operations. *Office of Water, Standards and Applied Sci. Div.* Washington, DC, *USEPA*.
- United States Environmental Protection Agency. 2000. National Primary Drinking Water Regulations: Ground Water Rule, Proposed Rule.
- United States Environmental Protection Agency. 2001a. Development document for the proposed revisions to the national pollutant discharge elimination system permit regulation and effluent limitation guidelines and standards for concentrated animal feeding operations (CAFOs). EPA-821-R-01-003. 2001. Washington, DC, *USEPA*.
- United States Environmental Protection Agency. 2001b. Method 1601: Male specific (F+) and somatic coliphage in water by two-step enrichment procedure. EPA-821-R-01-030. Office of Water, Engineering and Analysis Div., Washington, DC, *USEPA*.
- United States Environmental Protection Agency. 2003. National pollutant discharge elimination system permit regulation and effluent limitation guidelines and standards for concentrated animal feeding operations (CAFOs). *Federal Register* 69(29):7176-7274.
- United States Environmental Protection Agency. 2004. Guidelines for water reuse. EPA 625/R-04/108. Cincinnati, OH, *USEPA*.
- United States Food and Drug Administration. 2007. FDA finalizes report on 2006 spinach outbreak. *FDA News*.
- United States Department of Agriculture. 2000. National Nutrient Management (Code 590), Natural Resource Conservation Service, Conservation Practice Standard.
- Valenzuela-Solano, C. and Crohn, D.M. 2006. Are decomposition and N release from organic mulches determined mainly by their chemical composition? *Soil Biology & Biochemistry* 38:377-384.
- Vanderlip, R.L., and Reeves, H.E. 1972. Growth stages of sorghum [*Sorghum bicolor*, (L.) moench]. *Agron. J.* 64:13-16.
- Van Veen, J.A., van Overbeek, L.S. and van Elsas, J.D. 1997. Fate and activity of microorganisms introduced into soil. *Microbiol. Mol. Biol. Rev.* 61:121-135.

- Vanotti, M.B. and Hunt, P.G. 1999. Solids and nutrient removal from flushed swine manure using polyacrylamides. *Trans. ASAE*. 42:1833-1840.
- Vanotti, M.B., Millner, P.D., Hunt, P.G. and Ellison, A.Q. 2005a. Removal of pathogen and indicator microorganisms from liquid swine manure in multi-step biological and chemical treatment. *Bioresour. Technol.* 96:209-214.
- Vanotti, M.B., Rashash, D.M.C. and Hunt, P.G. 2002. Solid-liquid separation of flushed swine manure with PAM: Effect of wastewater strength. *Trans. ASAE*. 45:1959-1969.
- Vanotti, M.B., Rice, J.M., Ellison, A.Q., Hunt, P.G., Humenik, F.J. and Baird, C.L. 2005b. Solid-liquid separation of swine manure with polymer treatment and sand filtration. *Trans. ASAE*. 48:1567-1574.
- Verwey, E.J.W., and Overbeek, J.Th.G. 1948. Theory of the stability of lyophobic colloids. *Elsevier*, Amsterdam.
- Wan, J. and Tokunaga, T.K. 1997. Film straining of colloids in unsaturated porous media: Conceptual model and experimental testing. *Environ. Sci. Technol.* 31:2413-2420.
- Wan, J. and Wilson, J.L. 1994a. Colloid transport in unsaturated porous media. *Water Resour. Res.* 30:857-864.
- Wan, J. and Wilson, J.L. 1994b. Visualization of the role of the gas-water interface on the fate and transport of colloids in porous media. *Water Resour. Res.* 30:11-23.
- Wan, J.M., and Tokunaga, T.K. 2002. Partitioning of clay colloids at air-water interfaces. *J. Coll. Interf. Sci.*, 247:54-61.
- Wang, D.S., Gerba, C.P., and Lance, J.C. 1981. Effect of soil permeability on virus removal through soil. *Appl. Environ. Microbiol.* 42:83-88.
- Wang, G., Zhao, T. and Doyle, M.P. 1996. Fate of enterohemorrhagic *Escherichia coli* O157-H7 in bovine feces. *Appl. Environ. Microbiol.* 62:2567-2570.
- Wang, Z., Jury, W.A., Tuli, A. and Kim, D.J. 2004. Unstable flow during redistribution: controlling factors and practical implications. *Vadose Zone J.* 3:549-559.
- Wang, Z., Wu, L., Harter, T., Lumia, D.S. and Jury, W.A. 2003. A field study of unstable preferential flow during soil water redistribution. *Water Resour. Res.* 39: 1075, doi:10.1029/2001WR000903
- Ward, M.H., deKok, T.M., Levallois, P., Brender, J., Gukus, G., Nolan, B.T. and VanDerslice, J. 2005. Workgroup report: drinking-water nitrate and health—recent findings and research needs. *Environ. Health Perspect.* 113:1607-1614.
- Watson, K.K. 1966. An instantaneous profile method for determining the hydraulic conductivity of unsaturated porous materials. *Water Resour. Res.* 2:709-715.
- Watts, D.B., Torbert, H.A., and Prior, S.A. 2007. Mineralization of nitrogen in soils amended with dairy manure as affected by wetting/drying cycles. *Communications in Soil Science and Plant Analysis* 38:2103-2116.
- Waybrant, K.R., Ptacek, C.J. and Blowes, C.W. 2002. Treatment of mine drainage using permeable reactive barriers: column experiments. *Environ. Sci. Technol.* 36:1349-1356.
- Webb, J. and Archer, J.R. 1994. Pollution of soils and watercourses by wastes from livestock production systems. In: *Pollution in livestock production systems*. CABI Publishing. Oxfordshire, UK. pp. 189-204.
- Weiss, W.J., Bouwer, E.J., Aboytes, R., LeChevallier, M.W., O'Melia, C.R., Le, B.T. and Schwab, K.J. 2005. Riverbank filtration for control of microorganisms results from field monitoring. *Water Res.* 39:1990-2001.
- WHO. 2006. WHO guidelines for the safe use of wastewater, excreta and greywater. Geneva, Switzerland, *World Health Organization*.
- Woodard, K.R., French, E.C., Sweat, L.A., Graetz, D.A., Sollenberger, L.E., Macoon, B., Portier, K.M., Wade, B.L., Rymph, S.J.,

- Prine, G.M., and Van Horn, H.H. 2002. Nitrogen removal and nitrate leaching for forage systems receiving dairy effluent. *J. Environ. Qual.* 31:1980-1992.
- Yao, K.M., Habibian, M.T., and O'Melia, C.R. 1971. Water and waste water filtration—concepts and applications. *Environ. Sci. Technol.* 5:1105-1112.
- Yates, M.V., Yates, S.R., Wagner, J. and Gerba, C.P. 1987. Modeling virus survival and transport in the subsurface. *J. Contam. Hydrol.* 1:329-345.
- Yeoman, S., Stephenson, T., Lester, J.N. and Perry, R. 1988. The removal of phosphorus during wastewater treatment: a review. *Environ. Pollut.* 49:183- 233.
- Zevi, Y., Dathe, A., McCarthy, J.F., Richards, B.K. and Steenhuis, T.S. 2005. Distribution of colloid particles onto interfaces in partially saturated sand. *Environ. Sci. Technol.* 39:7055-7064.
- Zhang, R.H. and Lei, F. 1998. Chemical treatment of animal manure for liquid separation. *Trans. ASAE.* 41:1103-1108.
- Zhang, R.H. and Westerman, P.W. 1997. Solid-liquid separation of animal manure for odor control and nutrient management. *Appl. Eng. Agric.* 13:657-664.



# ISSUE



PRESORTED STANDARD  
POSTAGE & FEES PAID  
EPA  
PERMIT NO. G-35

Office of Research and Development (8101R)  
Washington, DC 20460

Official Business  
Penalty for Private Use  
\$300



Recycled/Recyclable  
Printed with vegetable-based ink on  
paper that contains a minimum of  
50% post-consumer fiber content  
processed chlorine free